STRUCTURAL STUDIES USING CHEMICAL IONISATION ION TRAP MASS SPECTROMETRY

Brian Leslie Williamson

A thesis submitted in partial fulfilment of the requirements of the Nottingham Trent University for the degree of Doctor of Philosophy

January 1996

ABSTRACT

Chemical ionisation (CI) studies have been carried out using quadrupole ion trap mass spectrometry. The reactions of benzoyl cations, of the type $[C_6X_5CO]^+$ (where X= H, F, 4-Me, 4-Bu^t), with compounds containing hydroxy, double bond and amine functionality have been investigated. The formation of $[M+C_6X_5CO]^+$, $[M-H]^+$ and $[M-OH]^+$ products with hydroxy compounds is determined by the hydroxy group environment in agreement with the known thermochemistry of these ions and a molecular modelling study of the electrophilic addition. The formation of $[M+C_6H_5CO]^+$, $[M-NH_2]^+$ and protonated benzamide ions with compounds containing the amino functionality is determined by the environment of the amine group. These mass selected reagent ions show limited reactivity towards other compounds. Substitution of the benzoyl cation with fluorine or a methyl group modifies the electrophilic character of the benzoyl cation, allowing the selectivity of its reactions to be controlled. The selectivity of the chemical ionisation reactions of the benzoyl ions is demonstrated by their reactions with analytes of pharmaceutical interest containing hydroxy, double bond and amine functionality.

Negative CI reactions of $[OH]^-$ and $[C_6H_5CO]^-$ have also been investigated in the ion trap. The reactions of the benzoyl anion, $[C_6H_5CO]^-$, formed as the $[M-H]^-$ ion from the $[OH]^-$ chemical ionisation reaction with benzaldehyde inside the ion trap are described. This ion reacted selectively as a nucleophile towards the carbonyl functional group of the aldehyde and ketone compounds investigated and may have potential as a selective chemical ionisation reagent for these classes of compounds.

The formation of gas-phase non-covalent inclusion complexes of crown ethers with protonated amines is reported. The effect of varying the structure of protonated amines of the type $[R-NH_3]^+$ (where R= C_3H_7, $C_6H_5C_2H_4$, $O_2NC_6H_4C_2H_4$ or $C_6H_5CH_2C(H)COOH$) on the interaction with the crown ethers 18-crown-6, benzo-18-crown-6 and (s)-phenyl-18-crown-6 to form non-covalent inclusion complexes has also been studied. This structure variation has a strong effect on the stability of the non-covalent inclusion complexes formed with the crown ethers. Ligand exchange and competition experiments have been used to assign the relative affinities of host-guest combinations.

ACKNOWLEDGEMENTS

First and foremost I thank my supervisor, Professor Colin S. Creaser for his support, advice and encouragement throughout the course of this study. I also thank Mr Brian Stockton and Dr Frank Cottee for their help and guidance.

I am grateful for the support and friendship I have received from all the members of CSC research group including Claudia, Colin, Derrick, Daniel, Karen, Mark, Russel, Sarah, Steve and Thomaś. I especially thank Tony and James for all their hard work, patience and friendship and also to Denise and Nicki for keeping me informed about life in general.

I thank my family and friends for their love and support during the past three years.

Finally I thank EPSRC and SmithKline Beecham Pharmaceuticals for their financial support of the project, enabling me to carry out this research.

TABLE OF CONTENTS

CHAPTER 1

INTRODUCTION

1.1 MASS SPECTROMETRY

The technique of mass spectrometry was pioneered in the early 1900's by J. J. Thompson [1] who used his parabola mass spectroscope to establish that elements such as neon have stable isotopes. Since then, the development of the mass spectrometer has been driven by the fact that it is a spectrometric technique capable of high sensitivity and unambiguous identification of compounds, giving a unique 'fingerprint' spectrum in many cases. The mass spectrometer has become increasingly sophisticated and the number of different applications of this technique is vast. Advances in ionisation techniques [2] allowing most compounds to be ionised or made to yield gas phase ions and in favourable cases with picograms or less being consumed in the process, mean that the mass spectrometry is potentially one of the most powerful analytical techniques available today.

A mass spectrometer is an instrument which produces ions from a sample, separates these ions into a spectrum according to their mass-to-charge (m/z) ratio and records the relative abundance of each species of ion present. Positive and negative ions may be detected although positive ion mass spectrometry is more common.

1.2 INLET SYSTEMS

Mass spectrometers operate at low pressure, typically 10^{-3} to 10^{-8} torr to eliminate scattering due to ion-molecule collisions. The inlet system bridges the gap between atmospheric pressure and the vacuum system of a mass spectrometer. It must also provide the conditions needed for involatile sample volatilisation.

A liquid reservoir inlet consists of a glass sample vial which is connected to the spectrometer *via* a fine control needle valve. It is suitable for samples which are volatile at room temperature and have a high vapour pressure. This inlet is most convenient way of introducing a reference compound such as perfluorotributylamine into the source for calibration or for carrying out long time scale experiments where a stable sample pressure is required.

For solids or extremely involatile liquids, introduction via a stainless steel solids probe may be the preferred mode of introduction. A sample is placed into a glass or quartz tube and inserted into the probe tip, inside a resistively heated coil. The whole assembly is then introduced into the mass spectrometer manifold *via* a vacuum lock. The tip can then be heated to temperatures upwards of 350 ^{o}C to volatilise the sample. Slow heating can distil samples to achieve some separation of mixtures on the basis of boiling points of individual components. Alternatively, very involatile samples can be coated onto a metal loop, fixed onto the probe tip which is resistively heated at a very high rate inside the mass spectrometer. This is

known as a direct exposure probe and helps to stop thermal degradation of involatile samples.

1.3 IONISATION METHODS

Sample molecules in the vapour phase must be ionised before mass separation can occur. During the early years of organic mass spectrometry electron ionisation (EI) was the normal ionisation method. When chemical ionisation (CI) was developed in the mid 1960's it provided a complementary ionisation technique. However, both EI and CI require the sample to be in the vapour phase. To extend mass spectrometry to large, involatile compounds such as most biological materials it was necessary to develop alternate ionisation methods. The most commonly used of these desorption ionisation techniques are laser desorption, fast atom bombardment (FAB) and electrospray.

1.3.1 Electron Ionisation

Electron ionisation (EI) is the oldest, most commonly used ionisation technique which was developed by Dempster [3] in the early 1920's. An EI source is shown in Figure 1.1. When a sufficient electric current is passed through a tungsten or rhenium filament, electrons are emitted by diffusion from their surface. Subjected to a 70V potential gradient across the source, a 70 eV beam is produced. On

interaction with a sample molecule (M), it is possible to remove an electron from the outer electron cloud of the molecule:

$$M + e^- \rightarrow M^{+\cdot} + 2e^-$$

(70 eV) (thermal)

A radical cation is formed known as the molecular ion.

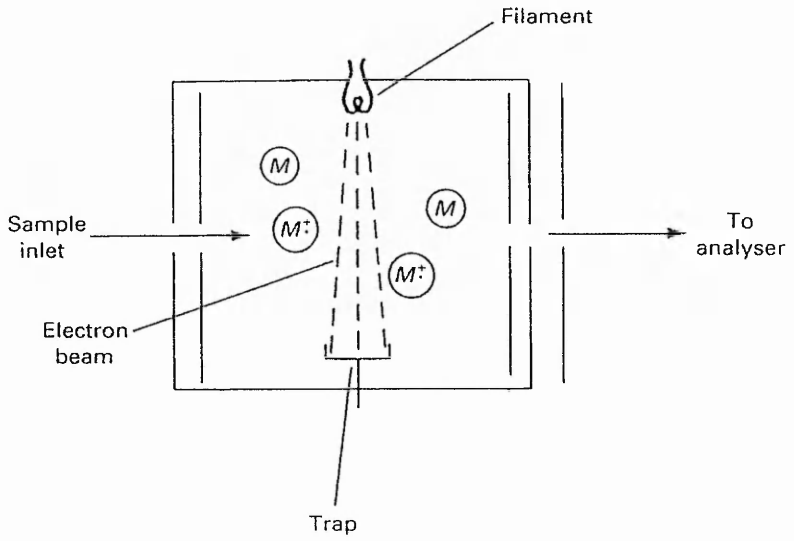

Figure 1.1. An electron impact ionisation source.

It is possible for other reactions, such as electron capture to form $M^{-\cdot}$ or energy transfer to form an electronically excited molecule to occur, however, the formation of positive ions is the most likely reaction. The efficiency of EI is low, less than 1 % of sample molecules are ionised.

An electron energy of 70 eV is normally used as this gives high ionisation efficiency and good reproducibility. Most organic molecules have ionisation

energies below 13 eV and the EI process will impart a large amount of excess energy into the radical cation. This can cause fragmentation to produce fragment ions which are often highly useful for structure determination. These fragmentations may be classified as shown below:

$$AB^{+\cdot} \rightarrow A^{+} + B^{\cdot} \quad \text{(Simple cleavage)}$$

$$AB^{+\cdot} \rightarrow A^{+\cdot} + B \quad \text{(Rearrangement)}$$

The distribution of charge and unpaired electron is by no means equal, the distribution depends entirely on the thermodynamic stability of the products of fragmentation. In some samples the degree of fragmentation is so great that it is impossible to determine the molecular weight of the sample, e.g. long chain hydrocarbons. To determine the molecular weight of such samples a much 'softer' ionisation technique is required such as chemical ionisation.

1.3.2 Chemical Ionisation

Since its invention in 1966 by Munson and Field, [4] chemical ionisation (CI) has become widely commercialised and applied to many different analytes. Conventional CI is based on the EI source, but the source is made virtually gas tight to contain a reagent gas such as methane or ammonia at 0.1 - 1 Torr. The generation of primary ions by EI gives rise to species which undergo ion-molecule

reactions owing to their small mean free path at these higher pressures. The primary ions may then react with neutral reagent molecules to form secondary reagent ions, for example for methane as reagent gas:

CH_4	+	e^-	→	$CH_4^{+\cdot}$	+	$2e^-$	Primary ion formation
$CH_4^{+\cdot}$	+	CH_4	→	CH_5^+	+	$CH_3^\cdot$	Reagent ion
CH_3^+	+	CH_4	→	$C_2H_5^+$	+	H_2	formation

On introduction of sample molecules (M) into the CI source, these reagent ions may react with sample molecules in several ways:

CH_5^+	+	M	→	MH^+	+	CH_4	Proton
$C_2H_5^+$	+	M	→	MH^+	+	C_2H_4	transfer
$C_2H_5^+$	+	MX	→	M^+	+	C_2H_5X	Anion abstraction

With other reagent gases such as ammonia other reactions can occur:

NH_4^+	+	M	→	$[M+NH_4]^+$			Electrophilic addition
$NH_3^{+\cdot}$	+	M	→	$M^{+\cdot}$	+	NH_3	Charge exchange

The most important of all these processes is proton transfer leading to the pseudo-molecular ion $[MH]^+$. The thermodynamics of the reaction depend on the difference in proton affinity between the sample and reagent molecules, where the proton affinity (PA) of a molecule is defined as:

$$PA\ (X) \quad \sim \quad -\Delta H^o\ (X+H \rightarrow XH^+)$$

The gas phase PA of some common CI reagent gases are given below:

Reagent Gas	Proton Affinity ($kJ\ mol^{-1}$)
H_2	423
CH_4	536
C_2H_6	585
H_2O	712
CH_3OH	762
CH_3CN	782
NH_3	847
CH_3NH_2	884

The difference in proton affinities for any combination of common reagent and sample molecules is much less than the excess energy associated with EI and therefore any $[MH]^+$ ions formed will have very little excess energy. Consequently CI is a 'soft' ionisation technique producing prominent molecular ions with little or

no fragmentation. By careful choice of reagent gases the exothermicity of the reaction can be tuned, for example methane will protonate nearly all organic compounds with some degree of fragmentation, where as ammonia will only protonate certain compounds, e.g. amines with little fragmentation. [5] This allows the possibility of selective ionising components in a mixture, for example the chemical ionisation by the ammonium reagent ion of nitrogen heterocycles in a gasoil sample. [6]

Negative chemical ionisation is possible, [7] by using reagents such as $[OH]^-$, $[Cl]^-$ and $[SF_6]^-$ from water, carbon tetrachloride and sulphur hexafluoride respectively. The major mechanisms of ionisation are proton abstraction, charge exchange, nucleophilic addition and nucleophilic displacement to produce $[M-H]^-$, $[M]^-$, $[M+R]^-$ and $[M-R]^-$ ions respectively. [8] These are all processes analogous to positive CI.

1.3.3 Fast atom Bombardment

Fast atom bombardment (FAB), also known as liquid secondary-ion mass spectrometry (LSIMS), is a liquid phase ionisation technique developed by Barber at the start of the 1980's. [9] Samples are dissolved in a suitable viscous liquid matrix (usually glycerol), placed on a target and aligned with an atom gun in the source. Bombardment by a primary beam of atoms or ions (Ar, Xe or Cs^+) having kinetic energies in the 8-35 kV range produces ions by a sputtering mechanism. [10] This is

illustrated in Figure 1.2. FAB spectra normally show both molecular weight and structural information, although FAB is classed as a 'soft' ionisation technique. The chemical noise in FAB spectra is higher than for other ionisation methods. The noise arises from matrix ions and degradation products formed during the bombardment process.

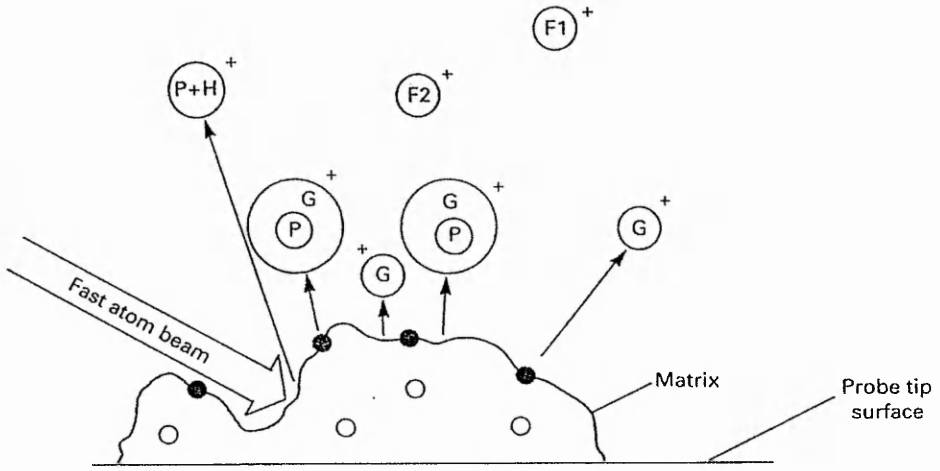

Figure 1.2. Sputtering phenomenon from liquid matrix during bombardment with fast atoms. G = matrix, P+G = parent solvate with matrix, P+H = pseudomolecular ion, F_1, F_2 = fragments ions.

1.3.4 Laser Desorption Ionisation

Laser desorption (LD) is a solid or liquid phase ionisation technique. In LD a high intensity laser beam is focused onto a sample to induce both volatilisation and ionisation. The laser must be pulsed to achieve the high power densities required.

The spectra most often consist of protonated or cationised molecular ions, although with sufficient laser power it is possible to perform multi-photon ionisation to give radical cations as the molecular species. [11] The LD technique had limited applications until the discovery of matrix assisted laser desorption / ionisation (MALDI). Here the sample is mixed with a matrix which is chosen because it assists ionisation, either by taking up energy from the laser and transferring that energy to the sample, [12] or by simulating a sputtering process analogous to FAB. [13] Examples of suitable matrices are nicotinic acid and 2,5-dihydroxybenzoic acid. In MALDI spectra matrix adduct ions may be formed together with other molecular ions. This technique has extended the upper mass limits of mass spectrometry to biomolecules of 500 kDa. [14]

1.4 MASS ANALYSERS

After their formation in the ion source, the ions are separated by their mass to charge ratio (m/z). There are a number of methods of mass analysis, all of which involve the use of magnetic and/or electric fields, but only four are commercially available. These are the magnetic sector, quadrupole, time-of-flight and ion-cyclotron-resonance (FT-ICR). Of these only magnetic sector and quadrupole mass spectrometers will be discussed here.

1.4.1 Magnetic and electric sectors

Sector analysers date back to 1898 when W. Wien demonstrated that a beam of positively charged particles could be deflected using magnetic and electric fields. A diagram of a magnetic sector is illustrated in Figure 1.3. The term magnetic sector arises because the beam trajectory traverses only a sector of the circular poles of the magnetic. Magnetic sector sources accelerate ions through a potential drop, V, which imparts kinetic energy equal to :

$$zeV = 1/2\ mv^2 \tag{1.1}$$

where ze is the ion charge, m is the mass and v is the velocity. On entering a magnetic field, ions experience a force perpendicular to their velocity, which is balanced by their own centripetal force:

$$Bzev = \frac{mv^2}{r} \tag{1.2}$$

where B is the magnetic field strength and r is the ion path radius.

Combining (1) and (2) yields the equation:

$$\frac{m}{ze} = \frac{B^2r^2}{2V} \tag{1.3}$$

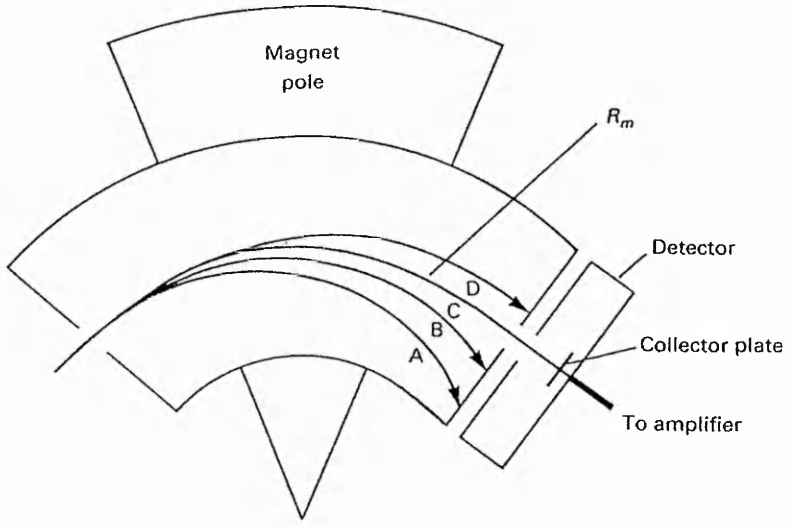

Figure 1.3. A representation of a magnetic sector mass spectrometer. Only ions following a trajectory of radius R_m will be focused.

A magnetic field will therefore separate ions according to their mass-to-charge ratios and by changing either B or V, ions of different m/z values can be focused on the detector. In practice, scanning the magnetic field strength B is most often used. A single magnetic sector can achieve a maximum resolution of approximately 6000, where resolution is defined as:

$$R = \frac{m}{\Delta m} \tag{1.4}$$

where two peaks of equal height and masses m and (m+Δm) are separated by a valley of 10 % of the peak height. The resolution limit is due to the kinetic energy spread of ions from the source. A solution to this problem is to use double focusing instruments.

In these instruments the magnetic sector is preceded (normal geometry) or followed (reverse geometry) by an electrostatic sector. This analyser consists of two stainless steel plates bent into segments of concentric circles. Ions entering the electric field experience a force perpendicular to their velocity vector, which is balanced by their own centripetal force:

$$Eze = \frac{mv^2}{r} \tag{1.5}$$

where E is the electric field strength applied. Combining equations (1.5) and (1.1) gives the simple relationship for radius of the ions:

$$r = \frac{2V}{E} \tag{1.6}$$

showing that the deflection in an electric field depends only upon V and E and therefore ions of the same energy and direction, regardless of their m/z ratio, will follow the same path. The electric sector analyser is therefore solely an energy and not a mass analyser. In a double focusing spectrometer, shown in Figure 1.4, the velocity dispersion of ions in the electric and magnetic sectors are equal and opposite, thus cancelling each other out and bringing divergent energy ions to a focus. Ions that directionally diverge are also focused by both sectors, hence the name of the instrument. Resolution in excess of 50,000 are possible with this

design. However, these are large, expensive devices with relatively low scan speeds.

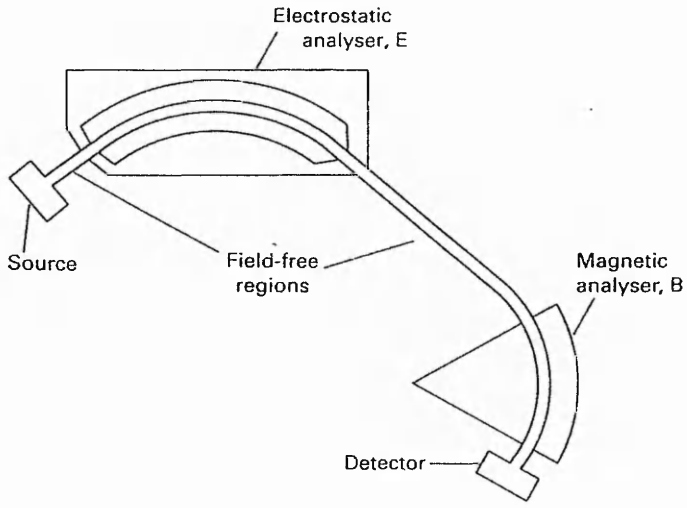

Figure 1.4. A double focusing mass spectrometer

1.4.2 Quadrupoles

Quadrupole mass spectrometers were first patented in 1956 by Paul and Steinwedel. [15, 16] The linear quadrupole consists of four parallel rods which have either hyperbolic or cylindrical surfaces as shown in Figure 1.5. Diagonally opposite pairs of rods are electrically connected and coupled to voltages consisting of a DC and a radio frequency (RF) component. The potentials applied to the two pairs are equal in magnitude, but the DC components are opposite in sign and the

RF part is shifted in phase by 180 °. Ions are accelerated out of the source and travel between the rods with an oscillatory motion. Only ions which posses a stable motion will pass through to the detector and all others will collide with the rods or go through the spaces to the manifold region.

Equations of motion for an ion may be derived from Newtons second law (force = mass x acceleration) to give second order differential equations known as the Mathieu equation [17] :

$$\frac{d^2u}{d\xi^2} + (a_u - 2q_u \cos 2\xi)\, u = 0 \qquad (1.7)$$

where u represents either x or y (see Figure 1.6) and ξ is πft where f is the RF frequency and t is time. a and q are dimensionless constants, which for ions in a quadrupole field are:

$$a_x = -a_y = \frac{8eU}{mr_o^2\Omega^2} \qquad q_x = -q_y = \frac{4eV}{mr_o^2\Omega^2} \qquad (1.8)$$

where an ion of mass m and single charge e travels through a quadrupole of radius r_o, operating with RF and DC voltage amplitudes V and U respectively and Ω is the angular frequency of the rf in radians per second.

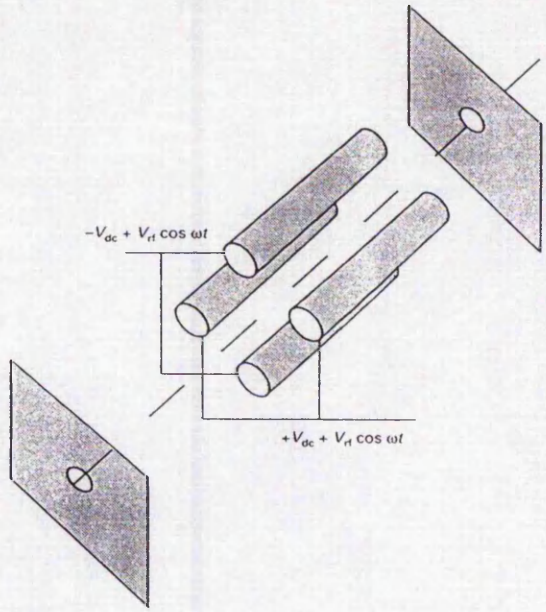

Figure 1.5. The linear quadrupole

Solving the Mathieu equation is a non-trivial task, but essentially solutions are sought where u remains finite as $\xi \rightarrow$ infinity, i.e. ions have stable trajectories. All other experimental parameters being constant, u depends only on a and q, thus conditions for finite u (or ion stability) can be represented on an a-q or stability diagram, shown in Figure 1.6. Ions have a stable motion if they have values of a and q which lie inside the stability boundaries. Ions in this region posses fundamental frequencies or secular frequencies, Ω_0

$$\Omega_o = \frac{\beta\Omega}{2} \tag{1.9}$$

where β is a parameter related to the ion frequency which can take values between 0 and 1.

The stability diagram is symmetrical about the q axis and for mass spectrometric analysis, the stability region near the origin is used. If the quadrupole voltages are scanned at a constant U/V ratio, then ions of increasing m/z ratio will have stable trajectories and pass down the quadrupole to strike the detector.

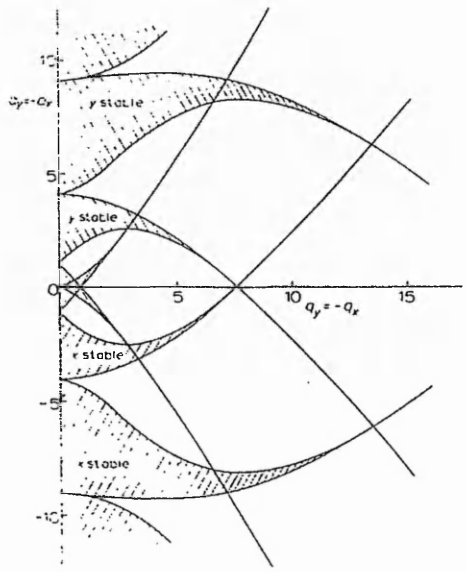

Figure 1.6. Graphical representation of stable solutions of the Mathieu equation plotted in (a, q) space

Using this technique of 'mass-selective-stability', the mass spectrum is obtained. Resolution is improved by increasing U, which moves the ion closer to the apex of the stability region, so that a narrower 'window' of m/z values are stable. Although the resolution can be improved, sensitivity is affected at higher resolutions. Hence, most quadrupole mass spectrometers operate at unit resolution. The advantages of such devices are relatively low cost, simple design, ease of use and compact size.

The majority of mass spectrometers in existence are 'benchtop' quadrupole instruments interfaced to gas chromatographs to allow GC-MS analysis.

1.4.3 Quadrupole ion traps

The quadrupole ion trap was patented as an alternative electrode arrangement of the linear quadrupole. This ion trap is the three dimensional solid of revolution of a two dimensional quadrupole, with the axis of rotation being the x or y axis, as shown in Figure 1.7. This creates a circular 'ring electrode' and two 'end cap electrodes', all having hyperbolic inner surfaces, illustrated in Figure 1.8. When a combination of rf and/or DC voltages applied to the quadrupole ion trap, the three electrodes create a rotational symmetric field in the space between them. In this field, ions exhibit complex periodic motion, now in three dimensions and the force exerted on an ion is proportional to its displacement from the centre of the trap.

Equations 1.7 and 1.8 can be solved to give a stability diagram for the ion trap, Figure 1.9(a). It is not symmetrical about the q axis due to the usual ion trap relationship

$$r_o^2 = 2z_o^2 \qquad (1.10)$$

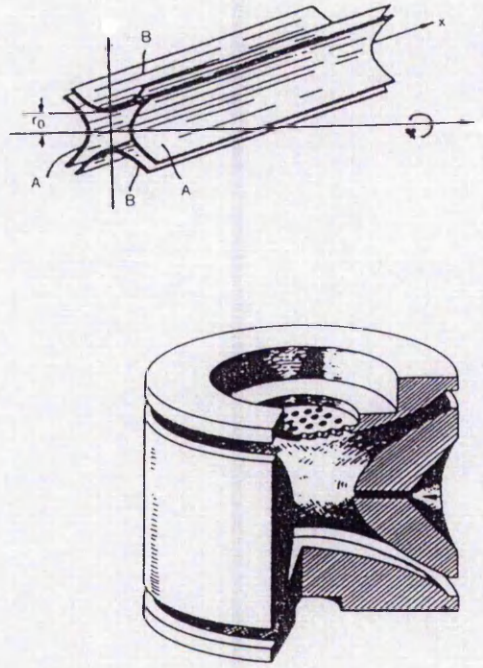

Figure 1.7. Electrode configuration of the ion trap.

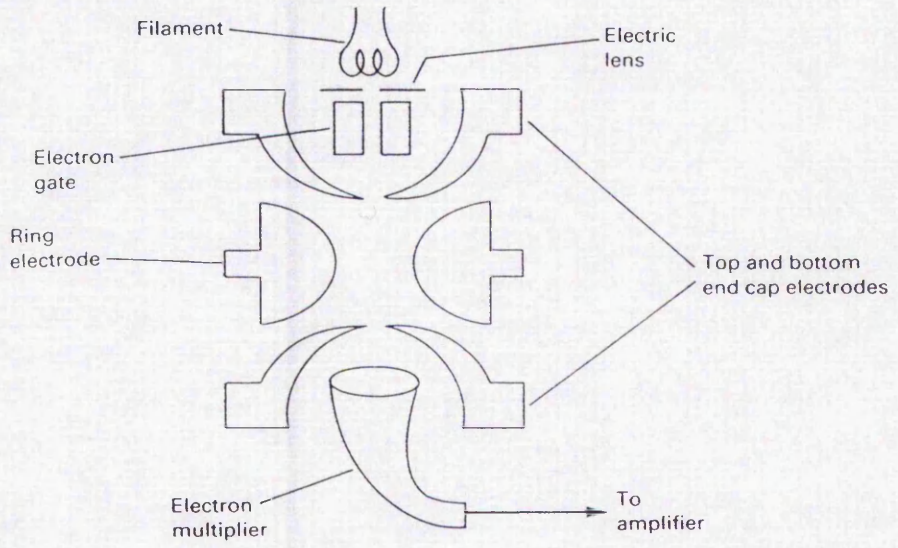

Figure 1.8. Schematic of the ion trap.

therefore

$$a_z = -2a_r = -\frac{8eU}{mr_o^2\Omega^2} \quad and \quad q_z = -2q_r = -\frac{4eV}{mr_o^2\Omega^2} \tag{1.11}$$

and the region for z stability is twice that for r stability. Where z and r stability regions overlap, ions will have stable trajectories in all directions and become 'trapped'. The overlapping region next to the origin is the area of most interest, this is enlarged in Figure 1.9(b). Ions lying on the marked iso-β lines posses the same secular frequency. An ion for which the a_z and q_z values fall within the stability region, exists in a potential well and providing the energy of the ion does not exceed the trapping potential of the trap, the ion will be trapped in a stable trajectory, an example of which is shown in Figure 1.10 for charged aluminium particles. [18]

In order for the ion trap to be used as a mass spectrometer, a method of scanning the trapped ions to measure their mass-to-charge ratio has to be utilised. A number of methods have been developed, one of the first being the resonance detection method. [19] A low voltage auxiliary RF signal is applied across the end cap electrodes and the frequency swept. When the applied frequency matches the secular frequency of ions of a particular m/z value, then resonance occurs and the resultant drop in the auxiliary Rf voltage can be detected. This was the method described in the original ion trap patent and was used for many years, however it was very cumbersome and lacked sensitivity.

(a)

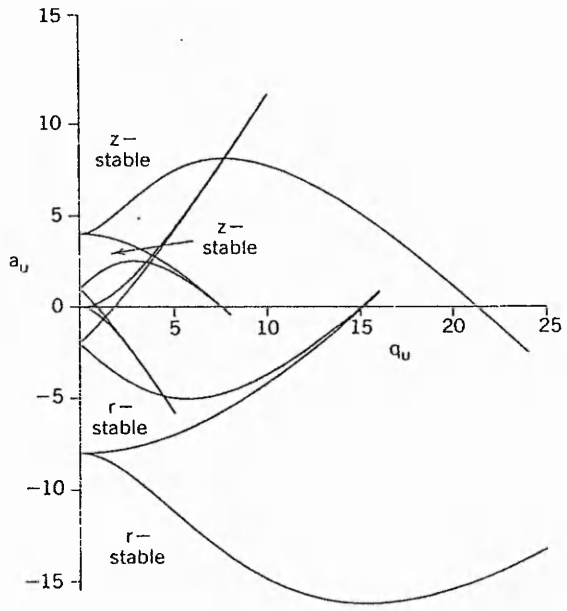

(b)

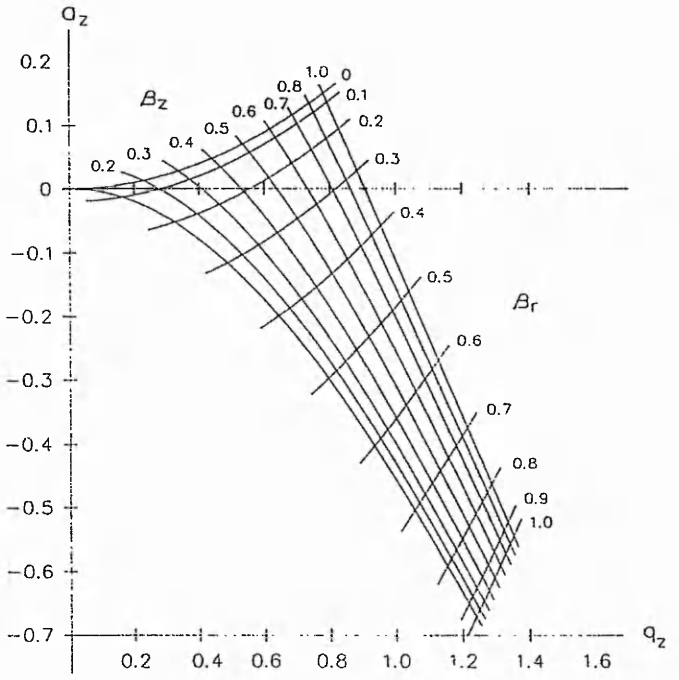

Figure 1.9. The Mathieu stability diagram for the quadrupole ion trap (a) with the region near the origin expanded (b).

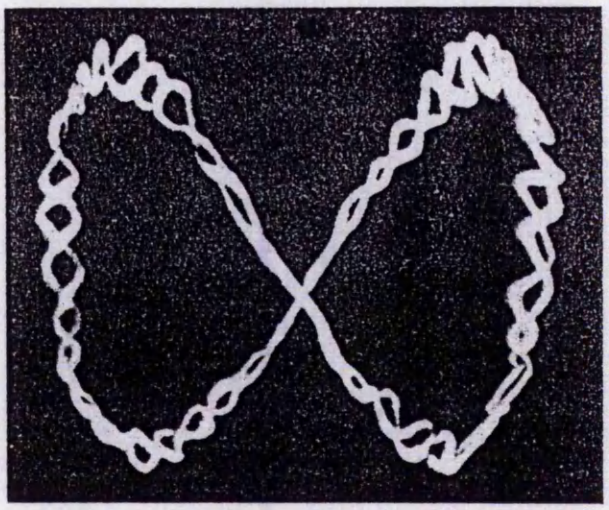

Figure 1.10. The trajectory of an aluminium micro-particles trapped in the r-z plane.

Dawson and Whetten patented the mass selective stability method of scanning the ion trap in 1970. [20] This method relates to that used on linear quadrupoles. By applying the correct RF and DC voltages, ions of a particular m/z ratio are placed at the lower apex of the stability diagram. All other ions are unstable and will be ejected from the trap. When ions have been isolated in this way, application of a sharp DC pulse to one of the end cap electrodes ejects the stored ions through holes in the exit endcap to an electron multiplier. By repeating the whole procedure, whilst slowly increases the RF and DC voltages at a constant ratio in order to isolate each m/z value, a mass spectrum is acquired. This scanning method is more

sensitive than resonance detection but for each mass scanned, a separate ionisation, ion isolation and detection stage must take place, leading to long scan times.

The scanning method known as mass selective instability, announced by Stafford and co-workers [21] in 1983 was the major breakthrough in ion trap scanning methods. The trap is operated using only RF voltages, consequently all trapped ions have an $a_{r,z}$ values of zero and will lie along the q axis, heavier ions to the left (lower q) and lower ions to the right (higher q). Ions are ejected from the trap by increasing the RF potential (V) applied to the ring electrode in a linear fashion, to a maximum of 15 kV (p-p). This has the effect of increasing the q_z value of the ions, until $q_z = 0.908$, at the boundary of the stability diagram. Here, $\beta_z = 1$ and the secular frequency $\Omega_0 = \Omega/2$. Resonant coupling of the drive and secular frequency occurs, ion oscillations in the z direction increase exponentially until ejection takes place. Ions leave the trap with an equal probability that they will pass through either end cap. By placing a multiplier behind one end cap electrode 50 % of the ions will be detected. Therefore, unlike scanning instruments, a large population of all ions formed are detected, making the ion trap operated in this way inherently sensitive. This le. to the commercialisation of the ion trap by Finnigan MAT, firstly as a benchtop GC-MS detector, the ITD™ and then as a more sophisticated research grade instrument, the ITMS™. Ion traps are now quite common and have been widely reviewed. [22, 23, 24] An ITMS schematic is shown in Figure 1.11, along with a scan routine (RF voltage applied to the ring electrode plotted against time) for a simple EI scan. This scan routine consists of two sequential steps, an ionisation step were ions are formed by electrons being gated into the trap and a

mass selective instability step that ejects the stored ions and an EI mass spectrum is recorded.

Stafford and co-workers also discovered that 10^{-3} Torr of a light buffer gas (usually helium) is necessary to achieve good resolution and sensitivity. Ion-helium collisions tend to focus the ion cloud down to the centre of the trap until the onset of instability, reducing the effect of higher fields (hexapole, octapole) caused by imperfections in the electrodes. [25] The ion-helium collisions also reduce ion velocity and minimise the effect of ion-neutral scattering.

Early ion traps suffered from a problem known as 'space-charging' which caused loss of mass resolution when the analyte concentration went above a certain limit. If a large number of ions are trapped, the mutual repulsion of the ions causes a perturbation of the properties of the charged cloud. Ions of the same m/z ratio occupy different points on the stability diagram and are ejected at different times during the mass scan, leading to peak broadening and also incorrect mass assignment. Ion-molecule reactions may also occur at high analyte concentration leading to enhanced $[M+H]^+$ ions.

To overcome space charge, 'Automatic Gain Control' (AGC) was developed. This incorporates two ionisation steps into each scan. The first, short ionisation step, the 'pre-scan' measures the number of ions being formed and then adjusts the ionisation time in the main analytical scan to avoid a large number of ions being formed. Ionisation times anywhere between 50 μs and 25 ms are possible. After

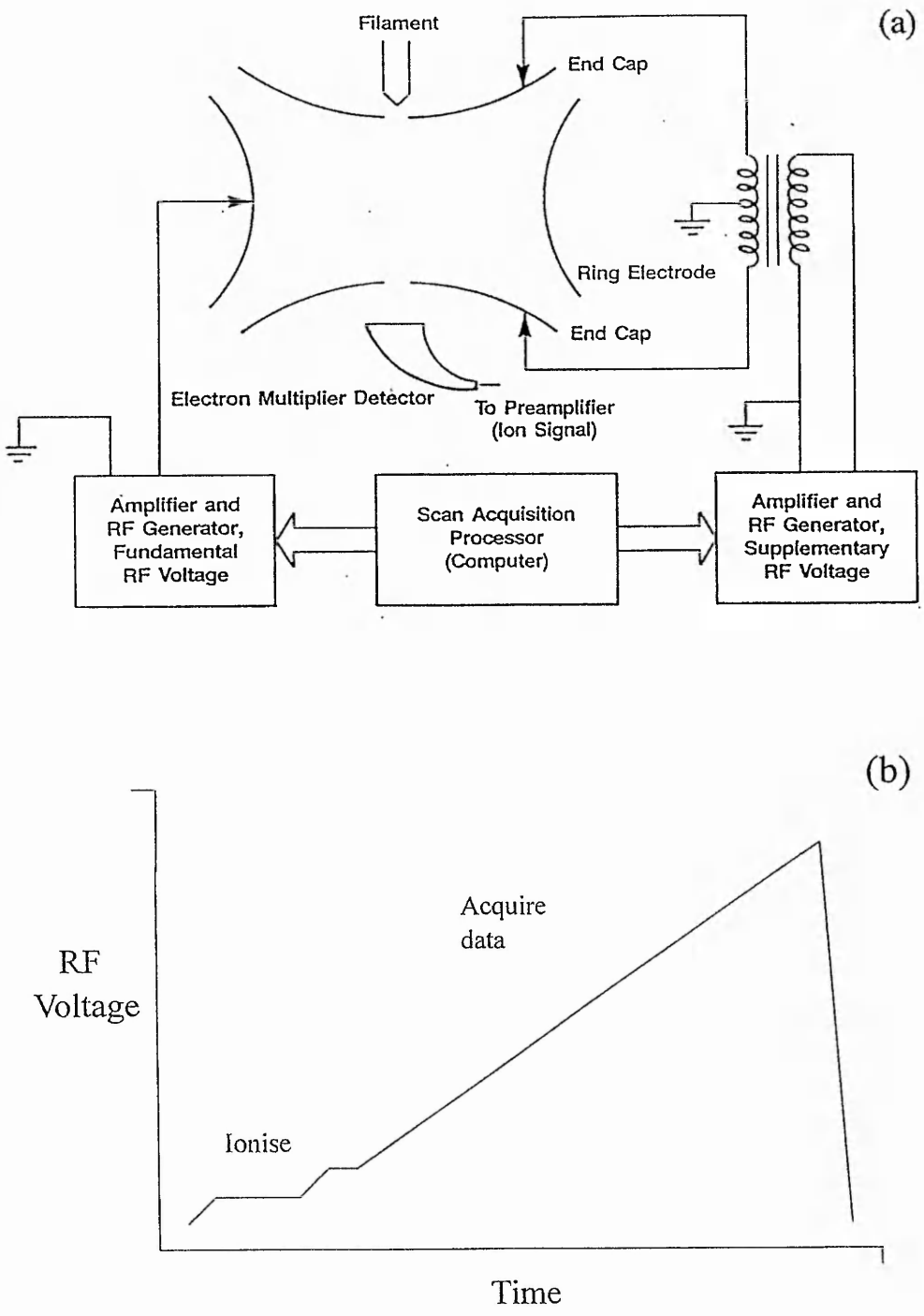

Figure 1.11. An ITMS schematic (a) and (b) a simple EI scan routine

each analytical scan the ion count is adjusted to take account of the ionisation time. Another technique to minimise space charge effects and improve resolution is 'axial modulation'. [26] A low (3-6 V_{p-p}) auxiliary RF voltage is applied to the end cap electrodes at a fixed frequency of approximately half the drive frequency (530 Khz). When ions reach the edge of the stability boundary ($\beta = 1$), both the drive frequency and the auxiliary frequency couple with the axial frequency of each ion, causing ejection to take place with ions much more tightly bunched.

This 'resonance ejection' technique can also be used to extend the mass range of the ion trap from its normal 0 - 650 amu. The mass range of the ion trap can be derived from equation 1.8 to give

$$(m/z)_{max} = \frac{4eV_{max}}{r_o^2 \Omega^2 q_{ej}} \qquad (1.12)$$

Increasing the maximum RF voltage or decreasing the drive frequency would increase the mass range, but both involve complex changes to the ion trap electronics. Reducing the radius of the electrodes has been demonstrated to increase the mass range to 2500 amu on a half size trap. [27] However, this involves building a new trap and this smaller traps are more susceptible to 'space charge'. By far the easiest way is to change q_{ej}. By using the resonance ejection technique to apply a frequency $<\Omega/2$, then ions will resonate through their secular frequency with the applied voltage at $\beta_z<1$ (equation 1.9). They will therefore be ejected earlier in the

scan cycle, effectively increasing the m/z_{max}. Ions upwards of 45,000 amu (from an external Cs^+ ion source) have been detected using this method. [28]

Decreasing the rate at which the drive voltage is increased during the mass selective instability scan can greatly enhance the resolution of the ion trap. Halving the scan speed in conjunction with resonance ejection can lead to an approximately doubling of the resolution. Very low scan speeds have produced some extremely high resolutions, over 10^7 FWHH at m/z 602. [29] However at these scan speeds the resolution is not very robust as it is extremely sensitive to trapping conditions such as space charge and helium pressure.

1.4.4 Ion Trap Chemical Ionisation

In ion-trap chemical ionisation (CI), the CI reagent gas is present at much lower pressure than in a conventional CI source, typically $1x10^{-6}$ Torr compared to $1x10^{-4}$ Torr. Primary ions are produced by EI of the CI reagent gas, and allowed to undergo ion-molecule reactions for upwards of 50 ms to produce secondary reagent ions (section 1.3.2). The chosen reagent ions are then isolated from other m/z ions, usually by the application of the appropriate RF/DC voltages to place the working point of the ions at the apex of the stability diagram (section 1.5.2). Another reaction period, typically 20-100 ms, allows the isolated reagent ions to ionise analyte molecules present in the trap. A mass selective instability scan then ejects the stored ions and a CI mass spectrum is recorded. [30, 31] These normally consist of

$[M+H]^+$ ions as adduct ions such as $[M+NH_4]^+$ present in conventional, high pressure CI, are less efficiently collisionally stabilised at the much lower pressures of ion trap CI and tend to dissociate. A CI scan routine is shown in Figure 1.12.

Ion trap CI has some important advantages over beam instruments. Firstly, because of the similar pressure regimes for EI and CI, no instrument down time is incurred whilst changing between the two. Secondly, reagent ions are isolated before analyte ionisation, therefore processes which compete with a desired ionisation reaction (such as proton transfer or charge transfer reactions) are suppressed. [6] This ion isolation allows specific ion-molecule reactions to be studied without interfering reactions taking place. This makes it a suitable device for studying selective gas phase ion molecule reactions. Several studies of such reactions [32] including some of analytical importance as a means of differentiating isomeric species, [33] locating the positions of double bonds [34] and of identifying ions containing certain functional groups [35] have been reported in an ion trap. Thirdly, it is possible to couple EI and CI or other scan routines together to collect several types of spectra in alternate scans, without the need to remove the reagent gas during the EI scan, a technique known as 'multiple-scan monitoring'.

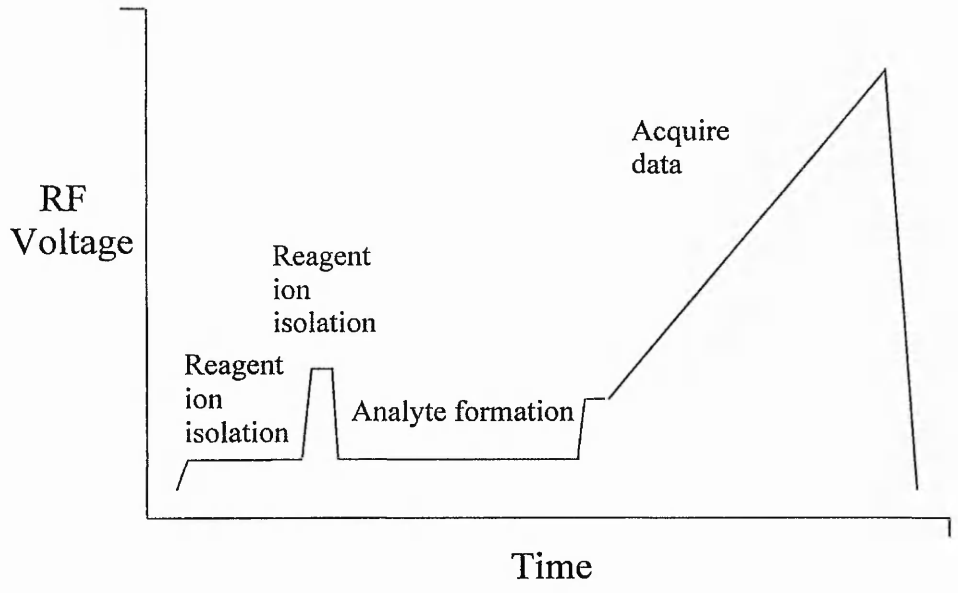

Figure 1.12. An ion trap CI scan routine

The CI gas present does not interfere with the EI routine, as during the EI period the RF voltage is set high enough to place the CI primary ions below the low mass cut-off and thus eject them. The only disadvantage of CI in the ion trap is that electron capture-negative ionisation cannot be performed efficiently unless a differentially pumped external source is used. This is because a high pressure of a moderating gas is needed to produce a large enough population of thermal electrons.

1.5 DETECTORS

No information could be gained from sources or analysers without a suitable detector being available. Here the ion current (typically 10^{-9} to 10^{-18} A) is amplified

and quantified. By far the most common detector in use today is the electron multiplier. There are two alternative designs, the discrete stage and the continuous channel (channeltron) multiplier. In the discrete stage device, shown in Figure 1.13, ions impinge upon a Be-Cu alloy plate, or dynode which cause a shower of electrons to be produced. These electrons impinge on a second dynode and produce yet more electrons. The process is repeated up to twenty times, in a cascade effect, the gain of which can be 10^{-6}. The signal on the final collector plate is converted to a voltage and subsequently processed under computer control to give a mass spectrum.

The channeltron device operates by a similar principle but there are no separate dynodes, instead a curved glass or ceramic tube is internally coated with lead doped glass. This material is a good secondary electron emitter. These devices are somewhat smaller and cheaper than their discreet stage competitors.

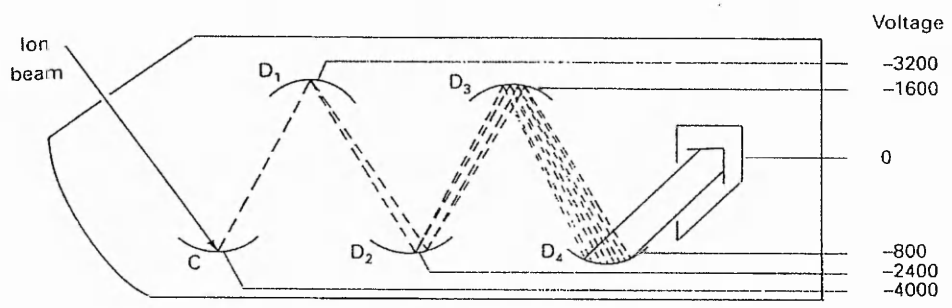

Figure 1.13. A discrete stage electron multiplier.

1.6 TANDEM MASS SPECTROMETRY

Many ionisation mechanisms are 'soft' techniques which impart little excess energy during ionisation and therefore few or no fragment ions are formed. The observation of a peak in a m/z spectrum does not of itself define any structural information. Accurate mass measurements may enable an empirical formula to be determined for the species but does not of itself, confirm a structure. The technique of tandem mass spectrometry (or mass spectrometry-mass spectrometry, MS/MS or MS^n) can be used to overcome this lack of structural information. [36, 37] Also, if complex mixtures are analysed, many different ions will be observed and the assignment of each component becomes difficult. In situations like this, tandem mass spectrometry can allow identification of each component. MS/MS may be defined as a procedure involving more than one stage of mass spectrometric analysis. The most common process, known as a product ion scan, is the dissociation of a preselected ion, known as the precursor ion, from a primary mass spectrum in the reaction region, to form product ions which are scanned in the second mass spectrometer to give a MS/MS spectrum. This is shown schematically in Figure 1.14. The precursor ion is not necessarily the molecular ion of the compound in question and may be a fragment ion produced in the initial ionisation process. Other scan types are possible, these include the precursor ion scan, where all ions formed during ionisation are fragmented sequentially and just one product m/z value is monitored. Therefore all ions that lose a specific fragment are detected. The constant neutral loss is another common scan, where both

spectrometers are scanned with a specific m/z difference between ions transmitted by the first and second analysers. Therefore all ions that lose a specific fragment are measured.

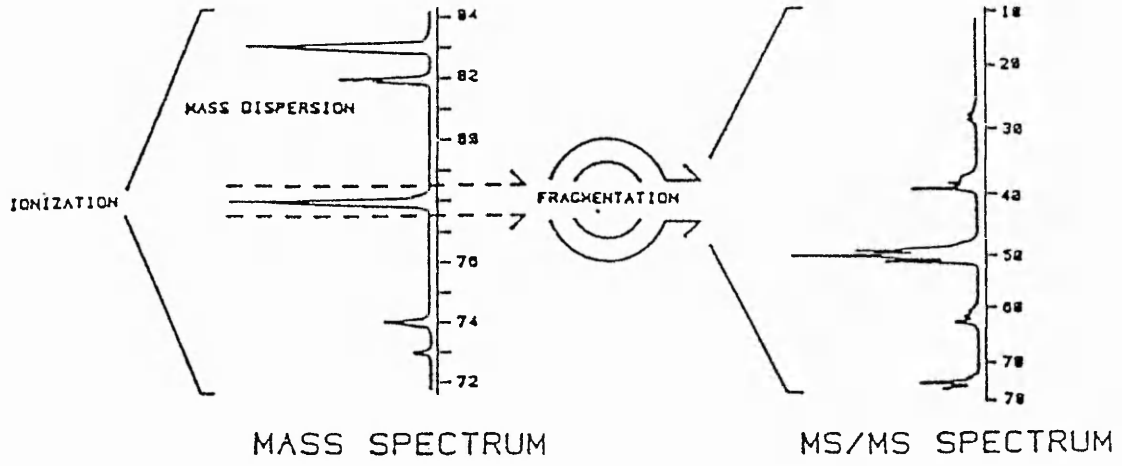

Figure 1.14. Schematic representation of a tandem mass spectrometry experiment

Precursor ions can be allowed to interact collisionally with light gases (collision-induced / activated-decomposition CID / CAD), [38] bombarded with photons (photodissociation, PD), [39] directed onto surfaces (SID) [40] or impacted with electrons (EID) [41] in order to fragment them. The most common ion dissociation method is CAD were light gases such as helium or other noble gases are used. It has been extensively studied [42] and is believed to follow a two step process. Upon collision with a neutral gas molecule, translational energy is transferred to the ion causing it to gain internal energy and become excited (activated). Energy transfer to the ion can be distributed in a variety of ways. Some of the transferred energy will

remain as translational (involved in direction changes, scattering etc.), whilst some will be distributed into the vibrational modes of the chemical bonds of the ion. If the energy transfer to the latter is sufficient then the ion will undergo unimolecular fragmentation. The level of internal energy deposition depends on the translational energy of the precursor ion, which will be in the low KeV range on sector machines, or in the low-to-mid eV range for quadrupole spectrometers. Nearly all mass analysers have been adapted for tandem operation, including multi-sector designs, time-of-flight instruments, ion-cyclotron-resonance (FTICR-MS) and hybrid machines. However only triple quadrupoles and ion traps will be described here.

1.6.1 Triple quadrupoles

One of the most widely used instruments for carrying out MS/MS experiments is the triple quadrupole, invented by Yost and Enke in 1978. [43] It is a QqQ device where Q denotes a quadrupole acting in the mass-selective-stability mode and q donates a RF-only quadrupole which will transmit all ions down to a low mass cut off. A schematic of a triple quadrupole mass spectrometer is shown in Figure 1.15. The first quadrupole, Q1 is used for precursor mass selection, ions of a particular m/z ratio are transmitted into the collision cell q which is filled usually with helium or argon. The products of decomposition are analysed by Q3. The collision energy for CAD is selected by varying the potential between Q1 and Q2 and the range available is usually of the order of 0-100 eV.

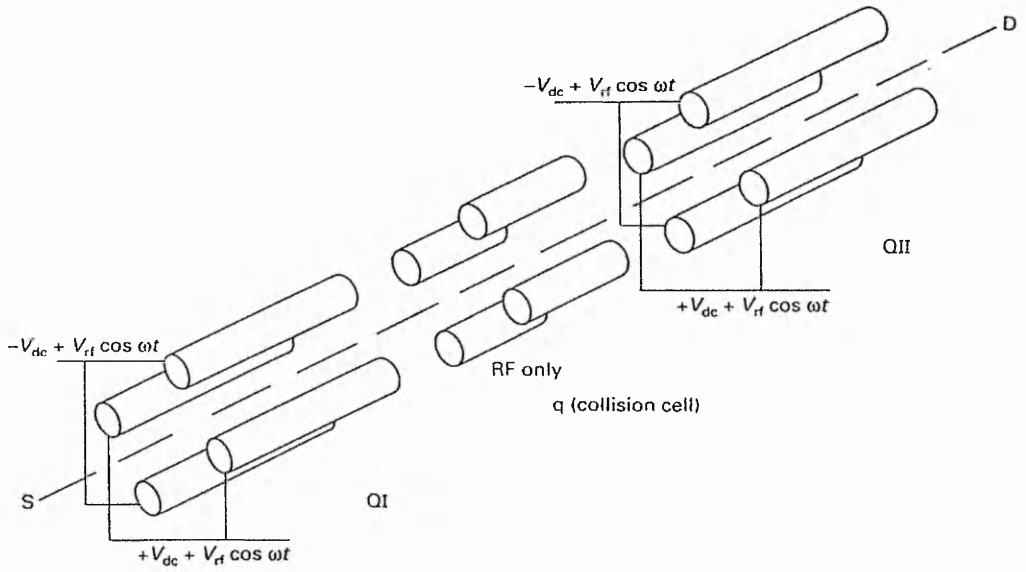

Figure 1.15. Arrangement in triple quadrupole systems. S = source and D = detector

1.6.2 Ion trap tandem mass spectrometers

Unlike conventional mass spectrometers where precursor ion isolation, fragmentation and product ion separation take place in different regions of the spectrometer, in the ion trap all these processes occur in the same region of space and the multiple mass spectrometry is distributed in time. [44, 45] This has led to the definition 'tandem-in-time' rather than 'tandem-in-space'. Therefore multiple stages of tandem mass spectrometry (MS^n) may be performed without spectrometers being connected together, with all the expense with which that infers.

There are several ion isolation methods available, shown diagramatically in Figure 1.16. Apex isolation [46] (Fig.1.16a) involves application of the appropriate RF and DC voltages to the ring electrode in order to move the working point of the ion of interest to the upper apex of the stability diagram. Ions of higher and lower masses become simultaneously unstable. Two-step DC isolation [47] (Fig.1.16b) is a similar technique, however ejection is achieved consecutively. Ejection of low masses is achieved by moving the ion of interest to a q_z of 0.85 followed by the application of a suitable negative DC pulse. The RF is then decreased so that the parent ion is placed at a q_z of 0.5 and then a positive DC pulse is applied to eject all ions of greater mass. The resonance hole technique [48] (Fig.1.16c) makes use of a low voltage auxiliary RF frequency applied to the end caps, the application of this auxiliary RF of chosen frequency places a 'resonance hole' along the a = 0 line. After the drive RF voltage applied to the ring electrode is ramped to remove ions of lower m/z ratio than that of the selected ion species. The drive RF voltage is then decreased to bring the ions of higher mass than the selected ion species sequentially into resonance with this auxiliary RF voltage. These ions rapidly become excited in the axial direction and are ejected from the trap. Very efficient isolation is possible using this method and no excitation of the isolated ion species occurs. A much quicker and easier method of ion isolation has recently been developed using a broad band frequency generator (Fig.1.16d). [49] Instead of one discrete axial frequency being applied to the end cap electrodes and ions successively being brought into resonance, a complex signal is applied having frequency components in resonance with all ions except the precursor ion. Thus all background ions are ejected simultaneously.

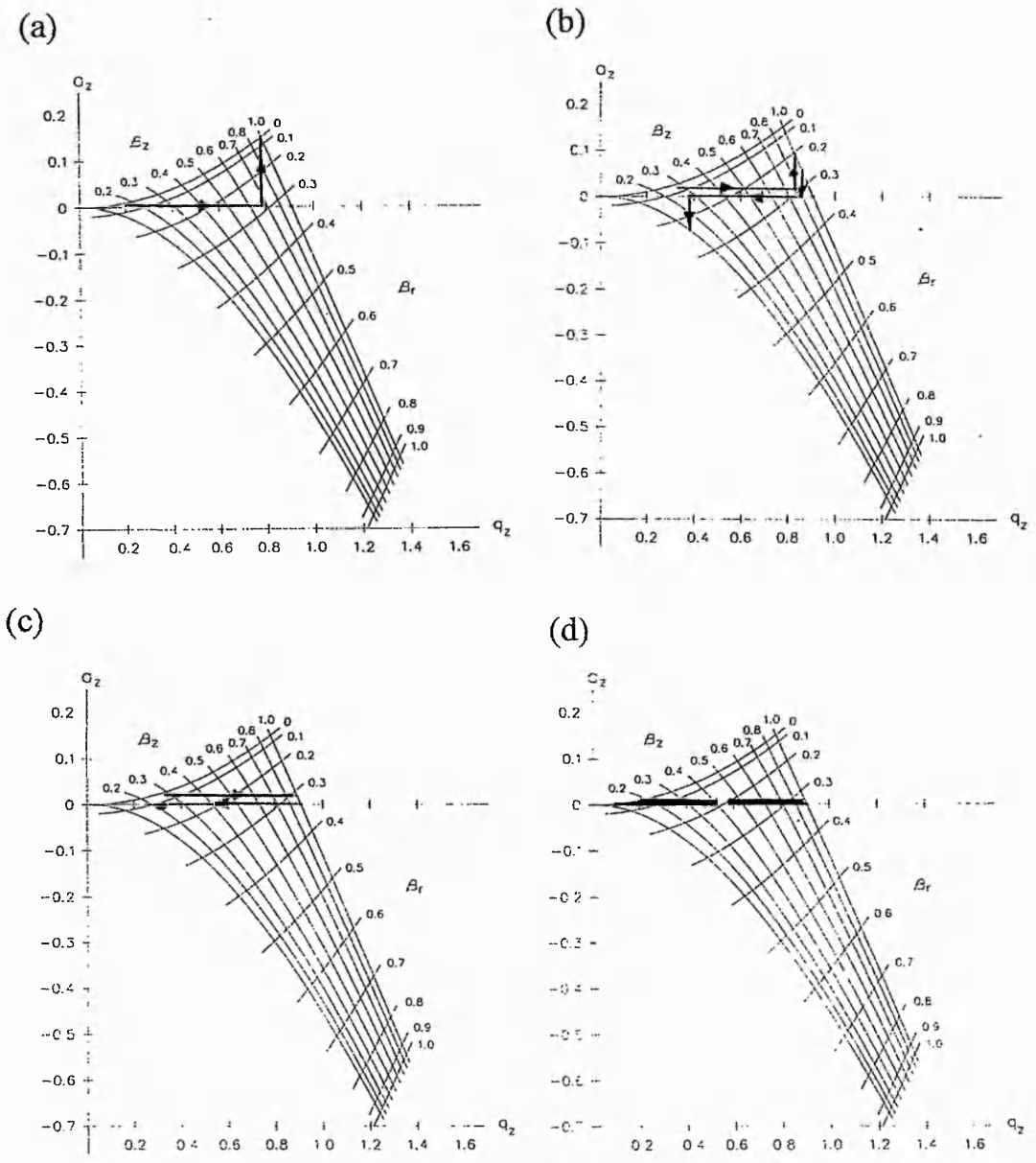

Figure 1.16. Illustration of the different isolation procedures, (a) apex, (b) two-step DC, (c) resonance hole and (d) filtered noise isolation

CAD is the most commonly used dissociation method used for ion trap tandem mass spectrometry. Figure 1.17 shows a typical ion trap MS/MS scan function. After parent ion isolation, fragmentation *via* CAD is usually achieved by applying a

small RF 'tickle' voltage across the end cap electrodes, at a frequency corresponding to the axial secular frequency of the precursor ion. This has the effect of moving the working point of the ions away from the centre of the trap to positions of high drive RF potential, where they acquire kinetic energy.

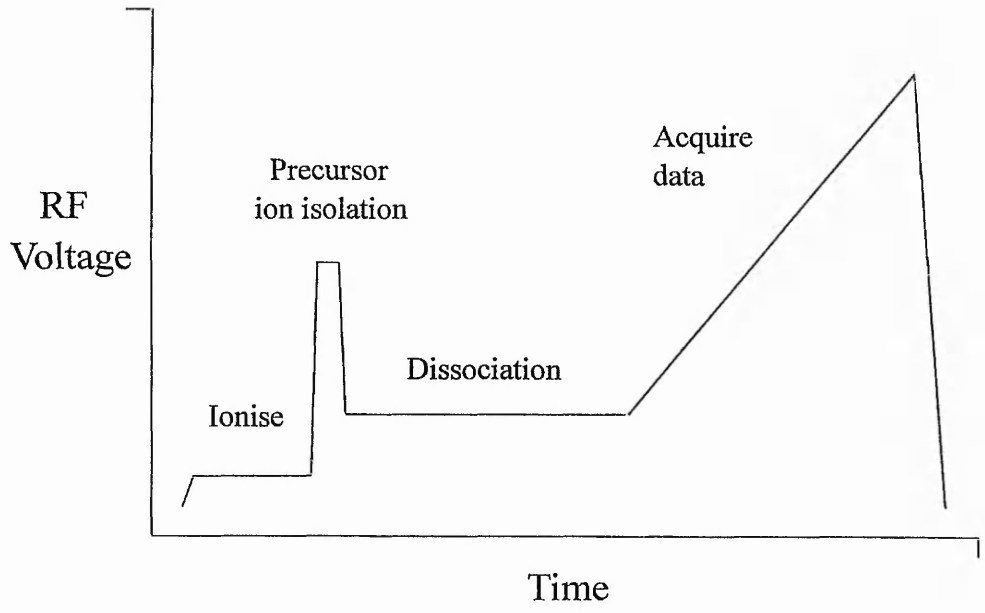

Figure 1.17. A typical ion trap MS/MS scan function

Following collisions with the helium buffer gas this kinetic energy can be converted to internal energy and dissociation may occur. The tickle signal can be applied for several milliseconds, so that each ion will undergo a large number of collisions. The dissociation products from the multiple events are accumulated in the trap and consequently high fragmentation efficiencies are possible, with values up to 100 % being reported. [50] Multiple tandem experiments (MS^n) are possible by

isolating selected product ions and dissociating them in turn to yield lower mass fragments. The current record is MS^{12}. [51]

Disadvantages of ion trap MS/MS are the difficulty of performing parent or neutral loss scan types, [52] the low energy of the CAD process (<6 eV) and the careful tuning of the applied tickle frequency which is necessary. However the last two have been the subject of much recent research. The secular frequency of a trapped ion is affected by the amount of space charge present. Therefore a MS/MS scan routine optimised at one concentration may not produce exactly the same fragmentation at another concentration if the parent ion is not completely in resonance with the applied tickle frequency. This is a particular problem with GC MS/MS where the secular frequency of the parent ion will change over the elution of a chromatographic peak. This can be overcome by varying slightly the drive RF over the tickle time to ensure that the parent ion comes into resonance, [53] applying a narrow range of frequencies rather than a discrete frequency [54] and also application of random noise to resonate all frequencies. [55] However with this last method the initial isolation step must be efficient. Non-resonant excitation is also possible by applying short DC pulses [56] to the end cap electrodes. This moves all ions away from the centre of the trap to regions of high RF potential and need little precise tuning. This leads to higher energy collisions than resonant excitation, upwards of 13 eV.

Boundary activated dissociation (BAD) is another fragmentation technique that needs no careful tuning for reproducible spectra and has received considerable

attention recently. [57,58] In this method, by application of the appropriate RF / DC voltages, the parent ions are held at a working point on the $\beta_z = 0$ boundary of the stability diagram, at a q_z value in the region of 0.3-0.5, for 10-100 ms. The ions 'pick-up' kinetic energy from the drive RF and subsequently fragments.

1.7 CHROMATOGRAPHIC SEPARATION

Chromatography covers a range of techniques capable of analysing nearly every type of molecule, but all methods are based on one principle: the separation of chemical mixtures into their individual components by reversible interactions with two phases, one stationary the other mobile.

1.7.1 Gas Chromatography

Gas chromatography (GC) was developed as a means of separating volatile organic mixtures. [59, 60] Components of a mixture are separated by partition between an inert carrier gas which serves as the mobile phase and a liquid stationary phase, which is chemically bonded or adsorbed onto a solid support. Different compounds travelling down a chromatographic column will spend different proportions of time dissolved in the mobile and stationary phases. This can be quantified by the partition co-efficient, K:

$$K = \frac{C_s}{C_m} \tag{1.13}$$

where C_s and C_m are the concentrations of analyte in the stationary and mobile phase respectively, and the phase ratio, β, of a column:

$$\beta = \frac{V_m}{V_s} \tag{1.14}$$

where V_m and V_s are the mobile and stationary volumes. Combining these equations gives the capacity factor, k', a measure of the amount of solute in each phase and hence of the time spent in each:

$$k' = \frac{C_s V_s}{C_m V_m} = \frac{K}{\beta} \tag{1.15}$$

The capacity factor is specific to a single solute in a given chromatographic systems and can be calculated by measuring the retention times of two solutes, one retained (t_r) and the other unretained (t_m).

$$k' = \frac{t_r - t_m}{t_m} \tag{1.16}$$

The selectivity factor, α, measures the relative time gap between one eluent (1) and another, later, eluent (2).

$$\alpha = \frac{t'_{R2}}{t'_{R1}} = \frac{k'_2}{k'_1} = \frac{K_2}{K_1} \qquad (1.17)$$

where t'_R is the adjusted retention time, $t_r - t_m$.

Since the introduction of capillary columns, with a gas flow of 1 to 2 ml min^{-1}, the direct coupling of GC and MS has been possible and has proved to be a powerful analytical combination.

Samples suitable for GC introduction must be volatile and thermally stable, or they will either be irreversibly bonded to the column or be degraded at the high temperature of the injector and column oven. It is possible to increase the volatility of analytes by derivatisation reactions and this is a common procedure for compounds containing one or more OH, SH, NH or COOH groups. For analysis, a small volume of the sample (0.1 - 3 μl) is injected into a heated sample port, into which the column is fitted. Levels of analyte up to 1μg may be used, depending on the internal diameter of the column. The volatilised sample passes from the injector onto the column, separation is achieved (although a suitable choice of stationary phases must be made) and then each component passes to the ion source to be ionised. The column is situated in a temperature controlled oven and samples may be eluted isothermally or, more often, by using a temperature programme. A schematic of a GC is shown in Figure 1.18. For a programmed analysis the oven temperature is initially low and then increased at a controlled rate to minimise the

run time whilst maintaining a good separation. Detection limits in the fg and pg range may be achieved using GC-MS.

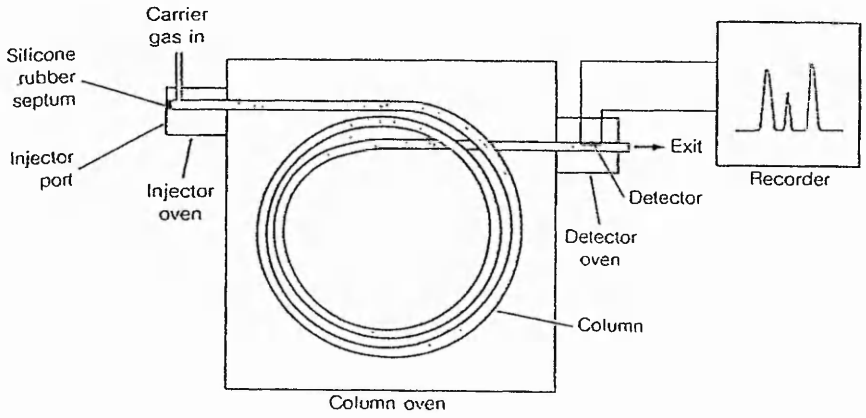

Figure 1.18. A GC schematic

1.8 REFERENCES

1. Thompson, J.J., *Rays of positive electricity and their application to chemical analyses, Longman Green and Co. Ltd.*, London (1913)

2. Burlingame, A.L., Boyd, R.K. and Gaskell, S.J., *Anal. Chem.* 634R-683R, **66** (1994)

3. Dempster, A.J., *Phys. Rev.*, 415, **18** (1921)

4 . Munson, M.S.B. and Field F.H., *J. Am. Chem. Soc.*, 2621, **88** (1966)

5. Speir, J.P., Gorman, G.S., Cornett, D.S. and Amster, I.J., Anal. Chem., 65, **63** (1991)

6. Creaser, C.S., Krokos, F., O'Neil, K.E., Smith, M.J.C. and McDowell, P.G., *J. Am. Soc. Mass Spectrom.*, 322, **4** (1993)

7. Dougherty, R.C., Daulton, J., Biros, F.J., *Org. Mass Spectrom.* 1171, **6** (1972)

8. Dougherty, R.C., *Anal. Chem.* 625A, **53** (1981)

9. Barber, M., Bordoli, R.S., Sedgewick, R.D. and Tyler, A.N., *J. Chem. Soc. Chem. Comm.*, 325, 7 (1981)

10. Behrisch, R. and Spinger, V., '*Sputtering by Particle Bombardment I. Springer Series Topics in Applied Physics*', **47** (1981)

11. Ehring, H., Karas, M. and Hillenkamp, F., *Org. Mass Spectrom.*, 472, **27** (1992)

12. Karas, M. and Hillenkamp, F., *Anal. Chem.*, 2299, **60** (1988)

13. Tanaka, K., Waki, H., Ido, Y., Akita, S., Yoshido, Y. and Yoshido, T., *Rapid Commun. Mass Spectrom.*, 151, **2** (1988)

14 . Overberg, A., Karas, M. and Hillenkamp, F., *Rapid Commun. Mass Spectrom.*, 128, **5** (1990)

15. Paul, W. and Steinwedel, H., *German Patent no.* 944,900 (1956)

16. Paul, W. and Steinwedel, H., *U.S. Patent no.* 2,939,952 (1960)

17. Mathieu, E., *J. Math. Pures. Appl.* (J. Liouville), 137, **13** (1868)

18. Wuerker, R.F., Shelton, H. and Langmuir, J., *J. Appl. Phys.*, 342, **30** (1959)

19. Rettinghaus, V. von G., *Z. Agnew. Phys.*, 321, **22** (1967)

20. Dawson, P.H., Whetten, N.R., *US Patent no.* 3,527,939, (1970)

21. Kelly, P.E., Stafford, G. C. Jr and Stephens, D.R., *U.S. Patent no.* 4,540,884 (1985)

22. Cooks, R.G., Glish, G.L., McLuckey, S.A. and Kaiser, R.E., *Chem. Eng. News*, 26, **69** (1991)

23. Todd, J.F.J., *Mass Spectrom. Rev.*, 3, **10** (1991)

24. March, R.E., Hughes, R.J., *Quadrupole Storage Mass Spectrometry*, J. Wiley & Sons, New York (1989)

25. Franzen, J., *Int. J. Mass Spectrom. Ion Phys.*, 63, **106** (1991)

26. Weber-Grabau, M., Kelly, P.E., Bradshaw, S.C. and Hoekman, D.J., *presented at the 36th annual meeting of the ASMS*, San Fransico, CA, USA (1988)

27. Kaiser, R.E., Cooks, R.G., Moss, J. and Hemberger, P.H., *Rapid Commun. Mass Spectrom.*, 50, **3** (1989)

28. Kaiser, R.E., Cooks, R.G., Stafford, G.C., Syka, J.E.P. and Hemberger, P.H., *Int. J. Mass Spectrom. Ion Proc.*, 79, **106** (1991)

29. Londry, F.A., Wells, G. J. and March, R.E., *Rapid Commun. Mass Spectrom.*, 43, 7 (1993)

30. Berberich, D.W., Hail, M.E., Johnson, J.V. and Yost, R.A., *Int. J. Mass Spectrom. Ion Proc.*, 115, **94** (1989)

31. Strife, R.J. and Keller, P.R., *Org. Mass Spectrom.*, 201, **24** (1989)

32. (a) Nourse, B.D., Cox, K.A. and Cooks, R.G., *Org. Mass Spectrom.*, 453, **27** (1992). (b) Donovan, T., Liou, C.C. and Brodbelt, J., *J. Am. Soc. Mass Spectrom.*, 39, **3** (1992). (c) Moini, M., *J. Am. Soc. Mass Spectrom.*, 631, **3** (1992). (d) Brodbelt, J. and Cooks, R.G., *Anal. Chim. Acta.*, 239, **206** (1988)

33. (a) Kascheres, C. and Cooks, R.G., *Anal. Chim. Acta.*, 223, **215** (1988) (b) Hart, K.J., McLuckey, S.A. and Glish, G.L., *J. Am. Soc. Mass Spectrom.*, 680, **3** (1992). (c) Glish, G.L., *Analyst*, 533, **119** (1994)

34. Einhorn, J., Kenttamaa, H.I. and Cooks, R.G., *J. Am. Soc. Mass Spectrom.*, 305, **2** (1991)

35. McCarley, T.D. and Brodbelt, J., *Anal. Chem.*, 2380, **65** (1993)

36. McLafferty, F.W., *Tandem Mass Spectrometry*, Wiley, New York (1983)

37. Busch, K.L., Glish, G.L. and McLuckey, S.A., *Mass Spectrometry /Mass Spectrometry: techniques and applications in tandem mass spectrometry*, VCH, New York (1988)

38. Yost, R.A., Enke, C.G., *Anal. Chem.*, 1251A, **51** (1979)

39. Louris, J.N., Brodbelt, J.S. and Cooks, R.G., *Int. J. Mass Spectrom. Ion Proc.*, 345, **75** (1987)

40. Mabud, M.A., DeKrey, M.J. and Cooks, R.G., *Int. J. Mass Spectrom. Ion Proc.*, 285, **67** (1985)

41. Cody, R.B. and Freiser, B.S., *Anal Chem.*, 547, **51** (1979)

42. Shukla, A.K. and Futrell, J.H., *Mass Spec. Rev.*, 211, **12** (1993)

43. Yost, R.A. and Enke, C.G., *J. Am. Chem. Soc.*, 2274, **100** (1978)

44. Louris, J.N., Cooks, R.G., Syka, J.E.P., Kelly, P.E., Stafford, G.C. and Todd, J.F.J., *Anal. Chem.*, 1677, **59** (1987)

45. Glish, G.L., McLuckey, S.A., and van Berkel, G.J., *Int. J. Mass Spectrom. Ion. Proc.*, 213, **106** (1991)

46. Weber-Grabau, M., Kelley, P.E., Syka, J.E.P., Bradshaw, S.C. and Brodbelt, J.S., *presented at the 35th annual meeting of the American Society for Mass Spectrometry*, Denver, Co, USA (1987)

47.Ardanaz, C.E., Traldi, P., Vettori, U., Kavka, J. and Guildugli, F., *Rapid Comm. Mass Spectrom.*, 5, **5** (1991)

48. Kelley, P.E., Syka, J.E.P., Ceja, P.C., Stafford, G.C., Louris, J.N., Grutzmacher, H.F., Kuck, D. and Todd, J.F.J., *presented at the 34th annual meeting of the American Society for Mass Spectrometry*, Cinncinatti, OH, USA (1986)

49. K. G. Asano, D. E. Goeringer, S. A. McLuckey, D. Hoekman, S. W. Stiller, *Proceedings of the 41st ASMS*, San Francisco, 1993, p 700a.

50. Johnson, J.V., Yost, R.A., Kelly, P.E. and Bradford, D.C., *Anal. Chem.*, 2162, **62** (1990)

51. Louris, J.N., Brodbelt-Lustig, J.S., Cooks, R.G., Glish, G.L., McLuckey, S.A. and van Berkel, G.J., *Int. J. Mass Spectrom. Ion Proc.*, 117, **96** (1990)

52. Todd, J.F.J., Penman, A.D., Thorner, D.A. and Smith, R.D., *Rapid Commun. Mass Spectrom.*, 108, **4** (1990)

53. Shaffer, B.A., Karnicky, J. and Butrill, S.E., *presented at the 41st annual meeting of the American Society for Mass Spectrometry*, San Fransisco, CA, USA (1993)

54. Julian, R.K.Jr. and Cooks, R.G., *Anal. Chem.*, 1827, **65** (1993)

55. McLuckey, S.A., Goeringer, D.E. and Glish, G.L., *Anal. Chem.*, 1455, **64** (1992)

56. Lammert, S.A., and Cooks, R.G., *J. Am. Soc. Mass Spectrom.*, 487, **2** (1991)

57. Curcuruto, O., Fontana, S., Traldi, P. and Celon, E., *Org. Mass Spectrom.*, 322, **27** (1992)

58. Creaser, C.S. and O'Neil, K.E., *Org. Mass Spectrom.*, 564, **28** (1993)

59. James, A.T., Martin, A.J.P., *Biochem. J.*, 679, **50** (1952)

60. James, A.T., Martin, A.J.P., *Analyst*, 915, **77** (1952)

CHAPTER 2

SELECTIVE CHEMICAL IONISATION REACTIONS OF THE BENZOYL CATION WITH COMPOUNDS CONTAINING A HYDROXY FUNCTIONAL GROUP.

2.1 INTRODUCTION

Gas phase ion-molecule reactions of the benzoyl cation have been the subject of a small number of studies. Reactions in the pressure and time regimes of the mass spectrometer using FT-ICR and quadrupole instruments have been reported for simple amines, [1] ammonia, [2] dienes, [3] and 1,3-dioxolanes. [4] The chemistry of the benzoyl ion has also been studied in the 90-650 torr pressure range for reaction periods of 15-20 months. In these experiments, the reactant ion was generated by β decay of [1,4-T_2]benzene in the presence of a large excess of carbon monoxide and neutral products were identified by radio GC and HPLC. [5, 6] The benzoyl ion has been characterised through these reactions as a mild, selective electrophile, preferring n-type nucleophile centres on the substrate rather than π-type centres, which undergoes benzoylation of phenol, aniline and anisole. [7] NMR studies on substituted benzoyl cations [8, 9, 10] have shown that electron donating substituents such as OCH_3 and CH_3 increase charge delocalisation into the aryl ring, whilst electron withdrawing groups such as F and CF_3 have the opposite effect, increasing the electrophilic nature of the benzoyl cation.

Reactions involving hydroxyl functional groups have been reported for the gas-phase nitrosonium ion, NO^+, [11] the trimethylsilyl ion, $(Me)_3Si^+$, [12, 13] the boron containing cations, $[MeOBOMe]^+$ and $[MeBMe]^+$, [14] and the dimethyl ether derived ion, $[MeOCH_2]^+$. [15] However, the selectivity of all these ions for hydroxy

groups is limited by their reactivity towards a variety of other functional groups, such as ketones, ethers and carboxylic acids.[16, 17, 18] This chapter, [19, 20] describes an ion trap mass spectrometric study of the selectivity of the ion-molecule reactions of benzoyl ions of the type $[C_6X_5CO]^+$, (X= H, F, 4-Me, 3,5-di-Bu^t) with hydroxy and other functional groups. The influence of experimental conditions such as helium buffer gas pressure and the ion trap q_z parameter on benzoyl ion reactivity have also been investigated.

2.2 EXPERIMENTAL

Experiments were performed using a quadrupole ion trap mass spectrometer (Finnigan MAT ITMS, San Jose, CA), operated at 120 °C. All chemicals were obtained from Aldrich Chemical Co. (Dorset, UK), except tert-butyl benzoate (TCI, Japan), and used without further purification. Liquid samples were introduced *via* a leak valve (Megg itt Avionics, Portsmouth, UK) and solid samples on a solids probe.

In a typical experiment, the benzoyl ion was generated as an electron ionisation fragment of acetophenone, isolated using resonance hole isolation, [21] and allowed to react with neutral sample vapour for 10 - 110 ms. Reaction times were varied using key sequences [22] to automatically increase the reaction time. Total reaction times were calculated from the end of the benzoyl ion isolation period, taking into account electron multiplier warm-up and the time taken to eject the benzoyl ion.

For ions lighter than the benzoyl ion, the total reaction time was calculated up to the time taken to eject those ions. Slight changes to the ionisation time were needed to ensure similar initial benzoyl ion intensities were present at the different q_z values of 0.17, 0.43, 0.86.

Pulsed valve introduction of reagent was carried out using a automobile fuel injector (Bosch, part no. 02EAC 4866). This was modified by first removing the two plastic inlet / outlet fittings. A male thread was machined onto the steel inlet of the valve to allow a stainless steel vacuum-tight compression connector to be attached with a viton 'O' ring seal. A short piece of 1/8" o.d. (1/16" i.d.) stainless steel tubing was welded to this connector. The valve exterior was cleaned ultrasonically with a variety of analytical grade solvents and the interior was purged with the same solvents whilst the solenoid was pulsed to allow a few millilitres of liquid to pass through the valve. A simple power supply was designed and built to drive the valve, which is shown in Figure 1.1. For pulsed introduction of acetophenone, the pulsed valve was positioned inside the vacuum manifold, just above the ion trap, which was assembled without the teflon spacers between the ring and end cap electrodes to aid removal of the neutral acetophenone (Figure 1.2).

The $[C_6F_5CO]^+$ and $[4\text{-}MeC_6H_4CO]^+$ ions were generated as EI fragments from 2',3',4',5',6'-pentafluoroacetophenone and 4'-methylacetophenone respectively. $[3,5\text{-}di\text{-}(t\text{-}C_4H_9)C_6H_3CO]^+$ ion was generated as an ammonia CI fragment of

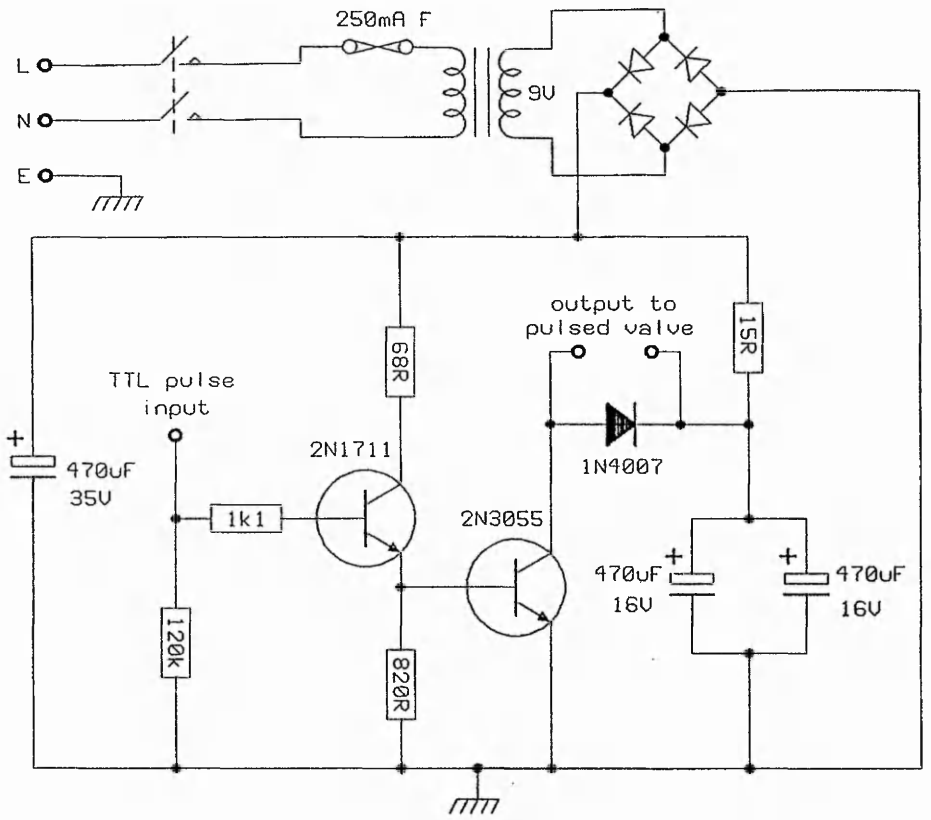

Figure 1.1. Pulsed-valve power supply

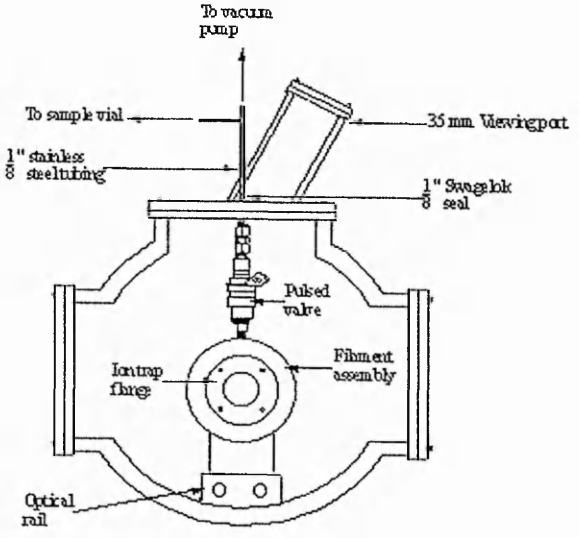

Figure 1.2. Pulsed valve schematic

3',5'-di-*tert*-butylbenzoic acid. Reagent pressure was $2x10^{-6}$ torr and sample pressures were typically 5×10^{-6} torr. Helium bath gas pressure was maintained at $1x10^{-4}$ torr (uncorrected). All pressures were measured by the ion trap vacuum chamber ion gauge.

Thermochemical data were taken from references 23 and 24 unless otherwise stated. Molecular modelling was carried out on a Silicon Graphics 4D35 Personal Iris machine using the VAMP programme (version 4.5), [25] with the PM3 hamiltonian,[26] using the 'PRECISE' keyword. Final geometries were characterised as true minima by the absence of negative eigenvalues in the Hessian matrix.

2.3 RESULTS AND DISCUSSION

A general scheme for the reaction of isolated benzoyl ions of the type $[C_6X_5CO]^+$ with hydroxy containing compounds in the quadrupole ion trap is shown in Scheme 2.1 (X=H). The three main products of the benzoylation reaction are the $[M+C_6X_5CO]^+$ adduct ion, $[M-OH]^+$ resulting from hydroxy abstraction and $[M-H]^+$ from hydride abstraction. The formation of adduct and hydroxy abstraction products is illustrated by the mass spectrum resulting from the reaction of $[C_6H_5CO]^+$ with 2-methylpropan-2-ol, (Figure 2.3a). The spectrum shows a strong $[M+105]^+$ adduct ion at m/z 179 (100 %) and a weak $[M-OH]^+$ ion at m/z 57 (4 %). These reaction pathways are shown in Scheme 2.2.

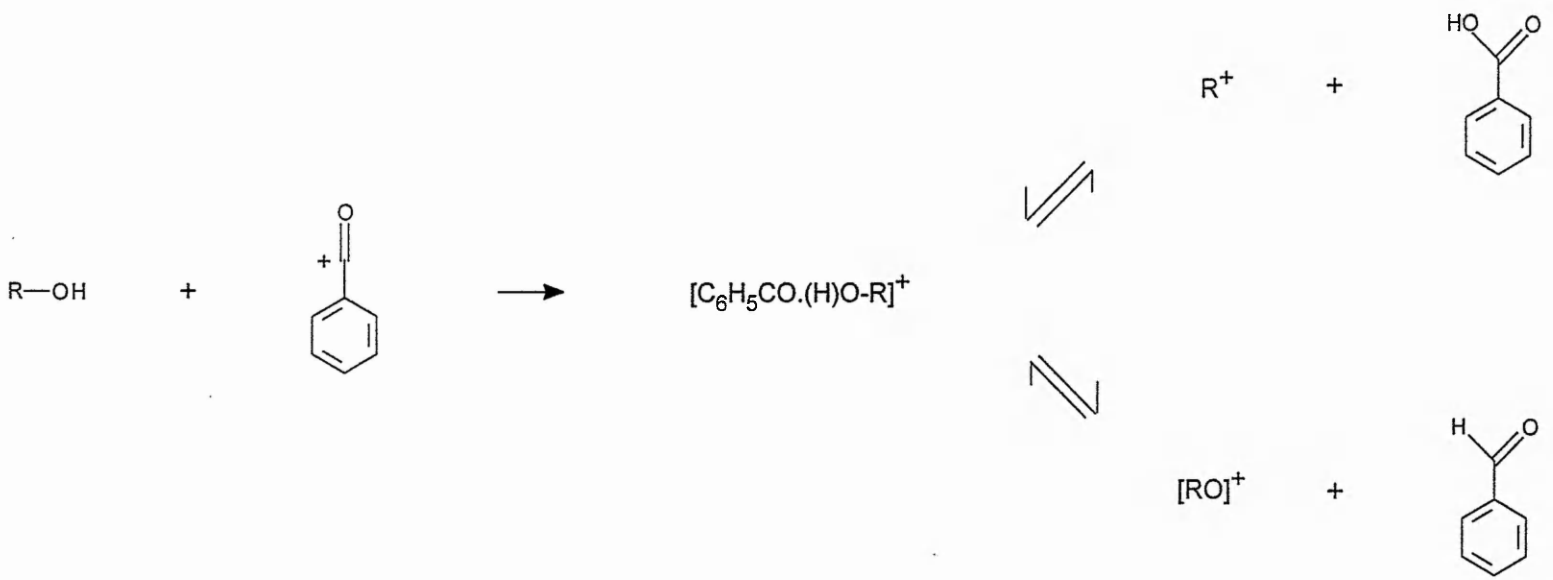

Scheme 2.1. The reaction of $[C_6H_5CO]^+$ with hydroxy containing compounds

A fragmentation product of the adduct, $[C_6H_5C(OH)_2]^+$, is observed at m/z 123 arising from loss of butene and this ion reacts further with water to yield the ion at m/z 141. The $[M\text{-}OH]^+$ ion forms an adduct with 2-methylpropan-2-ol, which dehydrates to form the $[C_8H_{17}]^+$ alkyl ion at m/z 113. These processes were confirmed by isolation of the $[M\text{-}OH]^+$ and $[C_6H_5C(OH)_2]^+$ ions, followed by reaction with the appropriate neutral. A protonated dimer ion of 2-methylpropan-2-ol is present in the spectrum at m/z 149, together with a product ion at m/z 93. The proton bound dimer ion has also been observed in an FT-ICR study of the proton transfer reactions of 2-methylpropan-2-ol. [27] The variation of product ion intensities for the reaction of the benzoyl ion with 2-methylpropan-2-ol over reaction times of up to 110 ms is shown in Figure 2.4.

A rapid decrease in $[C_6H_5CO]^+$ ion intensity occurs within the first 50 ms. The m/z 179 adduct ion intensity reaches a maximum during this period and then gradually decreases. There is no significant increase in fragment ion intensity to account for the loss the adduct ion, which may arise because of proton transfer to acetophenone, since the intensity of protonated acetophenone rapidly increases at longer reaction times. This explanation is supported by the observation that if the $[M+105]^+$ ion was isolated and held in the trap for a few milliseconds, protonated acetophenone (m/z 121) appeared in the spectrum. The $[M\text{-}OH]^+$ hydroxy abstraction ion (m/z 57) decreases over the reaction time since it reacts with 2-methylpropan-2-ol to produce m/z 113, which increases initially and then levels off at reaction times greater than 50 ms. The principal fragment ion (m/z 123)

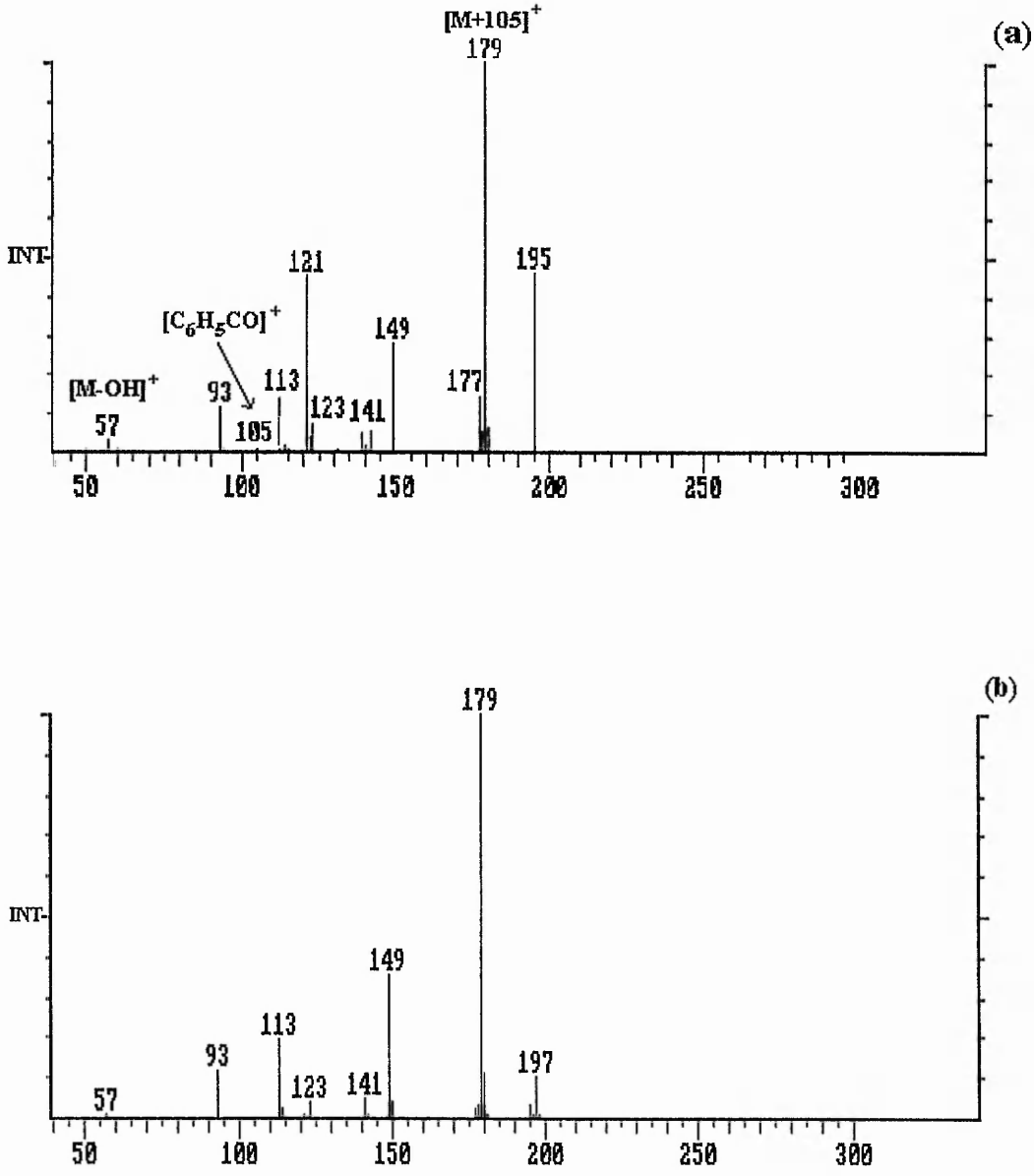

Figure 2.3. Reaction of $[C_6H_5CO]^+$ with 2-methylpropan-2-ol, without (a) and with (b) pulsed-valve introduction of acetophenone.

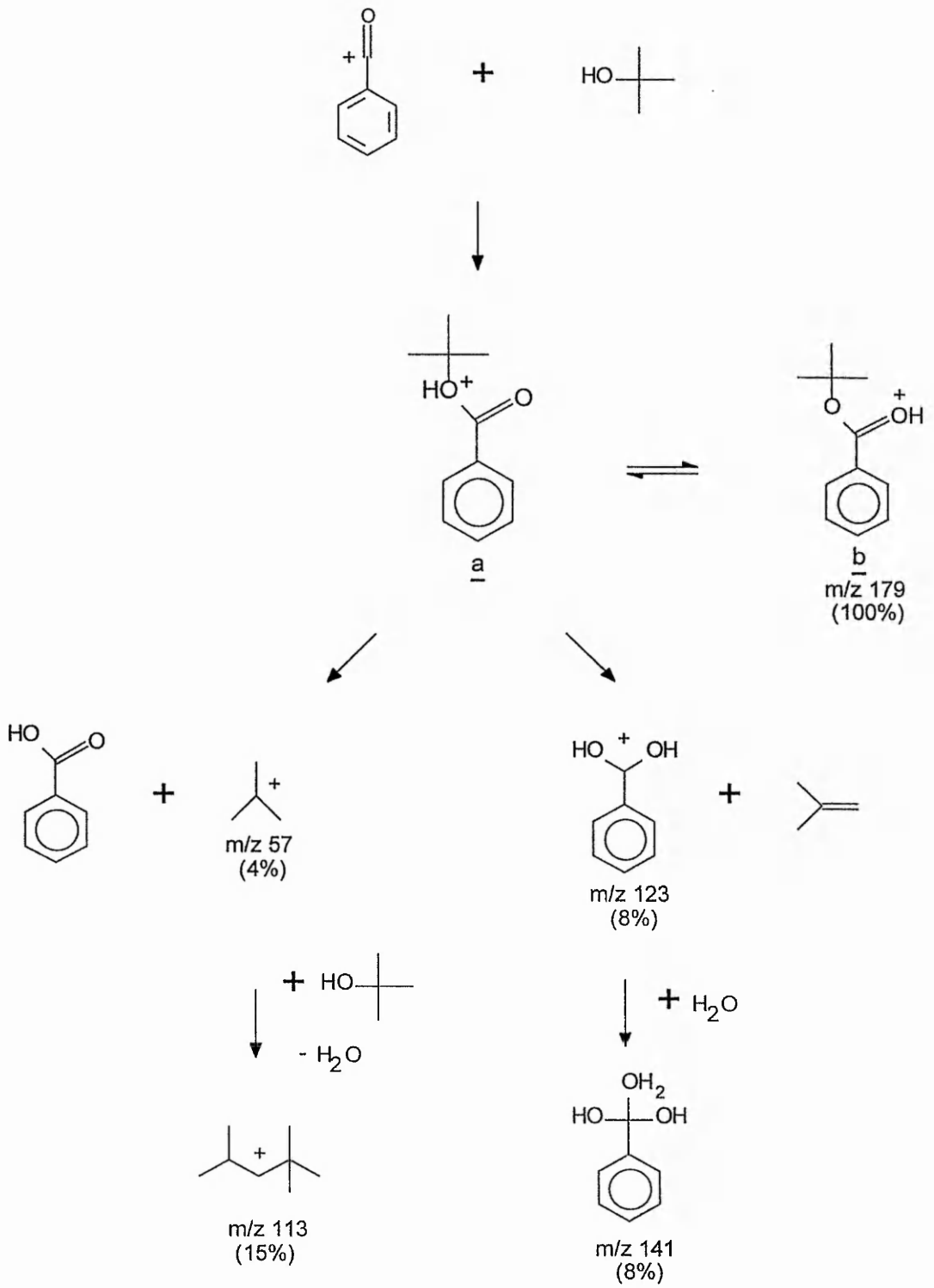

Scheme 2.2. Reaction pathway of $[C_6H_5CO]^+$ with 2-methylpropan-2-ol.

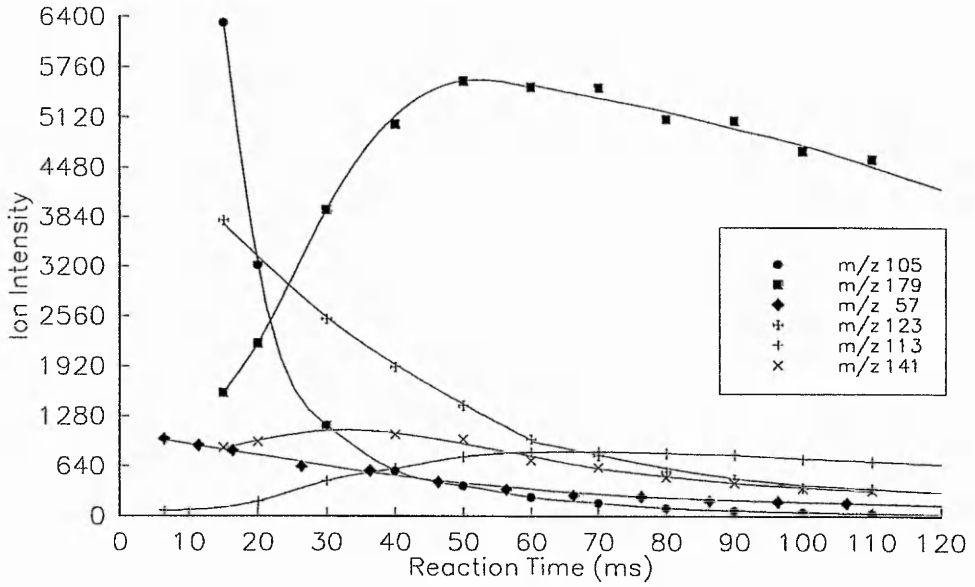

Figure 2.4. Ion intensity versus reaction time for the reaction of $[C_6H_5CO]^+$ with 2-methylpropan-2-ol

decreases throughout the reaction times, as does the product of its reaction with water, m/z 141, probably as a result of a deprotonation reaction with acetophenone.

Acetophenone, which is present in the trap as the precursor for the $[C_6H_5CO]^+$ ion, is readily protonated to form $[C_6H_5C(OH)Me]^+$ (m/z 121) and this ion undergoes competing reactions with 2-methylpropan-2-ol, leading to the formation of ions at m/z 195 (M+121), m/z 177 (M+121-H_2O) and m/z 139 (M+121-butene). The variation of the intensities of these ions over the 110 ms reaction time is shown in Figure 2.5 which illustrates the rapid increase in $[C_6H_5C(OH)Me]^+$ and $[M+121]^+$ ion intensities. The origin of these ions were confirmed by isolating the $[C_6H_5C(OH)Me]^+$ ion followed by a 100 ms reaction time which produced the

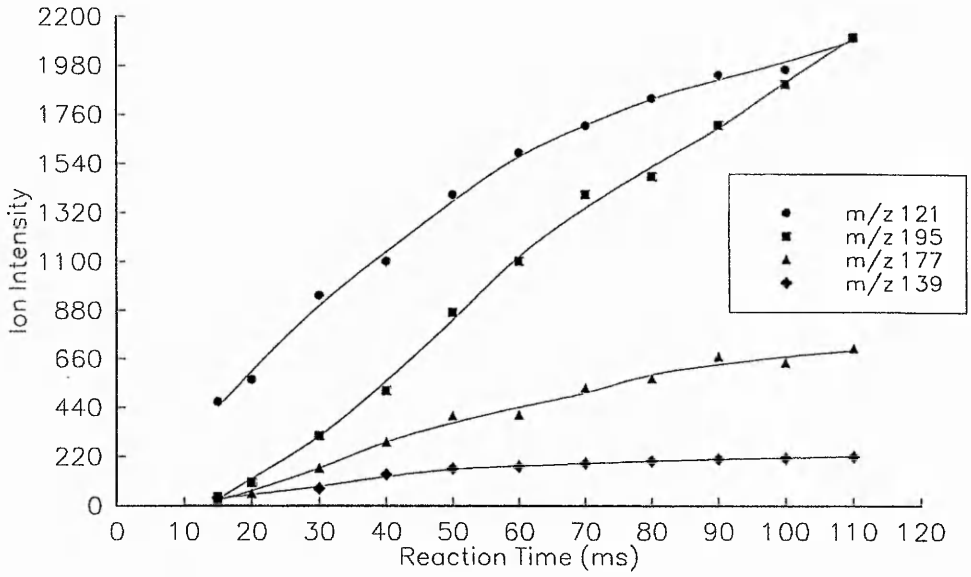

Figure 2.5. Ion intensity versus reaction time for the reaction of $[C_6H_5C(OH)Me]^+$ with 2-methylpropan-2-ol.

expected ions at m/z 195, m/z 177 and m/z 139. CAD of the isolated $[M+121]^+$ ion at m/z 195 also resulted in the formation of the m/z 177, m/z 139 and m/z 121 ions, illustrated in Figure 2.6. This reaction pathway is illustrated in Scheme 2.3.

Pulsed introduction of acetophenone into the quadrupole ion trap *via* a pulsed valve (5 ms wide band width) virtually eliminates these side reactions, since most of the neutral acetophenone is pumped away before the end of the benzoyl ion isolation period, allowing a clear distinction between product ions arising from protonated acetophenone and those from the benzoyl ion (Figure 2.3b). The time taken for the acetophenone to be removed from inside the trap was calculated by introducing a

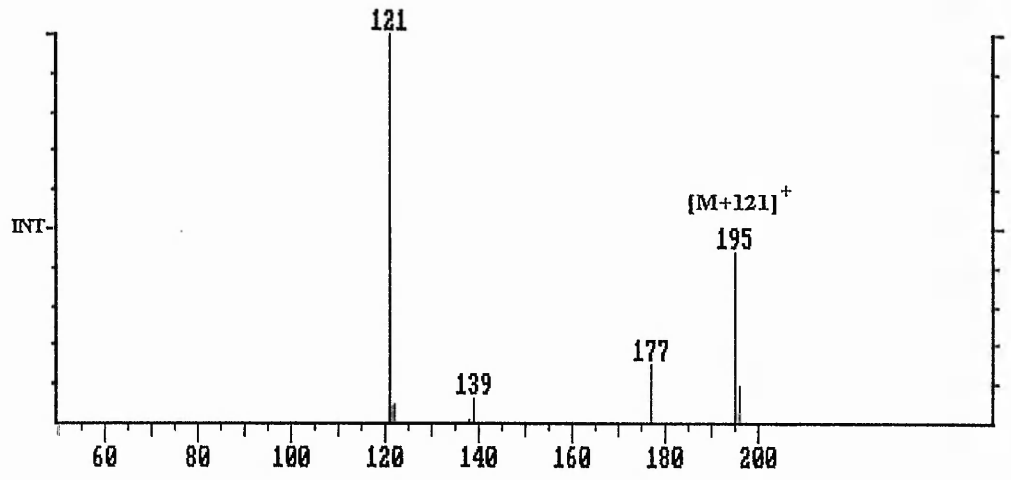

Figure 2.6. Mass spectrum resulting from the CAD of the $[M+121]^+$ ion at m/z 195.

pulse of acetophenone, followed by a variable delay before electron ionisation of residual sample. The resulting $[C_6H_5CO]^+$ intensity gave an indication of how much neutral sample vapour was still resident inside the trap, Figure 2.7. These experiments established that the acetophenone concentration in the ion trap fell to 10 % of the peak pulse concentration within 5 ms of the start of the pulse. This compares well with commercial pulsed valve systems. [28]

The reaction products of $[C_6H_5CO]^+$ with a selection of hydroxy containing compounds in the ion trap are summarised in Table 2.1. Butan-2-ol reacts to produce the characteristic $[M+105]^+$ adduct ion and an $[M-H]^+$ ion resulting from hydride abstraction, but not the $[M-OH]^+$ ion observed for 2-methylpropan-2-ol. No reaction is observed with butan-1-ol. The other aliphatic alcohol studied, cyclohexanol, yielded only the $[M-H]^+$ ion on reaction with $[C_6H_5CO]^+$.

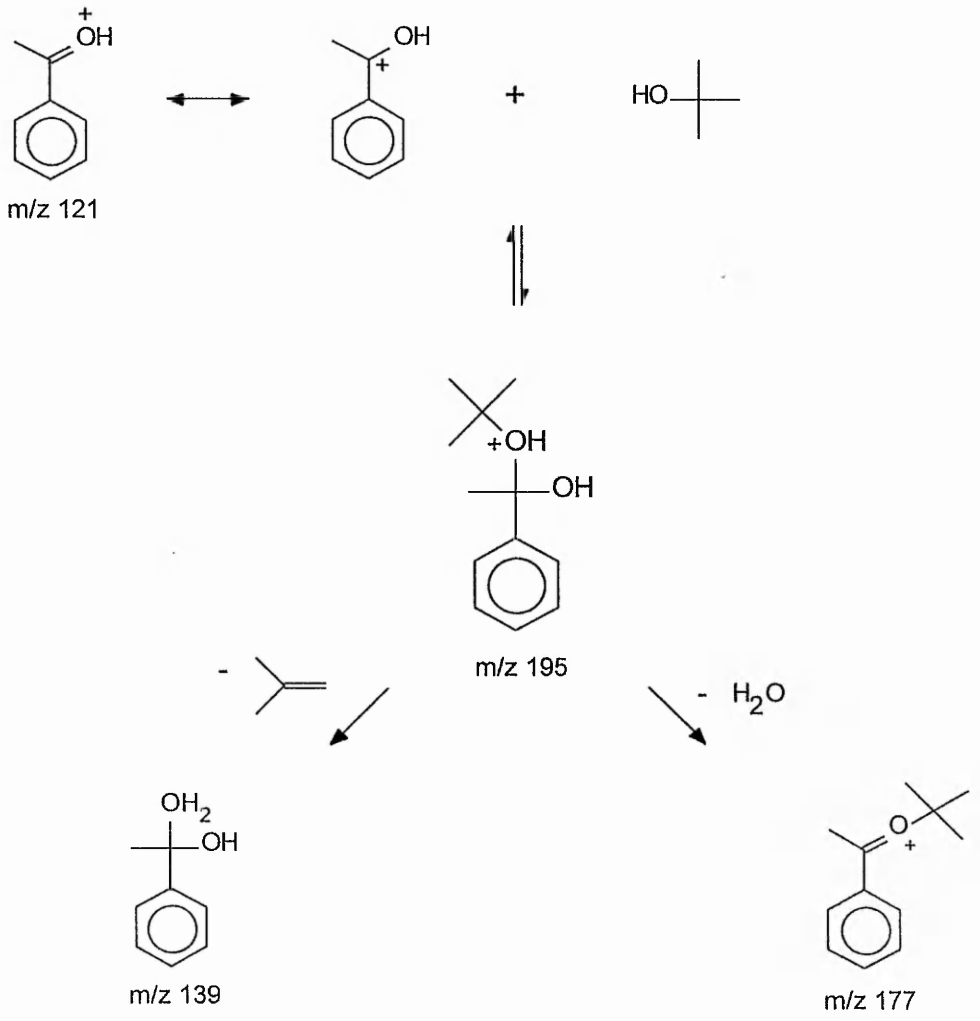

Scheme 2.3. Reaction pathway for $[C_6H_5C(OH)Me]^+$ ion with 2-methylpropan-2-ol.

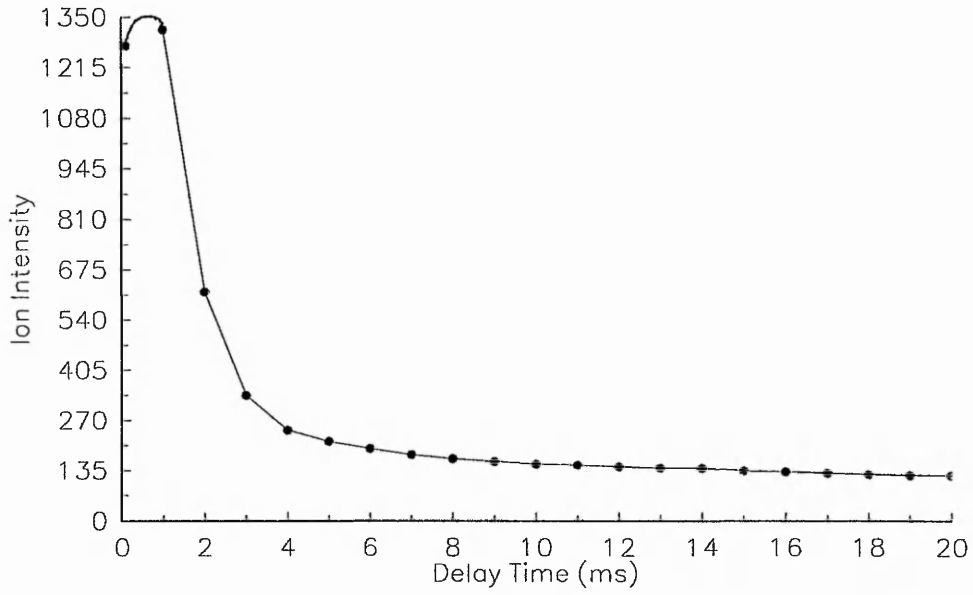

Figure 2.7. $[C_6H_5CO]^+$ intensity versus ionisation delay time for the pulsed introduction of acetophenone.

In contrast, the aromatic benzyl alcohol and benzhydrol both produce strong $[M\text{-}OH]^+$ hydroxy abstraction ions, with no adduct formation or hydride abstraction observed, but benzoylation of phenol does not occur in the trap. These reactions are consistent with the known thermochemistry of the benzoyl cation.

The formation of benzoic acid from $[C_6H_5CO]^+$ is strongly exothermic ($\Delta H_f \sim$ -999 kJ mol^{-1} under standard conditions) and the reaction to form $[M\text{-}OH]^+$ from the neutral precursor might therefore be expected to be favoured so long as hydroxy abstraction is endothermic by less then this amount. Hence, the $[C_7H_7]^+$ ion is observed as the only product for the reaction of the $[C_6H_5CO]^+$ ion with benzyl alcohol since this reaction is exothermic (ΔH_r = -24 kJ mol^{-1}), calculated using Equation 2.1.

Table 2.1. Product ions observed for the reaction of $[C_6H_5CO]^+$ with some hydroxy containing compounds (% relative abundance).

Compound	$[M+105]^+$	$[M-OH]^+$	$[M-H]^+$	Other ions
2-Methyl propan-2-ol	179 (100%)	57 (4 %)	-	113 (15 %) 123(8 %) 141(3 %)
Butan-2-ol	179 (55 %)	-	73 (21 %)	123(100 %) 129(23 %) 147(13 %) 131(11 %)
Butan-1-ol		no reaction		
Cyclohexanol	-	-	99 (100%)	-
Benzhydrol	-	167 (100%)	-	-
Benzyl alcohol	-	91 (100%)	-	197(19 %) 181(17 %) 169(8 %) 211(6 %)
Pentafluorobenzyl alcohol		no reaction		
Phenol		no reaction		
Trans 1,2-cyclopentadiol	207 (71 %)	-	-	189(100 %) 67(16 %)
Cis 1,2-cyclopentadiol		no reaction		
Flutriafol	406 (26 %)	284 (100 %)	-	
Fluconazole	411 (100 %)	289 (43 %)	-	248 (12 %)
4-(2-hydroxyethyl) oxindole	282 (23 %)	160 (100 %)	-	

However, the $[C_4H_9]^+$ ion is not formed from the reaction of the benzoyl ion with butan-1-ol, or butan-2-ol, since both these reactions are endothermic (ΔH_r = +125 kJ mol^{-1} and +62 kJ mol^{-1} respectively), as is that for phenol (ΔH_r = +292 kJ mol^{-1}). A weak $[Bu^t]^+$ ion is detected following the reaction with 2-methylpropan-2-ol, even though the overall reaction is slightly endothermic (ΔH_r = +6 kJ mol^{-1}). The reaction leading to the appearance of the $[M-H]^+$ from butan-2-ol, is also calculated to be slightly endothermic (ΔH_r = +8 kJ mol^{-1}), taking the formation of benzaldehyde from $[C_6H_5CO]^+$ to be exothermic by 742 kJ mol^{-1}. [23] This thermochemistry for the reaction of the benzoyl ion with a selection of hydroxy containing compounds is summarised in Table 2.2. However the effective temperature of an ion in the quadrupole ion trap is a complex function of the trap temperature and the applied rf voltages and this will influence these weakly endothermic reactions. [29]

$$[C_6H_5CO]^+ + ROH \rightarrow C_6H_5C(O)OH + R^+$$

$$\Delta H_r = \Delta H_f R^+ - \Delta H_f ROH - \Delta H_f [C_6H_5CO]^+ + \Delta H_f \text{ benzoic acid} \qquad (2.1)$$

Trans-1,2-cyclopentadiol reacts with $[C_6H_5CO]^+$ to produce a strong $[M+105]^+$ adduct ion, which dehydrates to yield the base peak ion at m/z 189. The spectrum from this reaction is shown in Figure 2.8, the ion at m/z 241 is the protonated dimer of acetophenone. In contrast *cis*-1,2-cyclopentadiol does not react because the configuration of the *cis*- isomer favours intramolecular hydrogen bonding between the hydroxy groups which prevents adduct formation with the benzoyl

cation. The electrophilic addition reaction therefore provides a simple method to distinguish between these isomeric forms. There is no reaction between $[C_6H_5CO]^+$ and pentafluoronated benzyl alcohol, as the strong withdrawing effect of the fluorine atoms causes the lone pairs on the oxygen to be less available for bonding.

Table 2.2. Thermochemical data for the reaction of the benzoyl ion with a selection of hydroxy containing compounds.

Compound / Ion	Heat of Formation (ΔH_f) (kJ mol^{-1})	Heat of Reaction (ΔH_r) (kJ mol^{-1})
$[C_6H_5CO]^+$	+ 705	
Benzoic Acid	- 294	
Benzaldehyde	- 37	
Butanol	- 275	
$[M\text{-}OH]^+$ $[n\text{-}C_4H_9]^+$	+ 849	+ 125
$[M\text{-}H]^+$ $[n\text{-}C_4H_9O]^+$	+ 521	+ 53
Butan-2-ol	- 295	
$[M\text{-}OH]^+$ $[sec\text{-}C_4H_9]^+$	+ 766	+ 62
$[M\text{-}H]^+$ $[sec\text{-}C_4H_9O]^+$	+ 455	+ 7
2-Methylpropan-2-ol	- 312	
$[M\text{-}OH]^+$ $[tert\text{-}C_4H_9]^+$	+ 693	+ 6
Cyclohexanol	- 286	
$[M\text{-}OH]^+$ $[C_6H_{11}]^+$	+ 733	+ 20
$[M\text{-}H]^+$ $[C_6H_{11}O]^+$	+ 461	+ 5
Benzyl Alcohol	- 100	
$[M\text{-}OH]^+$ $[C_7H_7]^+$	+ 875	- 24
Phenol	- 96	
$[M\text{-}OH]^+$ $[C_6H_5]^+$	+ 1193	+ 290

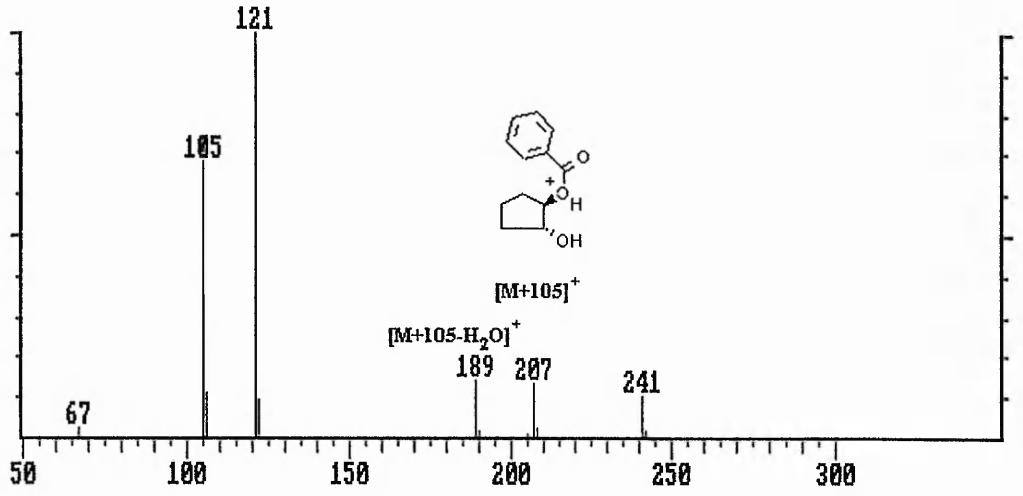

Figure 2.8. Spectrum resulting from the reaction of $[C_6H_5CO]^+$ with trans-1,2-cyclopentadiol.

Flutriafol (I) (a broad-spectrum systemic fungicide, Zeneca, UK), fluconazole (II) (an anti-fungal drug, Pfizer, UK) and 4-(2-hydroxyethyl) oxindole (III) (an intermediate in the production of Ropinirole, an anti-Parkinson's drug, SB, UK) all produce strong $[M\text{-}OH]^+$ ions (Table 2.1), as expected for hydroxy containing compounds with an adjacent aromatic ring. Adduct ions are also formed between $[C_6H_5CO]^+$ and compounds I-III.

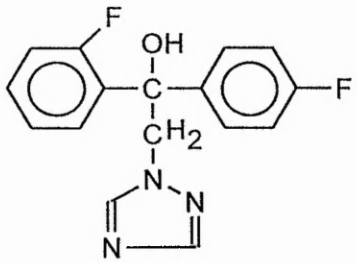

I

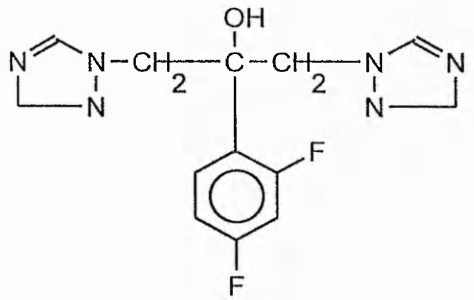

II

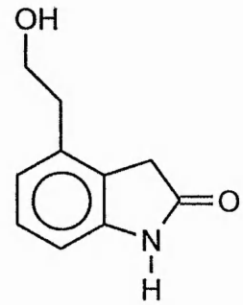

III

These observation on the reactivity of the range of hydroxy containing compounds listed in Table 2.1, suggest that the $[C_6H_5CO]^+$ ion interacts with the hydroxy functional group in a specific and predictable way, making it a potentially useful probe for the presence and chemical environment of hydroxy groups.

The behaviour of the benzoyl ion towards a number of carboxylic acids (4-chlorobenzoic acid, phenyl acetic acid, isobutyric acid), ethers (anisole, diphenyl ether, ethylphenyl ether), ketones (benzophenone, acetophenone), amines (diethyl amine, benzyl amine, n-butyl amine, butyl-2-amine, t-butyl amine, aniline) and molecules containing a carbon-carbon double bond (styrene and dienstrol) has also been investigated. Amines (which will be discussed in chapter 3) and molecules containing a carbon-carbon double bond reacted with the $[C_6H_5CO]^+$ ion, but none of the acids, ketones or ethers yielded ionic products in the lower pressure regime (*ca* 10^{-3} torr) of the quadrupole ion trap mass spectrometer. This is in contrast to reactivity of the benzoyl ion with anisole which has been reported in the 90 - 650 torr region. [7] This difference in reactivity probably arises because of

the slow rate of collisional stabilisation of the excited adduct ion relative to the dissociation of the adduct, that occurs inside the ion trap. The dominant process in this case being the dissociation of the adduct to yield the reactants. At the higher pressures (e.g. 760 torr) the rate of collision cooling of the excited adduct ion population exceeds that of the reverse reaction, making back dissociation the less favoured pathway.

Molecular modelling studies of the electrophilic addition of $[C_6H_5CO]^+$ to 2-methylpropan-2-ol suggest that the adduct formed initially, **a**, is unstable, since no energy minima could be found. However, rearrangement to **b**, which has the

a **b**

proton on the carbonyl oxygen, gave a stable adduct. The formation of adduct **b** with 2-methylpropan-2-ol, was calculated to be exothermic by 85 kJ mol^{-1}, whilst production of $[M\text{-}OH]^+$ from this adduct was calculated to endothermic, by 93 kJ mol^{-1}. These observations support the view that formation of the $[M\text{-}OH]^+$ ion proceeds preferentially *via* adduct ion **a** and this pathway competes with formation of the more stable adduct ion, **b**. This is further supported by a comparison of the CAD tandem mass spectrum of the m/z 179 ion formed by the reaction of the benzoyl ion with 2-methylpropan-2-ol, with the $[M+H]^+$ ion of t-butylbenzoate

generated by ammonia chemical ionisation of the parent compound, which is also expected to have the structure **b**. Both precursor ions yielded the m/z 123 product ion *via* the loss of butene, illustrated in Figure 2.9, suggesting that **b** is the most likely structure of the m/z 179 ion, whilst the m/z 57 ion expected from structure **a** was not observed.

The reaction of $[C_6H_5CO]^+$ with hydroxy deuterated 2-methylpropan-2-ol, $(CH_3)_3OD$, produced a 1:2 intensity ratio for the deuterated (m/z 180) and undeuterated (m/z 179) $[M+105]^+$ adduct ions, illustrated in Figure 2.10, indicating that proton transfer might not be a simple rearrangement, but may involve an intermolecular exchange *via* a third body. The formation of the rearranged carbonyl protonated product **c**, for the benzoylation of benzyl alcohol was calculated from molecular modelling data to be exothermic by 102 kJ mol^{-1} and production of $[M-OH]^+$ from this rearranged ion was calculated to be endothermic by 110 kJ mol^{-1}.

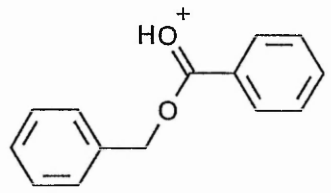

c

The transfer of the hydroxy group must therefore occur rapidly following electrophilic addition of the benzoyl ion, since $[M-OH]^+$ is the only product ion

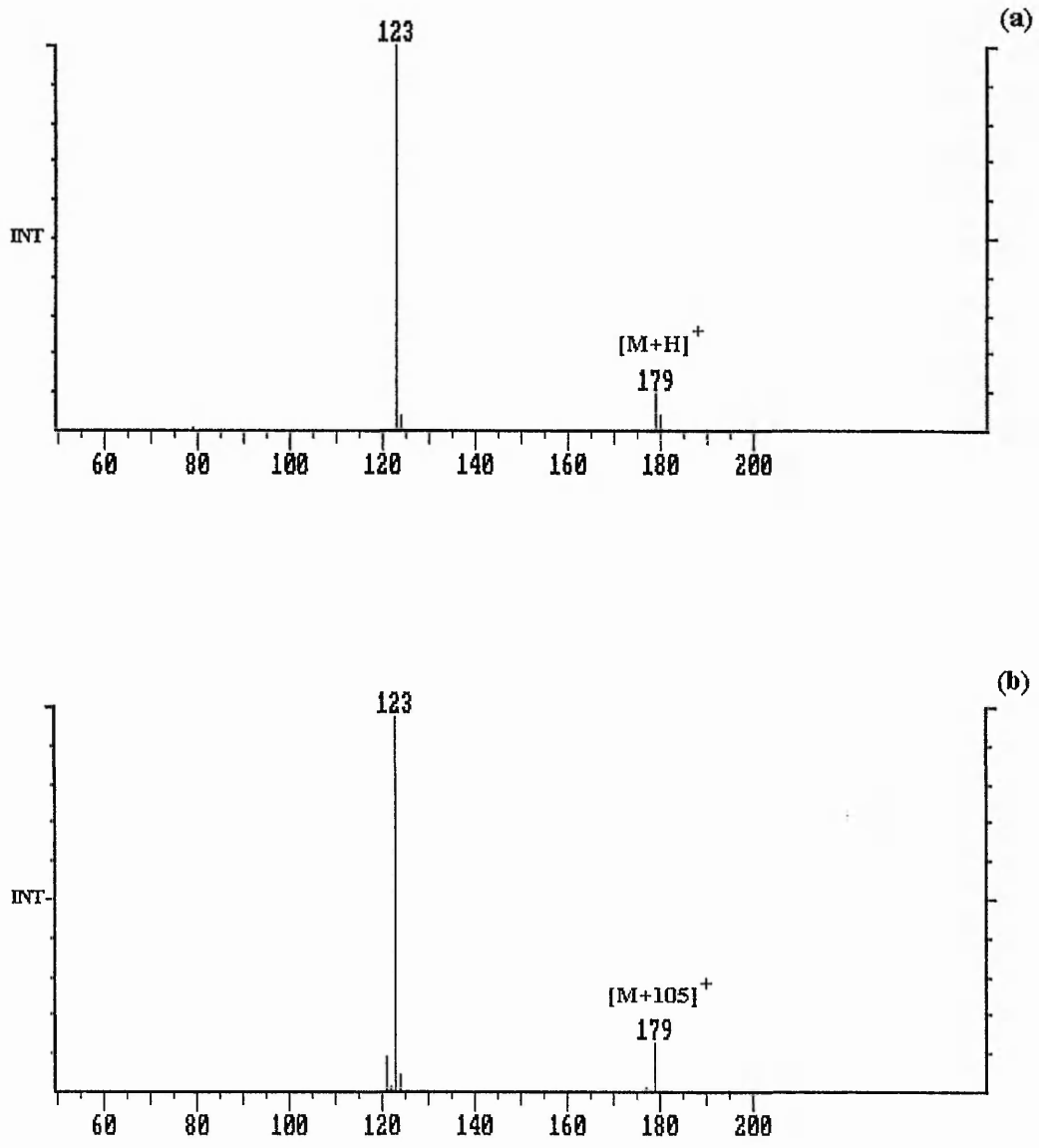

Figure 2.9. Comparison of the CAD of (a) $[M+H]^+$ from the methane CI of t-butylbenzoate and (b) $[M+105]^+$ benzoyl adduct of 2-methylpropan-2-ol.

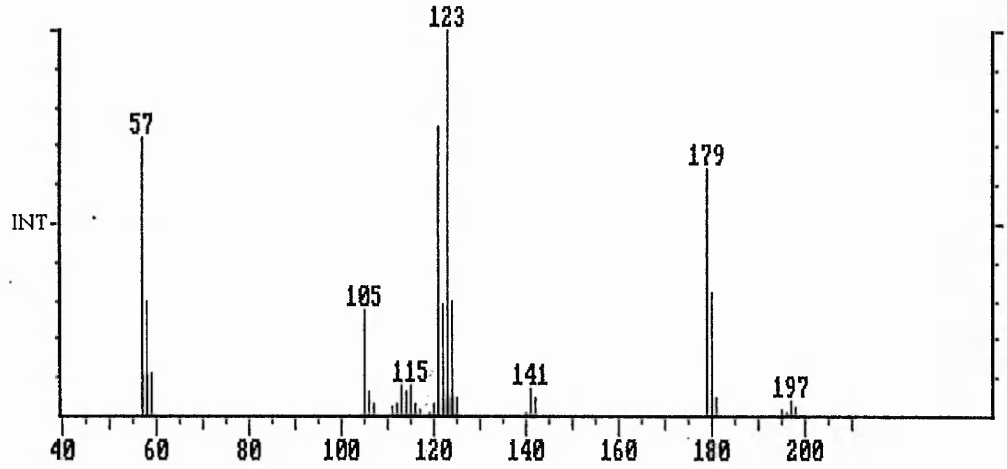

Figure 2.10. Spectrum resulting from the 100 ms reaction of $[C_6H_5CO]^+$ with $(CH_3)_3OD$

observed for benzyl alcohol. The formation of the rearranged carbonyl protonated adduct with butan-1-ol was calculated to be exothermic by 95 kJ mol^{-1}, but the electrophilic addition production was also not detected for the reaction with the benzoyl ion.

Generation of the $[M\text{-}OH]^+$ and $[M\text{-}H]^+$ ions from the stable adduct were calculated to be endothermic by 112 kJ mol^{-1} and 95 kJ mol^{-1} respectively and these ions were likewise not detected. These observations are explained if the rearrangement to the more stable adduct is less favoured than the dissociation pathway for the electrophilic addition product of butan-1-ol.

Ion trap operating conditions were observed to have a considerable influence on the reactions of the benzoyl ion. The effect of helium pressure on the stability of the adduct was investigated at three different helium pressures, $1x10^{-4}$, $8x10^{-5}$ and $5x10^{-5}$ torr (uncorrected ion gauge reading) for the reaction of 2-methylpropan-2-ol

with the benzoyl ion. At a helium pressure of $1x10^{-4}$, the adduct ion intensity was observed to increase, (11 % higher) relative to the intensity at $8x10^{-5}$ torr. Decreased fragmentation was also observed at this higher helium pressure, 4 % less relative to the fragment intensity at $8x10^{-5}$ torr. At the lowest helium pressure of $5x10^{-5}$ torr, decreased adduct ion intensity (21 % less relative to adduct ion intensity at $8x10^{-5}$ torr) and increased fragmentation (8 % higher relative to fragment ion intensity at $8x10^{-5}$ torr) was observed. This effect of the variation of helium pressure on the intensity of the adduct ion and the fragment ion at m/z 123 is illustrated in Figure 2.11. The adduct appears to be more efficiently collisionally stabilised at higher helium pressures, resulting in an increased intensity of the adduct ion and less fragmentation. These observation are consistent with the differing reaction pathways noted earlier for the interaction of the benzoyl ion with anisole in the ion trap and 90-650 torr pressure regimes.

The effect of varying the kinetic energy of the benzoyl ion was studied for the product ion distribution of the reaction with 2-methylpropan-2-ol. The kinetic energy of ions in the quadrupole rf field of an ion trap is related to their q_z value, given by equation 2.2.

$$q_z = - \frac{4eV}{mr_o^2\Omega^2} \qquad (2.2)$$

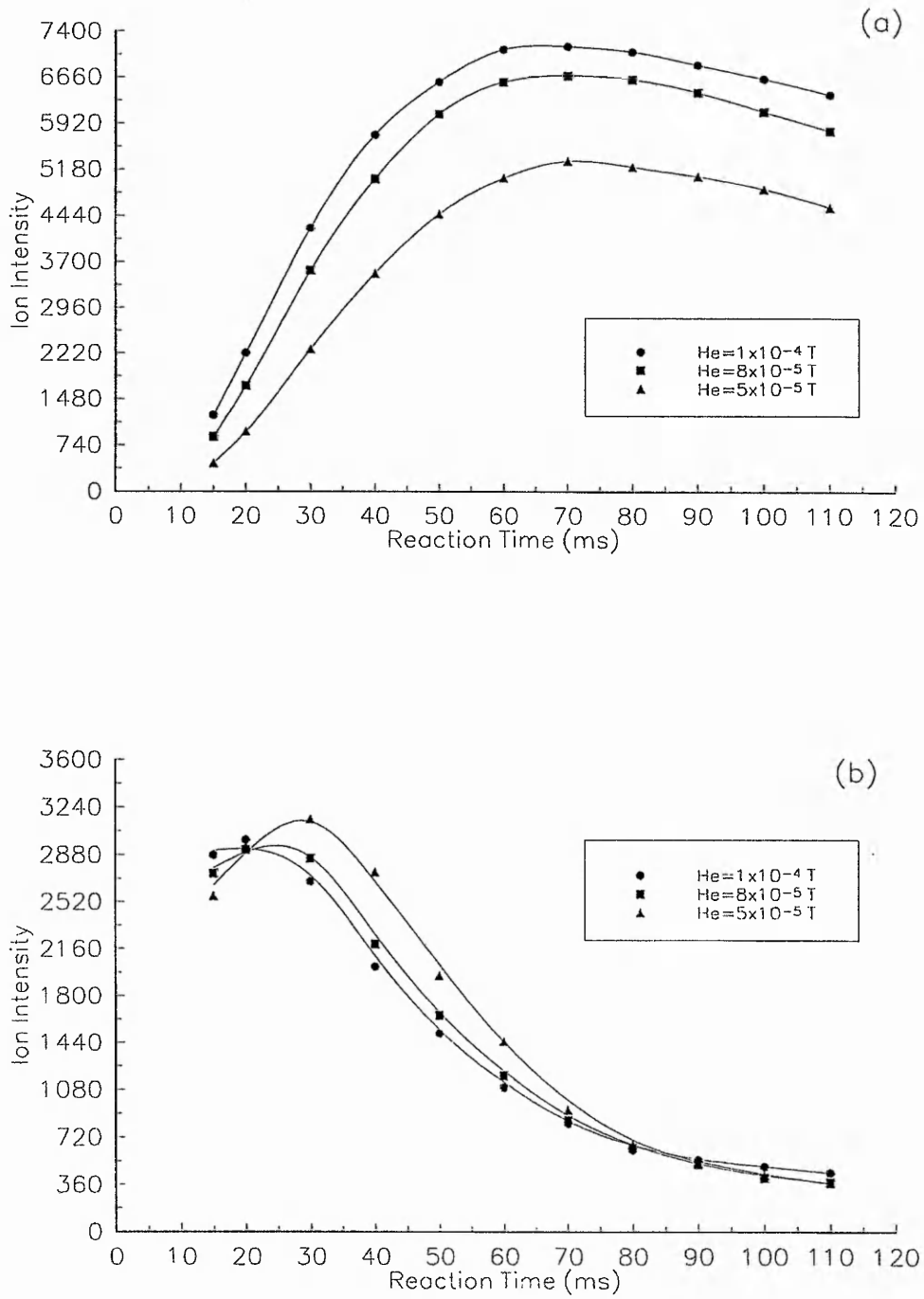

Figure 2.11. The variation of helium pressure on (a) adduct ion intensity and (b) m/z 123 fragment ion intensity.

where **V** is the applied rf voltage amplitude, **e** is the charge on the ion, **m** is the mass of the ion, $\mathbf{r_0}$ is the internal radius of the trap ring electrode and Ω is the angular frequency of the rf field.

Ions having a larger q_z value will possess greater kinetic energy and storing the benzoyl ion at a high q_z value during the reaction period therefore 'heats' the reactant, allowing the effect on the benzoyl ion and product abundances to be studied.

Increasing the q_z of the benzoyl ion resulted in a decrease in the relative rate of the reaction, illustrated in Figure 2.12 by the slopes of the lines for Ln [I] ($[C_6H_5CO]^+$ intensity) versus time at three different q_z values for the reaction of $[C_6H_5CO]^+$ with 2-methylpropan-2-ol. At a q_z of 0.17 the line deviates from linearity at reaction times below 30 ms, but the reason for this is not clear. The faster rate of decrease in the $[C_6H_5CO]^+$ intensity at low q_z is accompanied by a corresponding increase in the $[M+105]^+$ adduct ion intensity and a decrease in the intensity of the $[M-OH]^+$ ion. These spectral changes may be attributed to an increased rate of formation of the adduct at lower q_z. This is consistent with the calculated exothermicity of this reaction. [30] Increasing the q_z value of the benzoyl ion during the reaction period is therefore less favourable for adduct and product ion formation.

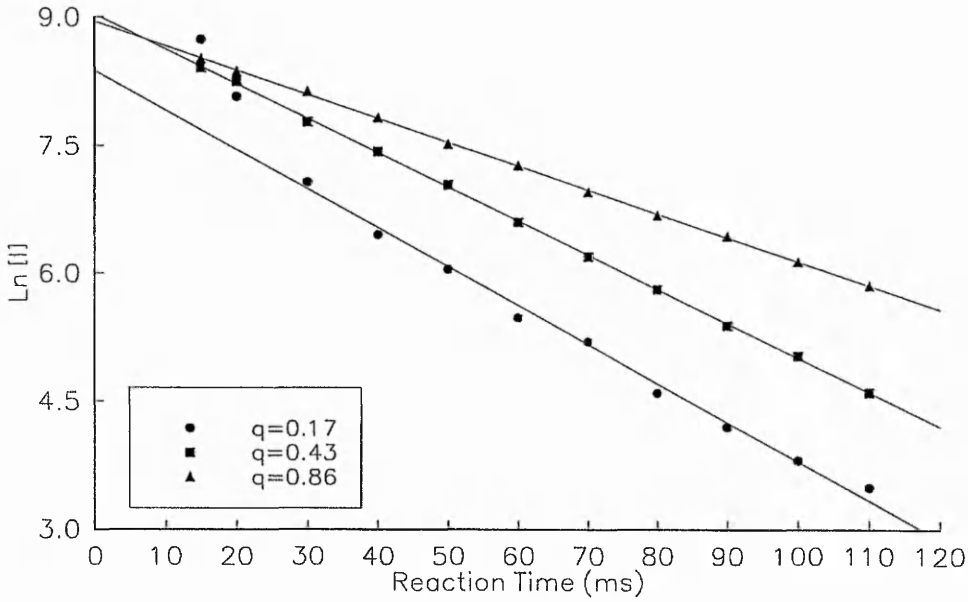

Figure 2.12. Ln [I] versus time for the reaction of the $[C_6H_5CO]^+$ ion with 2-methylpropan-2-ol at three different q_z values

The reactions of the substituted benzoyl ions $[C_6X_5CO]^+$ (X= H, F, 4-Me or 3,5-di-Bu^t) were investigated in the quadrupole ion trap to determine the influence of substitution on the relative reactivities of these ions and the observed ionic products. Table 2.3 shows the product ion abundances for the reactions of these substituted benzoyl ions with some oxygenated compounds. $[C_6F_5CO]^+$ is a much stronger electrophile than $[C_6H_5CO]^+$ because of the electron-withdrawing properties of the fluorine substituents. This causes the ion to be significantly more reactive, forming an $[M\text{-}OH]^+$ ion with isobutyric acid, and an $[M+195]^+$ adduct ion with diphenyl ether and phenol, as well as the expected reaction products with benzyl alcohol and 2-methylpropan-2-ol. In the reaction with 2-methylpropan-2-ol, increased intensity for the $[M\text{-}OH]^+$ ion was observed compared to the $[C_6H_5CO]^+$

Table 2.3. Product ions observed for the reactions of substituted benzoyl ions (% relative abundance).

Compound	$[C_6F_5CO]^+$	$[C_6H_5CO]^+$	$[4\text{-}CH_3C_6H_4CO]^+$	$[(C_4H_9)_2C_6H_3CO]^+$
2-methyl propan-2-ol	$[M+195]^+$ (33 %) $[M-OH]^+$ (7 %) $[C_6F_5COOH]$ (100 %)	$[M+105]^+$ (100 %) $[M-OH]^+$ (4 %)	$[M+119]^+$ (20 %) $[M+119-C_4H_8]^+$ (100 %)	no reaction
Benzyl alcohol	$[M-OH]^+$ (100 %)	$[M-OH]^+$ (100 %)	$[M-OH]^+$ (100 %)	no reaction
Phenol	$[M+195]^+$ (100 %)	no reaction	no reaction	no reaction
Isobutyric acid	$[M-OH]^+$ (100 %)	no reaction	no reaction	no reaction
Diphenyl ester	$[M+195]^+$ (100 %)	no reaction	no reaction	no reaction

ion. In contrast, $[3,5\text{-di-}(Bu^t)C_6H_3CO]^+$ is a much weaker electrophile, because of the electron-donating properties of the *tert*-butyl groups. This results in the ion being unreactive towards all of the oxygenated compounds in Table 2.2. The neutral parent compound is in fact a strong electrophile, illustrated in Figure 2.13a by the formation of a strong $[M+NH_4]^+$ adduct ion, which is unusual in the low pressure regime of the ion trap. The origin of this ion was confirmed by CAD which produced the $[M+H]^+$ ion and the $[M-OH]^+$ ion ($[3,5\text{-di-}(Bu^t)C_6H_3CO]^+$),

illustrated in Figure 2.13b. The $[4\text{-}CH_3C_6H_4CO]^+$ and $[C_6H_5CO]^+$ ions show reactivities which are intermediate between the pentafluoro- and di-*tert*-butyl-substituted ions, with the $[4\text{-}CH_3C_6H_4CO]^+$ the weaker electrophile of the two because of the electron donating properties of the methyl group.

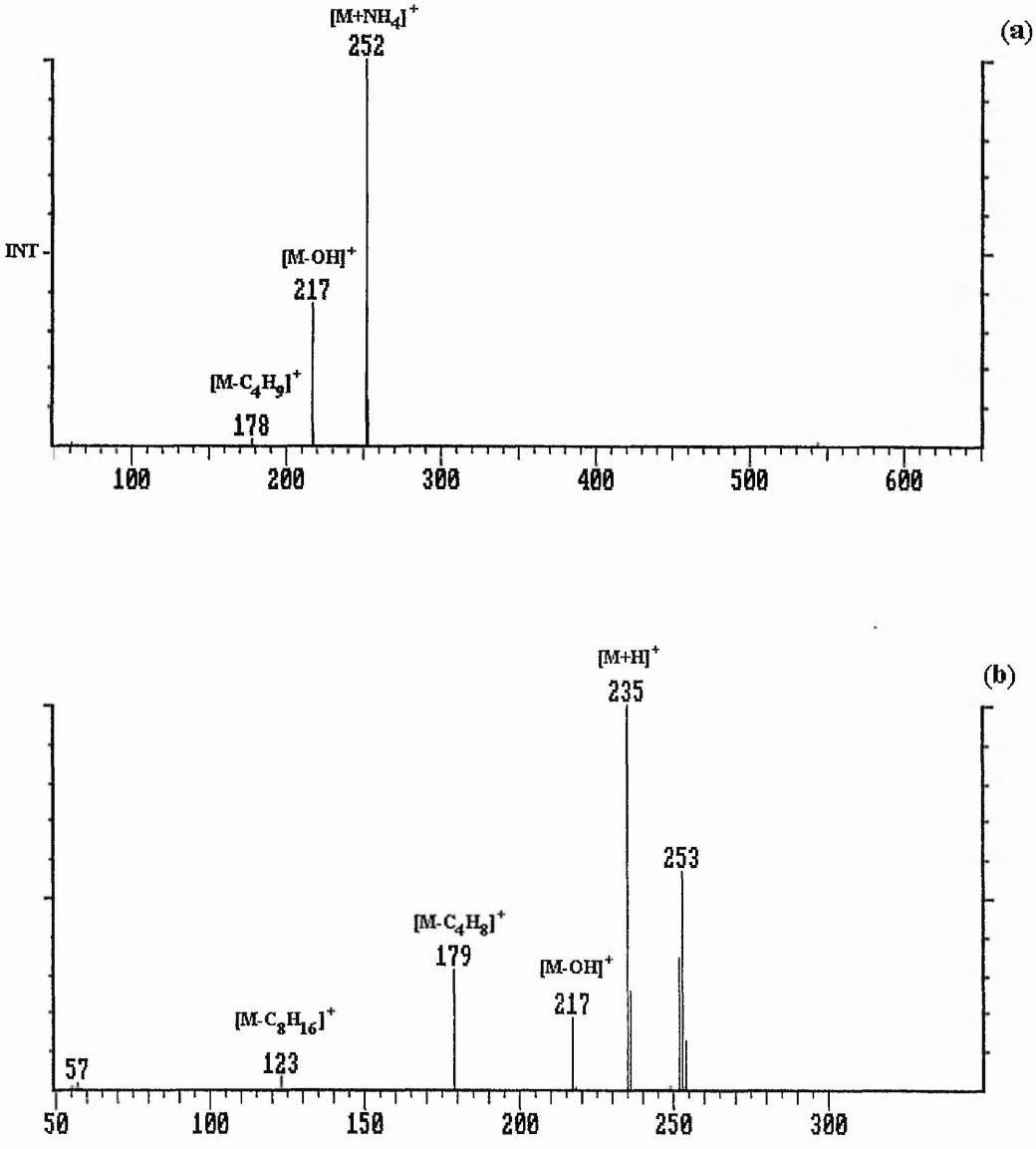

Figure 2.13. Ammonia CI of 3,5-di-tert-butylbenzoic acid (a) and (b) CAD of the $[M+NH_4]^+$ ion.

2.4 CONCLUSION

The $[C_6X_5CO]^+$ ions (X= H, F, 4-Me, 4-Bu^t) react within the pressure and time regimes of the quadrupole ion trap mass spectrometer with compounds containing hydroxy functionality to yield characteristic $[M+C_6X_5CO]^+$, $[M-OH]^+$ and $[M-H]^+$ products. Product distributions are determined by the hydroxy group environment in agreement with the known thermochemistry of these ions, making these reagent ions potentially useful probes for establishing the presence and chemical environment of hydroxy groups. Storing the benzoyl ion at a low q_z value during the reaction period, as well as at increased pressure stabilises adduct formation. The gas-phase chemistry of the benzoyl ions in the quadrupole ion trap is strongly influenced by the substituents on the phenyl ring.

2.5 REFERENCES

1. Bruins, A.P. and Nibbering, N.M.M., *Tetrahedron Lett.*, 4491, **50** (1975)

2. White, E.L., Tabet, J.C. and Bursey, M., *Org. Mass Spectrom.*, 132, **22** (1987)

3. Eberlin, M.N. and Cooks, R.G., *J. Am. Chem. Soc.*, 9226, **115** (1993)

4. Eberlin, M.N. and Cooks, R.G., *Org. Mass Spec.*, 679, **28** (1993)

5. Occhiucci, G., Patacchiola, A., Sparapani, C. and Speranza, M., *J. Chem. Soc., Chem. Commun.*, 1269 (1982)

6. Occhiucci, G., Speranza, M. and Cacace, F., *J. Chem. Soc., Chem. Commun.*, 723 (1984)

7. Occhiucci, G., Cacace, F. and Speranza, M., *J. Am. Chem. Soc.*, 872, **108** (1986)

8. Olah, G.A., Iyer, P.S., Surya Prakash, G.K. and Krishnamurthy, V.V., *J. Am. Chem. Soc.*, 7073, **106** (1984)

9. Olah, G.A., Iyer, P.S., Surya Prakash, G.K. and Krishnamurthy, V.V., *J. Org. Chem.*, 4317, **49** (1984)

10. Brownlee, R.T.C. and Craik, D.J., *J. Am. Chem. Soc.*, 872, **105** (1983)

11. Hunt, D.F., Harvey, T.M., Brumley, W.C., Ryan, J.F. and Russell, J.W., *Anal. Chem.*, 492, **54** (1982)

12. Orlando, R., Strobel, F., Ridge, D.P. and Munson, B., *Org. Mass Spectrom.*, 597, **22** (1987)

13. Blair, I.A., Phillipou, G. and Bowie, J.H., *Aust. J. Chem.*, 59, **32** (1979)

14. Ranatunga, T.D. and Kenttamaa, H.I., *Proceedings of the 41st ASMS Conference on Mass Spectrometry and Allied Topics*, San Francisco, CA. (1993)

15. Keough, T., *Anal. Chem.*, 2540, **54** (1982)

16. Doorn, R. van and Nibbering, N.M.M., *Org. Mass Spectrom.*, 527, **13** (1978)

17. Vairmani, M., Mirza, U.A. and Srinivas, R., *Mass Spectrom. Rev.*, 235, **9** (1990)

18. Ranatunga, T.D. and Kenttamaa, H.I., *J. Am. Chem. Soc.*, 8600, **114** (1992)

19. Creaser, C.S. and Williamson, B.L., *J. Chem. Soc., Chem Commun.*, 1677 (1994)

20. Creaser, C.S. and Williamson, B.L., *J. Chem. Soc., Perkin 2*, in press

21. Kaiser, R.E., Cooks, R.G., Syka, J.E.P. and Stafford, G.C., *Rapid Commun. Mass Spectrom.* 30, **4** (1990)

22. Todd, J.F.J., Penman, A.D., Thorner, D.A. and Smith, R.D., *Rapid Commun. Mass Spectrom.* 108, **4** (1990)

23. Lias, S.G., Bartmess, J.E., Liebmann, J.F., Holmes, J.L., Levin, R.D. and Mallard, W.G., *J. Phys. Chem. Ref. Data* suppl. 1, **17** (1988)

24. Franklin, J.L., Dillard, J.G., Rosenstock, H.M., Herron, J.T., Draxl, K. and Field, F.H., *Ionisation potentials, appearance potentials and heats of formation of gaseous positive ions*, National Bureau of Standards (1969)

25. Clark, T., Rauhut, G. and Chandrasekhar, J., VAMP4.5, Erlangen (1992)

26. Stewart, J.J.P., *J. Computer Aided Molecular Design*, 1, **4** (1990)

27. Moody, S., Underwood, N.J. and Watts, P., *presented at the 21 st BMSS meeting*, Manchester (1995)

28. Coopersmith, B.I., Yost, R.A., *J. Am. Soc. Mass Spectrom.*, 976, **6** (1995)

29. Basic, C., Eyler, J.R. and Yost, R.A., *J. Am. Soc. Mass Spectrom.*, 716, **3** (1992)

30. Wu, H.F., Brodbelt, J.S., *Int. J. Mass Spectrom. Ion Process.*, 175, **124** (1993)

CHAPTER 3

SELECTIVE CHEMICAL IONISATION REACTIONS OF THE BENZOYL CATION WITH AMINES.

3.1 INTRODUCTION

The benzoyl cation, $[C_6H_5CO]^+$, has been shown in Chapter 2 to undergo selective ion-molecule reactions with the a range of compounds containing the hydroxy functional group. Reactions have also been reported for unsaturated compounds [1, 2] and 1,3-dioxolanes. [3] However, the reactions of the benzoyl cation with the amine functional group has been little studied.[4-6]

The formation of $[C_6H_5CONH_3.(NH_3)_n]^+$ cluster ions (n = 0,1,2,3) has been reported for the reaction of the benzoyl ion with ammonia in the collisional cell of a triple quadrupole mass spectrometer. [4] $[C_6H_5CO]^+$ ions were generated by CI of phenyl benzoate using isobutane as reagent gas in the source of the mass spectrometer. The reaction of $[C_6H_5CO]^+$ with the simple aliphatic amines; methylamine, dimethyl amine and trimethylamine, have been studied in an FT-ICR mass spectrometer, resulting in the production of adduct ions, however no amino abstraction or protonated benzamide ions were reported. [5] Adduct formation between the benzoyl cation and aniline in the 90-650 torr pressure range has also been reported. [6] In these experiments, $[C_6H_5CO]^+$ was generated by β decay of multitritiated benzene in excess carbon dioxide (90-630 torr) and reaction with aniline (5-10 torr) took place in a Pyrex vessel (500-1000 mL) at 100 °C for periods of 15 - 20 months. The products, extracted in ethyl acetate, were analysed by radio GLC and HPLC.

Ionisation of compounds containing the amine functional group have been reported by conventional chemical ionisation techniques with reagent ions such as CH_5^+, [7] HCO^+, [8] and NH_4^+. [9] In the CH_4 CI mass spectra of butylamines, the $[MH\text{-}NH_3]^+/MH^+$ ion intensity ratios were reported to be 0.04 for n-butylamine, 0.07 for s-butylamine and 2.3 for t-butylamine. [7] The HCO^+ CI mass spectra of a selection of C_3 to C_5 alkylamines have been determined, resulting in only low intensity MH^+ ions being observed for the n-butylamine, although much more intense MH^+ ions were observed for secondary and tertiary amines. [8] The two major fragmentation reactions of the MH^+ ion were reported as:

$$RNH_3^+ \rightarrow R^+ + NH_3$$

$$\rightarrow NH_4^+ + [R\text{-}H]$$

The differentiation of primary, secondary and tertiary amines has been reported by obtaining two mass spectra, one with NH_4^+ and the other with ND_4^+ as reagent ions. [10] Primary amines with two labile hydrogens gave ions at $[M+4]^+$ and $[M+24]^+$. For secondary amines they appeared at $[M+3]^+$ and $[M+23]^+$ and for tertiary amines at $[M+2]^+$ and $[M+22]^+$. This method was illustrated with the isomeric anilines 2,6-di-methylaniline, N-ethylaniline and N,N-dimethylaniline, and among the more than two dozen simple amines tested at the time, no exceptions to the generalisation were found. This method has also been extended to several other classes of amine found in coal tar, with confirmation of the observations above. [11] However, the selectivity of all these

reagent ions for amines was limited by their reactivity towards a variety of other functional groups. [12]

This chapter describes an ion trap mass spectrometric study of the selectivity of the ion molecule chemical ionisation reactions of $[C_6H_5CO]^+$ ion with compounds containing the amine functional group, which has not been previously described.

3.2 EXPERIMENTAL

Experiments were performed using a quadrupole ion trap mass spectrometer (Finnigan MAT ITMS, San Jose, CA), operated at 120 °C. All chemicals were obtained from Aldrich Chemical Co. (Dorset, UK), except 4-[2-(dipropylamino)ethyl]-1,3-dihydro-2H-indol-2-one (Ropinirole), which was obtained from SmithKline Beecham (Tonbridge, Kent, UK). These compounds were used without further purification. Acetophenone was introduced into the mass spectrometer *via* a leak valve (Meggitt Avionics, Portsmouth, UK) at a pressure of 2×10^{-6} torr (uncorrected). All other samples were introduced on a solid probe. Helium bath gas pressure was maintained at 1×10^{-4} torr (uncorrected). All pressures were measured by the ion trap vacuum chamber ion gauge.

The benzoyl ion was generated as an electron ionisation fragment of acetophenone, isolated using resonance hole isolation and allowed to react with neutral sample vapour for 100 ms. A scan routine for this experiment is shown in Figure 3.1. Standard heats of formation (ΔH_f) for benzamide and n-protonated benzamide were taken from reference 4. All other thermochemical data was taken from reference 13.

Tandem mass spectrometry [14, 15] using collisionally activated dissociation [16, 17] was employed to give structural information on adduct ions. Resonance hole isolation [18] was employed to isolate the precursor ion followed by the application of a tickle voltage to the end cap electrodes to resonately excite the precursor ion.[19]

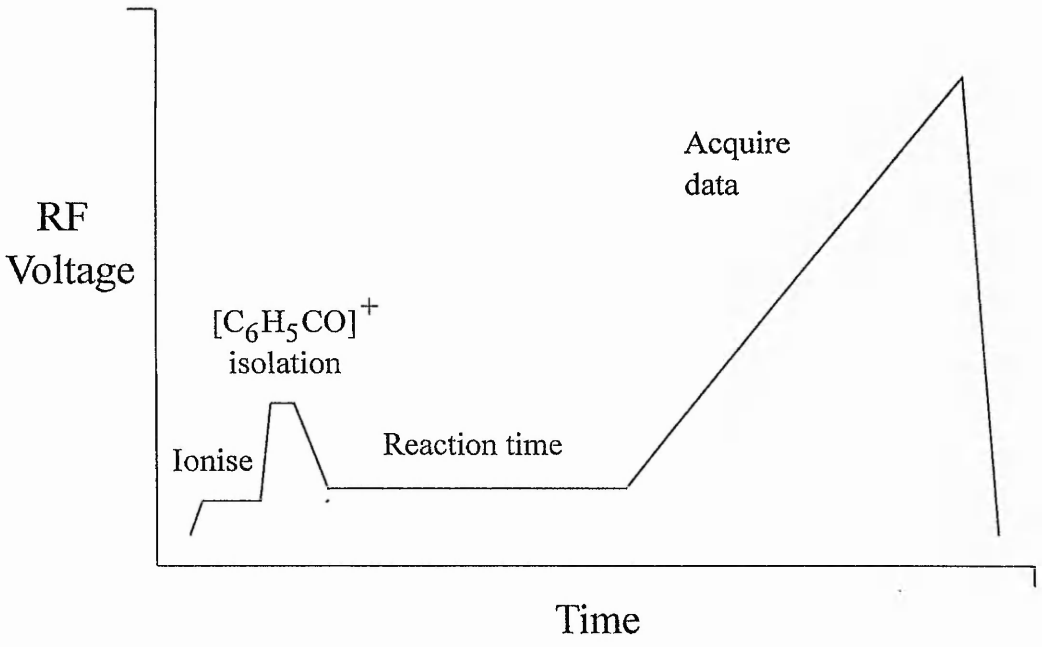

Figure 3.1. Scan routine for the reaction of the benzoyl ion with compounds containing the amine functional group.

3.3 RESULTS AND DISCUSSION

The spectra resulting from the reaction of the benzoyl ion with three aliphatic amines; t-butylamine (2-methylpropan-2-amine), sec-butylamine (butyl-2-amine) and n-butylamine (butyl-1-amine) are shown in Figure 3.2. The reaction with t-butylamine, Figure 3.2(a), produced an $[M+105]^+$ adduct ion at m/z 178 and a $[M-NH_2]^+$ amino abstraction ion at m/z 57. These product ions are equivalent to those for the reaction of $[C_6H_5CO]^+$ with 2-methylpropan-2-ol, which produced an adduct and a hydroxy abstraction ion (Figure 2.3). However, the base peak resulting from the reaction with t-butylamine was the protonated benzamide ion, $[C_6H_5C(O)NH_3]^+$ at m/z 122. The most likely origin of this ion is the adduct ion at m/z 178. This was investigated by tandem mass spectrometry using collisionally activated dissociation (CAD) with resonance excitation. The resulting product ion spectrum, Figure 3.3, shows the m/z 122 ion as the only product confirming that the protonated benzamide ion is derived from the adduct.

The m/z 122 ion was also present in the product spectrum of the $[C_6H_5CO]^+$ reaction with sec-butylamine, Figure 3.2(b). The reaction with sec-butylamine also produced a $[M+105]^+$ adduct ion at m/z 178, but no $[M-NH_2]^+$ ion was present. The reaction of the benzoyl cation with n-butylamine is illustrated in Figure 3.2(c). An $[M+105]^+$ adduct ion was present at m/z 178. However, neither $[C_6H_5C(O)NH_3]^+$ or $[M-NH_2]^+$ ions were

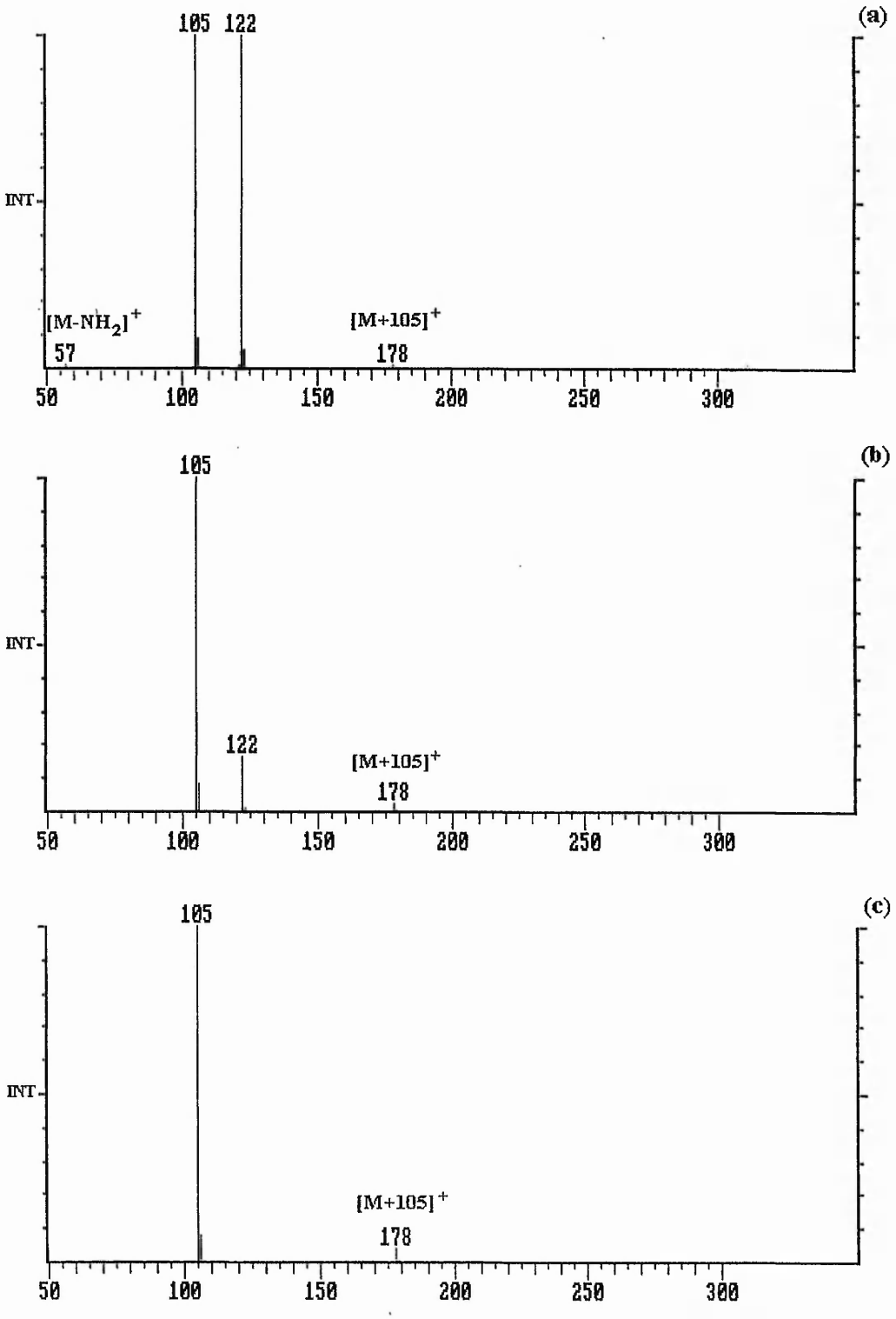

Figure 3.2. The spectra resulting from the reaction of $[C_6H_5CO]^+$ with (a) t-butylamine, (b) sec-butylamine and (c) butylamine.

observed for the reaction of $[C_6H_5CO]^+$ with n-butylamine. This is in contrast to the reaction of $[C_6H_5CO]^+$ with butan-1-ol (Table 2.1), in which no reaction was observed, consistent with the increased nucleophilicity of the amine group. The selective chemical ionisation reactions of the benzoyl ion are therefore capable of distinguishing between the three aliphatic amines which is a non trivial task by conventional CI techniques. [6, 7, 8]

The reaction of the benzoyl cation with 4-chlorobenzylamine is illustrated in Figure 3.4(a). No adduct ion was present in the spectrum, however an $[M\text{-}NH_2]^+$ ion was present in the spectrum at m/z 125/127 together with an ion at m/z 91, tentatively assigned to $[C_7H_7]^+$. The reaction of $[C_6H_5CO]^+$ with aniline, Figure 3.4(b), produced

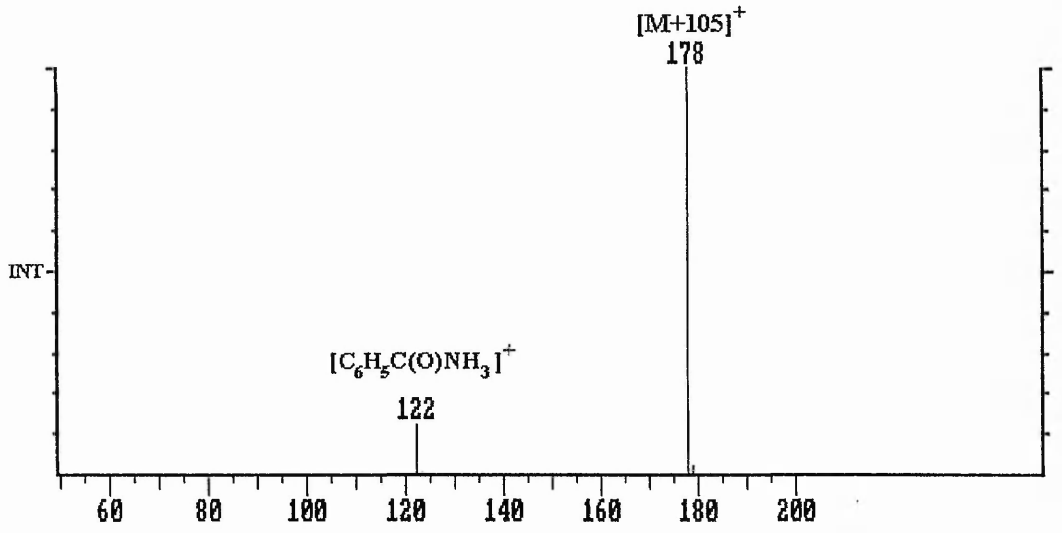

Figure 3.3. The CAD spectrum of the benzoyl ion / t-butylamine adduct ion

an adduct ion at m/z 198 and the $[C_6H_5C(O)NH_3]^+$ ion at m/z 122. This is in contrast with the reaction of $[C_6H_5CO]^+$ with phenol were no reaction was observed, which again can be explained by the increased nucloephilicity of the amine compared to the hydroxy functional group. Scheme 3.1 illustrates the generalised reaction pathway for the formation of adduct, $[M\text{-}NH_2]^+$ and protonated benzamide ions from the reaction of $[C_6H_5CO]^+$ with amino containing compounds. This work suggests that the protonated benzamide ion at m/z 122 may be a possible diagnostic ion for the presence of primary amines, however the absence of this ion does not necessary indicate a primary amine group is not present. This is in agreement with earlier work reported on the reaction of the benzoyl ion with ammonia, [4] in which protonated benzamide was observed, and with the work of Nibbering [5] where no protonated benzamide was observed between $[C_6H_5CO]^+$ and secondary and tertiary amines.

The formation of benzamide from $[C_6H_5CO]^+$ is strongly exothermic ($\Delta H_f \sim$ - 828 kJ mol^{-1} under standard conditions) and the reaction to form $[M\text{-}NH_2]^+$ from the neutral precursor would be favoured if amino abstraction is endothermic by less than this amount. Hence the $[Bu^t]^+$ ion was observed for the reaction of the $[C_6H_5CO]^+$ ion with t-butylamine, since this reaction is exothermic (ΔH_r = -14.1 kJ mol^{-1}, calculated using the equation 3.1). However, the $[C_4H_9]^+$ ion was not formed from the reaction of the benzoyl ion with n-butylamine or sec-butylamine, since both these reactions are endothermic (ΔH_r = +113 kJ mol^{-1} and + 37 kJ mol^{-1} respectively), as is that for aniline

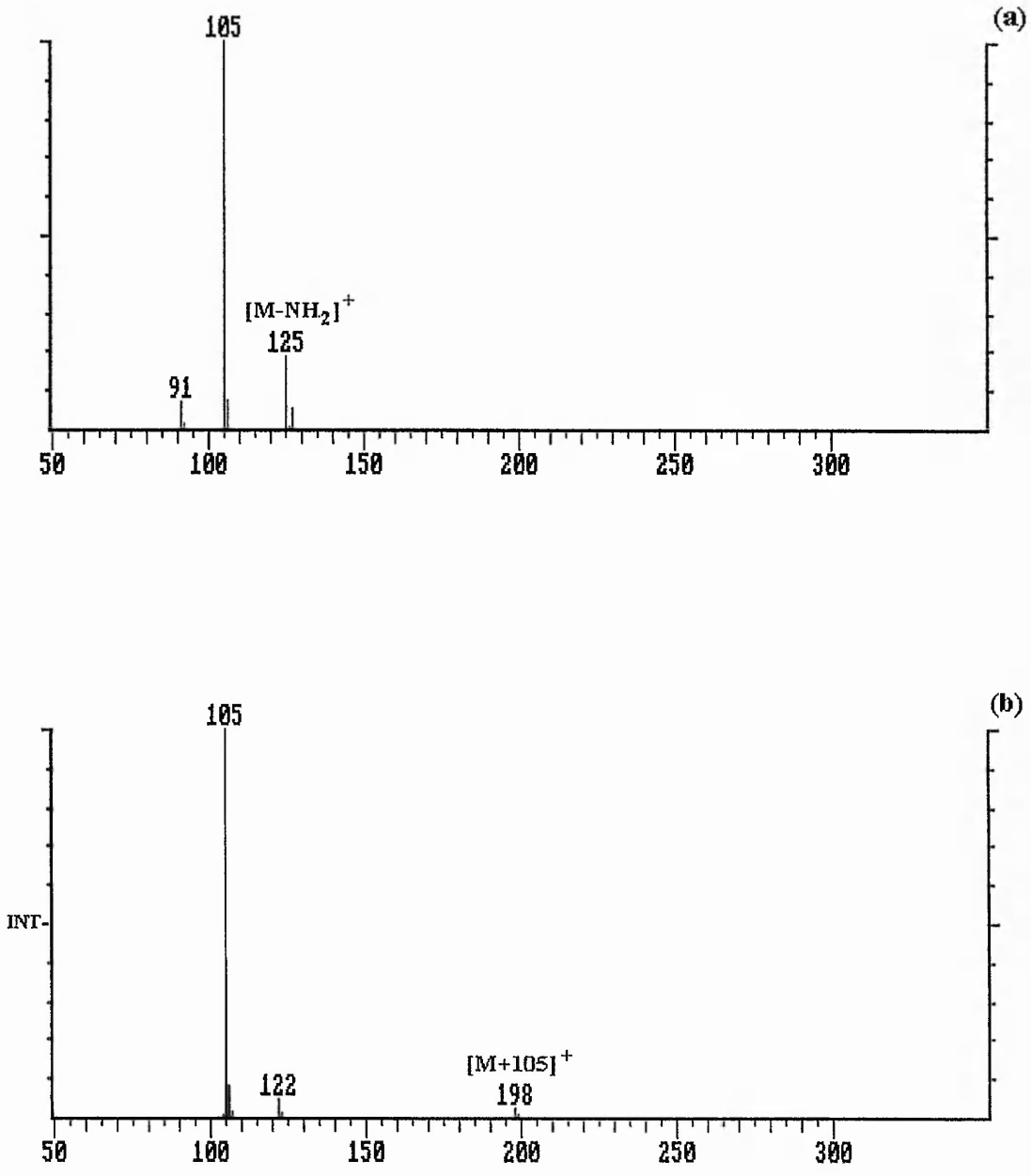

Figure 3.4. Spectra resulting from the reaction of $[C_6H_5CO]^+$ with (a) 4-chlorobenzyl amine and (b) aniline.

Primary amines

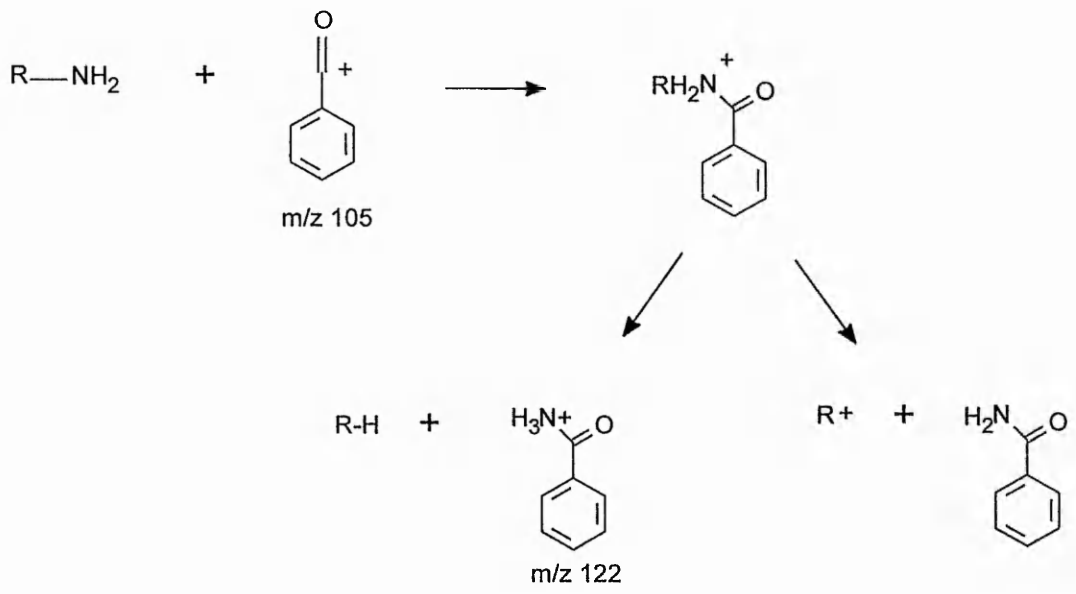

Scheme 3.1. The reaction pathways for the reaction of the benzoyl ion with primary amines

(ΔH_r = +278 kJ mol^{-1}). The appearance of the $[M\text{-}NH_2]^+$ ion from 4-chlorobenzylamine is calculated to be exothermic (ΔH_r = -37 kJ mol^{-1}) and indeed this ion was observed.

$$[C_6H_5CO]^+ + RNH_2 \rightarrow C_6H_5C(O)NH_2 + R^+$$

$$\Delta H_r = \Delta H_f(R^+) - \Delta H_f(RNH_2) - \Delta H_f([C_6H_5CO]^+) + \Delta H_f(\text{benzamide}) \qquad (3.1)$$

The formation of N-protonated benzamide from $[C_6H_5CO]^+$ is calculated to be exothermic by -161 kJ mol^{-1}, [4] and therefore the reaction to form the $[C_6H_5C(O)NH_3]^+$ ion should therefore be expected to be favoured if abstraction of NH_3 from the neutral

amine is endothermic by less than this amount. Hence, the $[C_6H_5C(O)NH_3]^+$ ion is observed for the reaction of the benzoyl ion with t-butylamine and sec-butylamine, since these reactions are calculated using equation 3.2 to be exothermic (ΔH_r = -57 kJ mol^{-1} and - 74 kJ mol^{-1} respectively).

$$[C_6H_5CO]^+ + RNH_2 \rightarrow [C_6H_5C(O)NH_3]^+ + (R\text{-}H)$$

$$\Delta H_r = \Delta H_f(R\text{-}H) - \Delta H_f(RNH_2) - \Delta H_f([C_6H_5CO]^+) + \Delta H_f([C_6H_5C(O)NH_3]^+) \quad (3.2)$$

The formation of the $[C_6H_5C(O)NH_3]^+$ ion from butylamine is also calculated to be exothermic (ΔH_r = - 69 kJ mol^{-1}), and it is therefore surprising that the $[C_6H_5C(O)NH_3]^+$ ion is not observed for the reaction with butylamine. Furthermore, the formation of the $[C_6H_5C(O)NH_3]^+$ ion from aniline is calculated to be strongly endothermic (ΔH_r = +568 kJ mol^{-1}) even though this ion is observed. It is not clear why the thermochemistry of some of these reactions do not relate to the observed spectra, but may be because the N-protonated benzamide ion formed initially undergoes a rearrangement process to form the stable ion at m/z 122.

Figure 3.5 shows the spectrum resulting from the reaction of $[C_6H_5CO]^+$ with Ropinirole (I), a drug used in the treatment of altzheimers disease (SmithKline Beecham). An $[M+105]^+$ adduct ion can be seen at m/z 365. There are two nitrogen

atoms on the molecule, therefore the adduct can posses two possible structures, **a** or **b**, illustrated in Scheme 3.2.

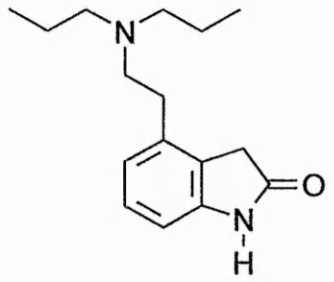

(I)

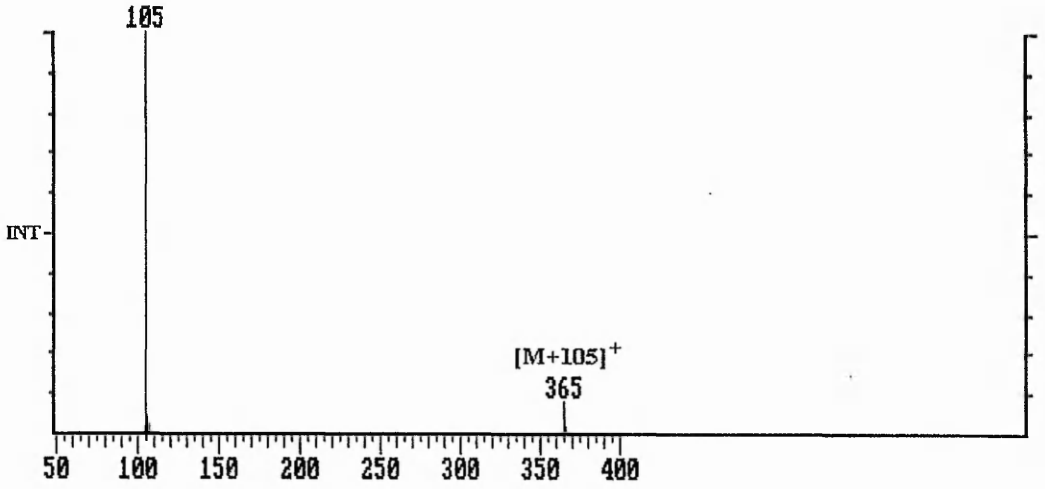

Figure 3.5. The spectrum resulting from the reaction of the benzoyl ion with ropinirole.

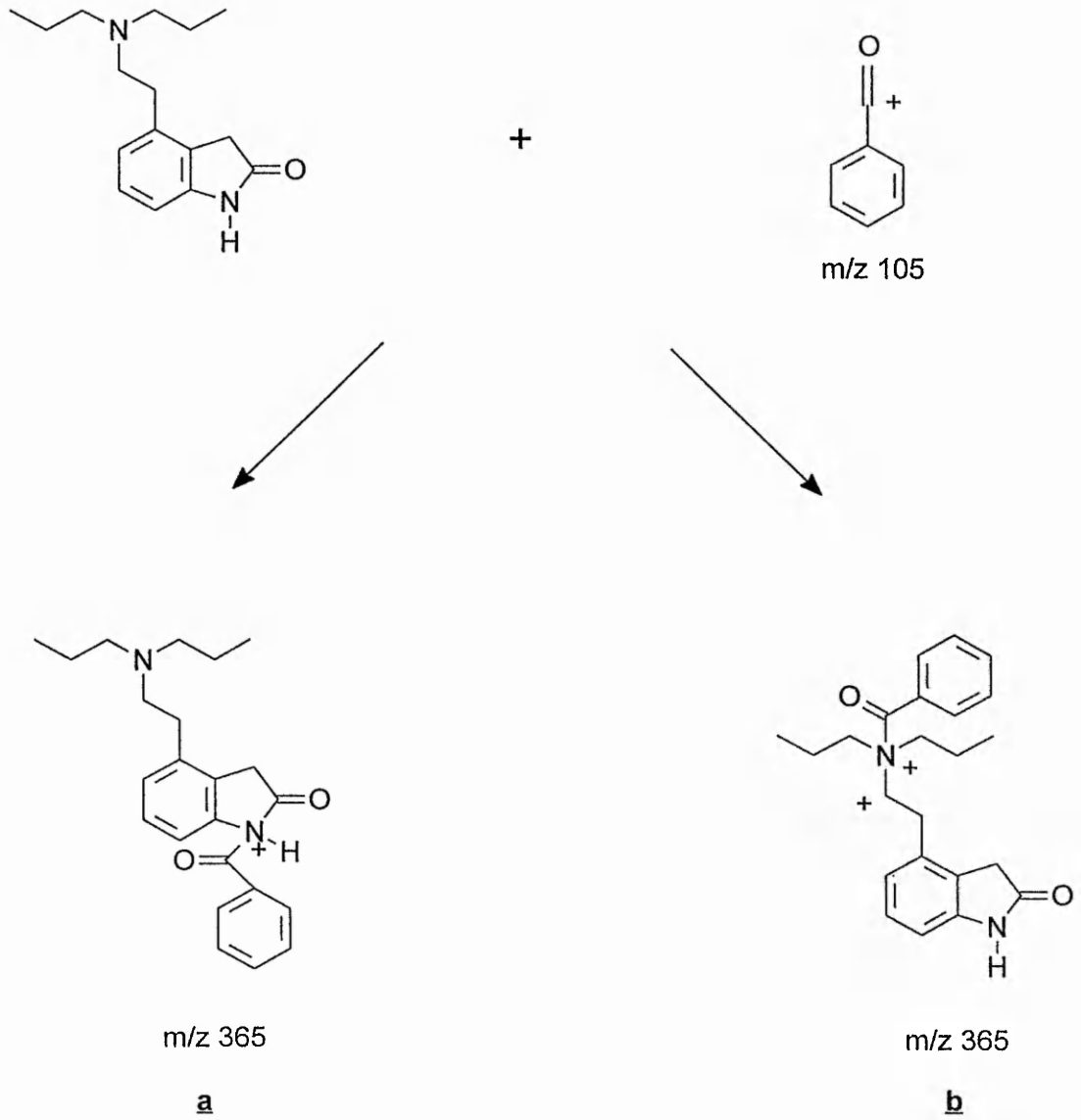

Scheme 3.2. Possible structures for the benzoyl ion - ropinirole adduct

Tandem mass spectrometry of the adduct using CAD with resonance excitation was employed to obtain structural information. The resulting product ion spectrum is shown in Figure 3.6. The base peak ion is at m/z 264, resulting from the loss of $(C_3H_7)_2NH$ from the adduct. Other important ions are those at m/z 321 $[M+105-C_3H_7]^+$, m/z 220 $[C_6H_5C(O)N(C_3H_7)_2CH_3]^+$ and m/z 114 $[(C_3H_7)_2NCH_2]^+$. These CAD processes are assigned in Scheme 3.3. The prominent m/z 264 ion indicates the possible structure for the adduct is that of structure **a**, as this ion results from the loss of $HN(C_3H_7)_2$ from the adduct, which is likely if benzoylation occurs on the ring nitrogen. Conversely, the weak ion at m/z 220 is likely to have been derived from the adduct of structure **b**, as this ion originates from benzoylation on the alkyl amine group. The product ion spectrum therefore suggests that electrophilic attack on the ring

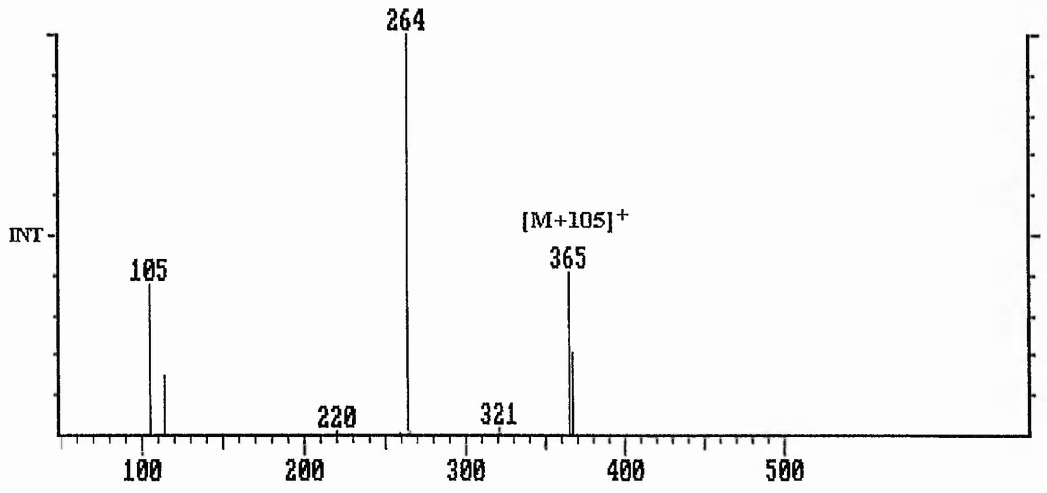

Figure 3.6. The CAD spectrum of the benzoyl ion-ropinirole adduct (m/z 365).

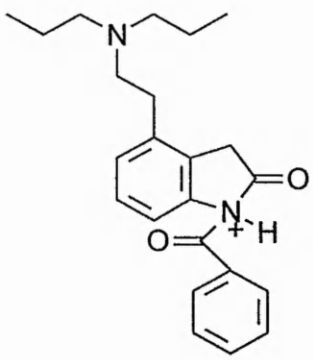

m/z 365

a

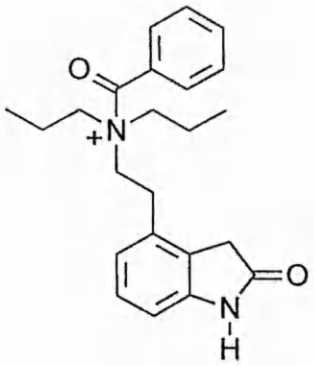

m/z 365

b

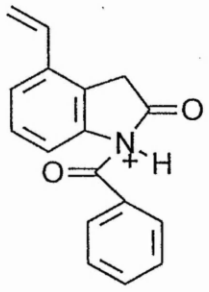

m/z 264

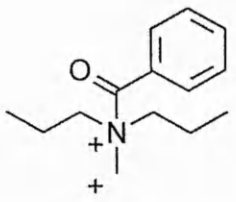

m/z 220

Scheme 3.3. CAD products of the benzoyl ion - ropinirole adduct

nitrogen to produce an adduct with structure **a** occurs predominately, probably due to adduct stabilisation *via* charge delocalisation through the aromatic ring.

3.4 CONCLUSION

Compounds containing the amine functional group undergo chemical ionisation reactions with the benzoyl cation within the pressure and time regimes of the quadrupole ion trap mass spectrometer to yield characteristic $[M+105]^+$, $[M-NH_2]^+$ and $[C_6H_5C(O)NH_3]^+$ ions. Product ion distributions are dependant on the amine group environment. These reactions suggest that the $[C_6H_5CO]^+$ ion is a potentially useful probe for the presence of the amino functional group. The ion at m/z 122 is a diagnostic ion for the presence of a compound possessing a primary amine functional group. For the case of Ropinirole, where adduct formation can occur at two nitrogen sites, attack of the nitrogen predominately on the ring is indicated by tandem mass spectrometric studies of the $[M+105]^+$ adduct ion. In a complex mixture, reactions of the benzoyl ion with hydroxy and amine functional groups would both occur, but the identity of these functional groups may be confirmed by the characteristic product ions produced by these reactions and also by tandem mass spectrometry on the adduct ions formed.

3.5 REFERENCES

1. Creaser, C.S. and Williamson, B.L., *J. Chem. Soc., Perkin Trans 2*, in press

2. Soni, M., Amy, J., Frankevich, V., Cooks, R.G., Taylor, D., Mckewan, A., Schwartz, J.C., *Rapid Comm. Mass Spectrom.*, 911, **9** (1995)

3. Eberlin, M.N. and Cooks, R.G., *Org. Mass Spectrom.*, 679, **28** (1993)

4. White, E.L.,Tabet, J.C. and Bursey, M., *Org. Mass. Spectrom.*, 132, **22** (1987)

5. Bruins, A.P. and Nibbering, N.M.M., *Tetrahedron Lett.*, 4491, **50** (1975)

6. Occhiucci, G., Cacace, F. and Speranza, M., J. Am. Chem. Soc., 872, **108** (1986)

7. Jardine, I. and Fenselau, C., *J. Am. Chem. Soc.*, 5086, **98** (1976)

8. Audier, H.E., Millet, A., Perret, C., Tabet, J.C. and Varenne, P., *Org. Mass Spectrom.*, 315, **13** (1978)

9. Westmore, J.B. and Alauddin, M.M., *Mass Spectrom. Revs.*, 381, **5** (1986)

10. Hunt, D.F., McEwen, C.N. and Upham, R.A., *Tetrahedron Lett.*, 4539, **47** (1971)

11. Buchanan, M.V., *Anal. Chem.*, 570, **54** (1982)

12. Harrison, A.G., *Chemical Ionisation Mass Spectra*, CRC (1992)

13. Lias, S.G., Bartmess, J.E., Liebmann, J.F., Holmes, J.L., Levin, R.D. and Mallard, W.G., *J. Phys. Chem. Ref. Data suppl.* 1, **17** (1988)

14. Busch, K.L., Glish, G.L., McLuckey, S.A., *Mass Spectrometry/Mass Spectrometry: techniques and applications in tandem mass spectrometry*, VCH, New York (1988)

15. McLafferty, F.W. (ed.), *Tandem Mass Spectrometry*, Wiley, New York (1983)

16. Yost, R.A., Enke, C.G., *Anal. Chem.*, 1251A, **51** (1979)

17. McLuckey, S.A., *J. Am. Chem. Mass Spectrom.*, 599, **3** (1992)

18. Kelly, P.E., Syka, J.E.P., Ceja, P.C., Stafford, G.C., Louris, J.N., Grutzmacher, H.F., Kuck, D. and Todd, J.F.J., *presented at the 34th annual meeting of the American Society for Mass Spectrometry*, Cinncinatti, OH, USA (1986)

19. Todd, J.F.J., *presented at the 2nd European Tandem Mass Spectrometry Conference*, Warwick, UK (1992)

CHAPTER 4

SELECTIVE CHEMICAL IONISATION REACTIONS OF THE BENZOYL CATION: PHARMACEUTICAL APPLICATIONS

4.1 INTRODUCTION

The benzoyl cation, $[C_6H_5CO]^+$, has been shown to undergo selective ion-molecule reactions with hydroxy compounds, Chapter 2 and amino containing compounds, Chapter 3. This ion has also been reported to react with unsaturated compounds, including isoprene, in a quadrupole ion trap. [1- 3] Reactions of the benzoyl ion using triple quadrupole and FT-ICR instruments have been shown for simple amines, [4] ammonia, [5] dienes [6] and 1, 3-dioxolanes. [7] The chemistry of the $[C_6H_5CO]^+$ ion has also been described in the 90-650 torr pressure range for periods of 15-20 months in which the benzoyl ion was generated by β decay of [1,4-T2]benzene in the presence of a large excess of carbon monoxide and products were identified by radio GC and HPLC. [8, 9] The $[C_6H_5CO]^+$ ion was characterised through these reactions as a mild, selective electrophile, preferring n-type nucleophile centres on the substrate rather than π-type centres, which undergoes benzoylation of phenol, aniline and anisole. [10] This ion shows limited reactivity towards other oxygenated compounds and therefore has potential as a selective reagent for chemical ionisation and as a probe for the presence of hydroxy, amino functionality or unsaturation.

The benzoyl cation has been shown to react with Flutriafol (a broad-spectrum fungicide, Zeneca, UK) and Flucanozole (an anti-fungal drug, Pfizer, UK) to produce $[M+105]^+$ and $[M-OH]^+$ ions (Chapter 2) and Ropinirole (an anti-

Parkinson's drug, SmithKline Beecham, UK) to produce an $[M+105]^+$ adduct ion (Chapter 3). In this chapter, an ion trap mass spectrometric study of the selectivity of the ion-molecule reactions of the benzoyl ions of the type $[C_6X_nH_{5-n}CO]^+$, (X= H, F, CH_3) with compounds of pharmaceutical interest containing hydroxy and other functional groups is described. The selectivity of the benzoyl cation as a selective CI reagent and as a probe for the presence of hydroxy, amino functionality or unsaturation is demonstrated by its reactions with the diketo / enol tautomers of methylacetoacetate, an analogue of a β-diketo ester used in the synthesis of the drug candidate SK&F96067 (SmithKline Beecham) [11] and also the product related intermediates of 2-(8-phenyloctyl)benzaldehyde (POB), [12] the precursor of SK&F104353 [13] (SmithKline Beecham), a peptidoleukotriene antagonist following GC separation.

4.2 EXPERIMENTAL

Experiments were performed using a quadrupole ion trap mass spectrometer (Finnigan MAT ITMS, San Jose, CA), operated at 120 °C. All chemicals were obtained from Aldrich Chemical Co. (Dorset, UK), except methylacetoacetate and the product related intermediates of 2-(8-phenyloctyl)benzaldehyde (POB), which were obtained from SmithKline Beecham R&D (Tonbridge, UK) and used without further purification. Acetophenone, 2',3',4',5',6'-pentafluoroacetophenone, 3',4',5'-trifluoroacetophenone and 4'-methylacetophenone were introduced *via* a leak valve (Megg itt Avionics, Portsmouth, UK). Reagent pressure was $2x10^{-6}$ torr

and helium bath gas, introduced *via* another leak valve (Meggritti Avionics, Portsmouth, UK) was maintained at a pressure $1x10^{-4}$ torr. All pressures were uncorrected and measured by the ion trap vacuum chamber ion gauge (Granville-Phillips).

In a typical experiment, the benzoyl ion was generated as an electron ionisation fragment of acetophenone, isolated using resonance hole isolation, [14] and allowed to react with neutral sample vapour for 100 ms. The $[C_6F_5CO]^+$, $[C_6H_2F_3CO]^+$ and $[4\text{-}MeC_6H_4CO]^+$ ions were generated as EI fragments from 2',3',4',5',6'-pentafluoroacetophenone, 2',3',4'-trifluoroacetophenone and 4'-methylacetophenone respectively. Tandem mass spectrometry [15, 16] using collisionally activated dissociation (CAD) [17, 18] was employed to give structural information on adduct ions. Resonance hole isolation was employed to isolate the precursor ion followed by the application of a tickle voltage to the end cap electrodes to resonantly excite the precursor ion.[19] The scan routine for this experiment is shown in Figure 4.1.

Samples were introduced using a Varian 3400 gas chromatograph coupled to the quadrupole ion trap. The capillary column used to separate the keto/enol tautomers of methylacetoacetate was a 15 m x 0.2 mm id HP-1 column (Hewlett Packard, Sunnyvale, CA, USA). The GC conditions were as follows: injector temperature, 280 °C; transfer line, 250 °C; 1μL splitless injector (split flow at 15 mL / min); helium head pressure, 5 psi. The column oven temperature was 50 °C for 1 min,

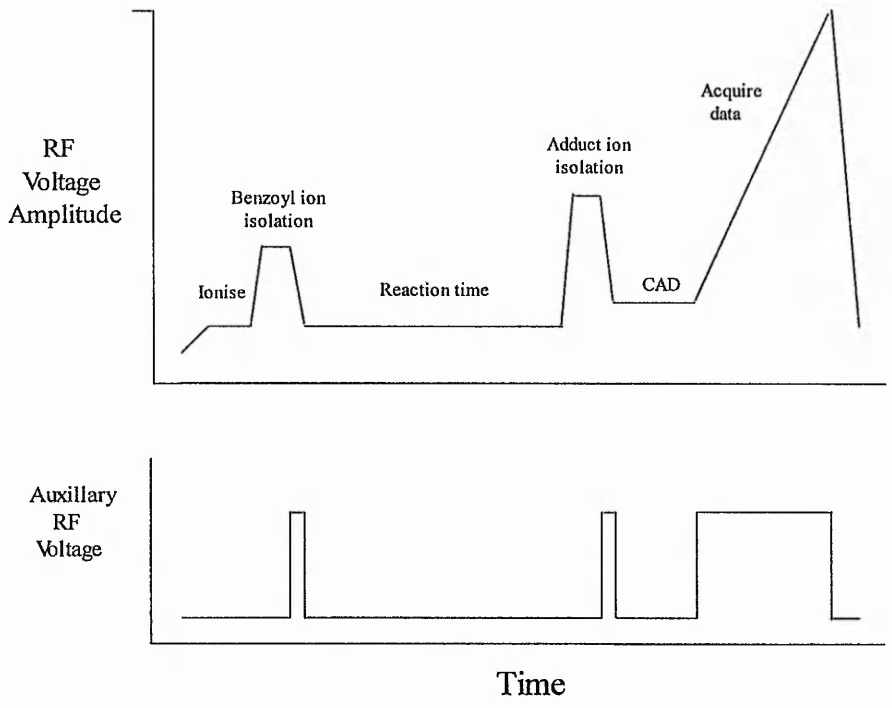

Figure 4.1. The scan routine for the CAD of adduct ions formed by reactions of the benzoyl ion

raised to 200 °C at 10 °C min^{-1}. The capillary column used to separate the POB components was a 30 m x 0.25 mm id DB17 column (J & W Scientific, California, USA). The GC conditions were as follows: injector temperature, 280 °C; transfer line, 250 °C; 1 μL splitless injection (split flow at 30 mL / min); helium head pressure, 15 psi. The column oven temperature was 40 °C for 1 min, raised to 280 °C at 20 °C min^{-1} and held for 10 min.

4.3 RESULTS AND DISCUSSION

4.3.1 Keto / enol tautomers of methylacetoacetate

Carbonyl compounds containing an alpha hydrogen can undergo keto-enol tautomerism as shown in Scheme 4.2. For simple compounds (R_3 = H, alkyl, OR etc.) the equilibrium lies well to the left due to the difference in bond energies between the two forms. However, if R_2 contains a multiple bond that may be conjugated with the enolic double bond, the equilibrium will be shifted to the right. During routine testing by GC, the β-diketo ester used in the synthesis of the drug candidate SK&F96067 exhibits poor peak shape which is postulated to be due to the partial separation of the keto-enol form from the diketo form, [11] as separation of aliphatic 1,3 diketones using GC has been previously reported. [20]

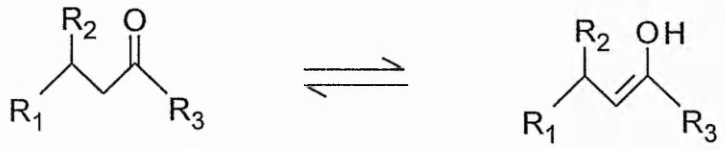

Scheme 4.2. Keto / enol tautomerism

The EI GC/MS chromatogram of the β-diketo ester methylacetoacetate (R_1 = CH_3, R_2 = O and R_3 = OCH_3) is shown in Figure 4.2(a) using the reported GC conditions. [11] The diketo / enol tautomers can be seen to be well resolved giving the EI spectra shown in Figure 4.3(a) and (b). The EI spectra could distinguish but

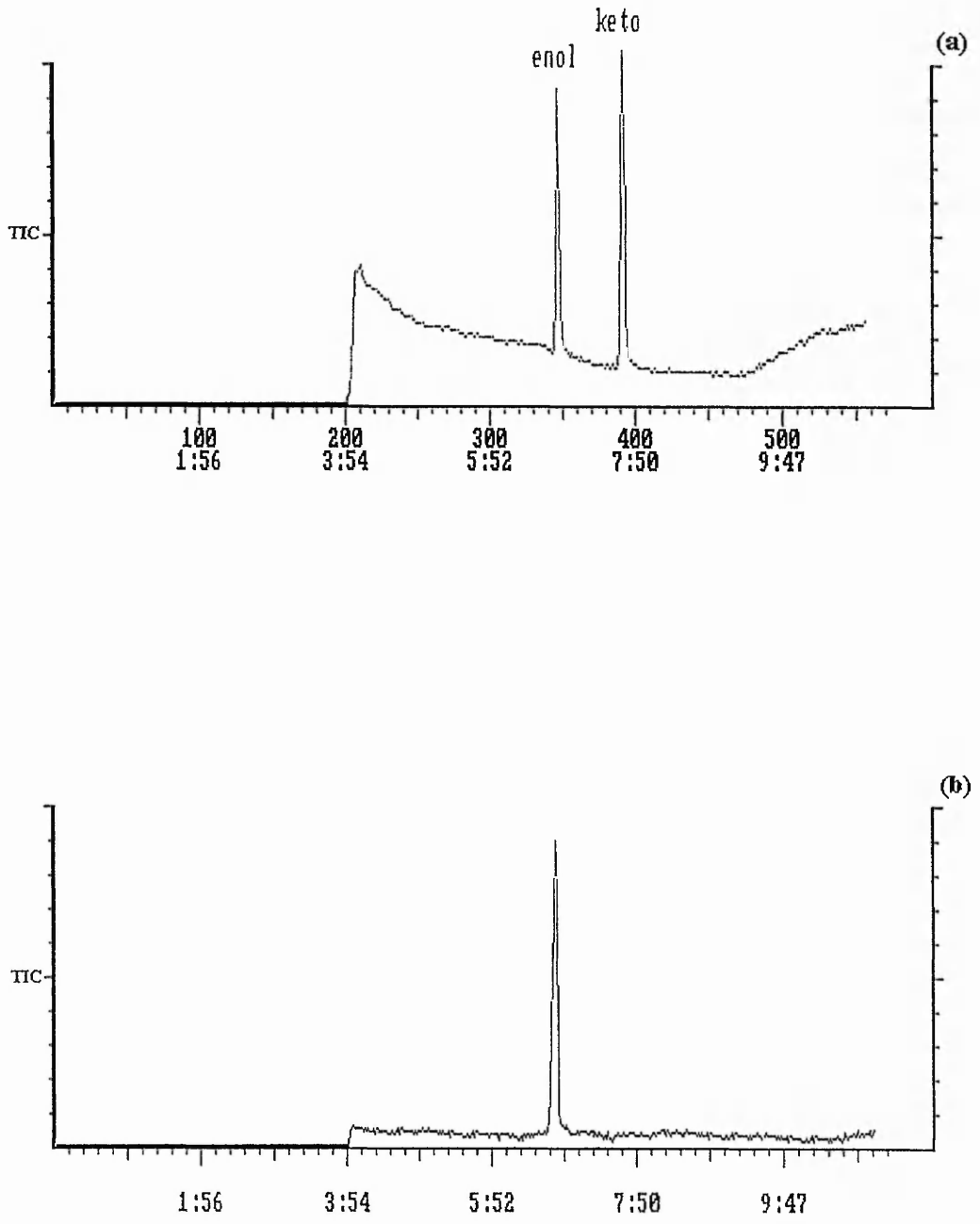

Figure 4.2. EI GC/MS (a) and (b) $[C_6H_5CO]^+$ CI GC/MS of methylacetoacetate.

not unambiguously assign these tautomers. The corresponding benzoyl cation, $[C_6H_5CO]^+$, selective CI GC/MS chromatogram of methylacetoacetate is shown in Figure 4.2(b). Residual precursor ion, m/z 105, was removed from the trap by resonance ejection prior to the spectral acquisition scan. Reaction with the enol tautomer is observed, Figure 4.3(c), in which two ions were observed at m/z 85 and m/z 161 assigned to fragment products of the electrophilic addition of $[C_6H_5CO]^+$ to the double bond of the enol tautomer. There was no reaction observed with the diketo tautomer and a mechanism for this reaction is proposed in Scheme 4.2. Reaction at the double bond is probably preferred due to intramolecular hydrogen bonding involving the hydroxy group. This allows assignment of the enol and keto peaks which was not possible by EI GC/MS.

The reactivity of the diketo / enol tautomers was further investigated by their reactions with the $[C_6F_3H_2CO]^+$ substituted benzoyl ion. The TIC for the reaction of $[C_6F_3H_2CO]^+$ with the keto-enol tautomers of methylacetoacetate is illustrated in Figure 4.4. Residual precursor was removed from the trap by resonance ejection prior to the spectral acquisition scan.

It can be seen that the a reaction is observed with the diketo tautomer as well as the enol tautomer, which may be attributed to the increased electrophilicity of the $[C_6F_3H_2CO]^+$ ion. The product ion abundance for the enol tautomer is greater by around a factor of three than that for the diketo tautomer. The spectra resulting from these reactions are shown in Figure 4.5. The spectra can be seen to differ,

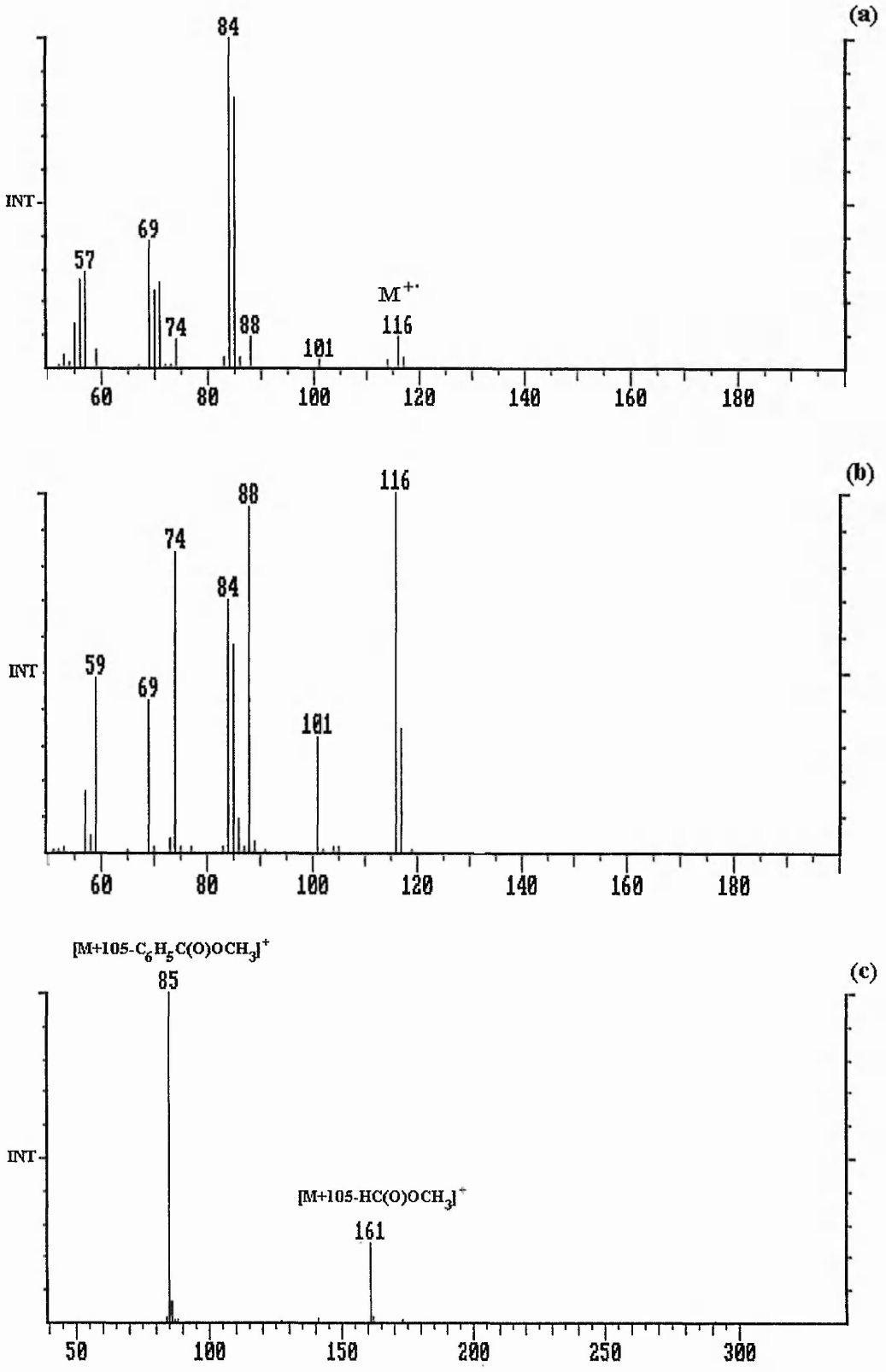

Figure 4.3. EI mass spectra of (a) enol and (b) diketo tautomers of methylacetoacetate and (c) mass spectrum resulting from the benzoyl ion reaction with the enol tautomer of methylacetoacetate.

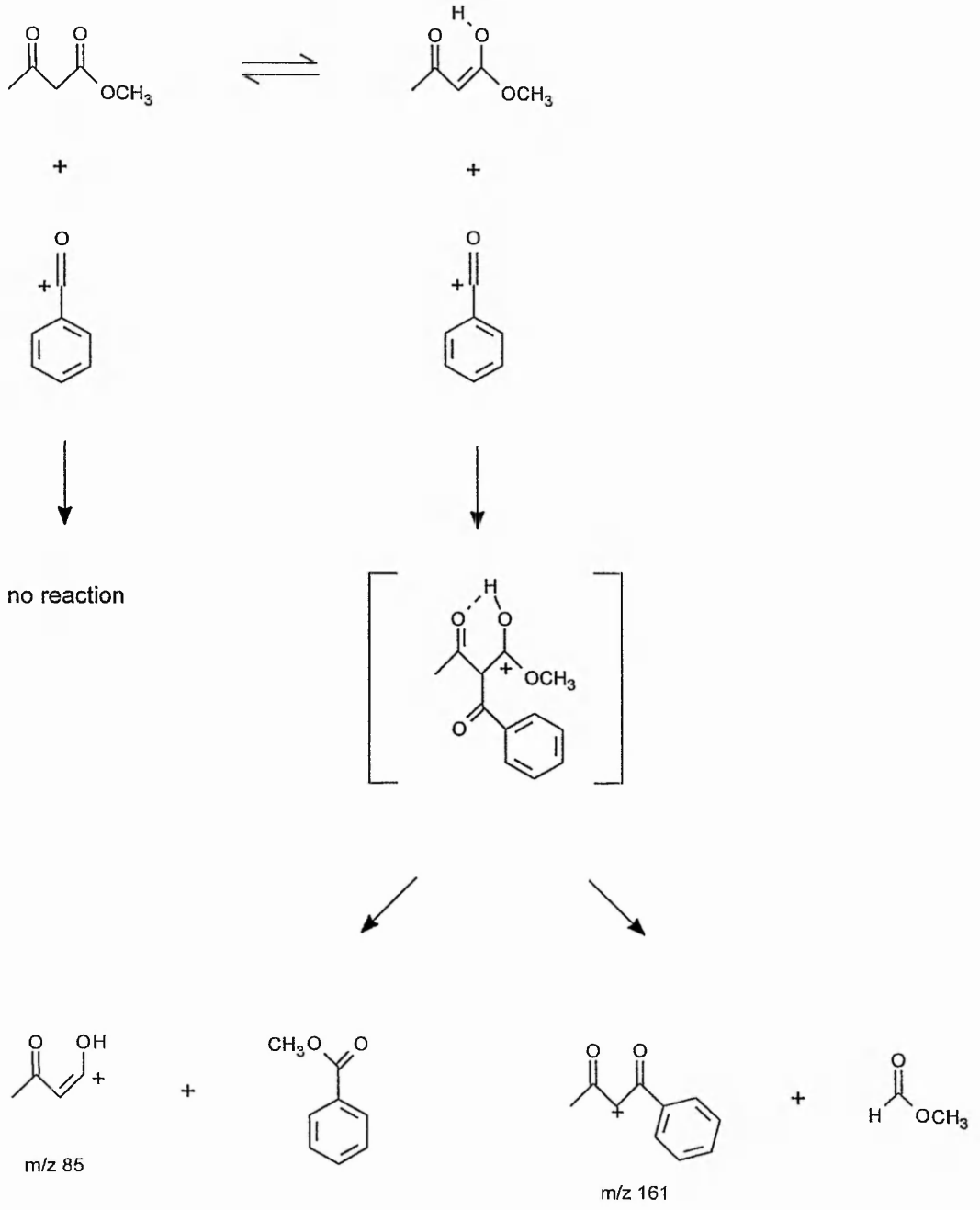

Scheme 4.2. Benzoyl ion CI of keto-enol tautomers of methylacetoacetate.

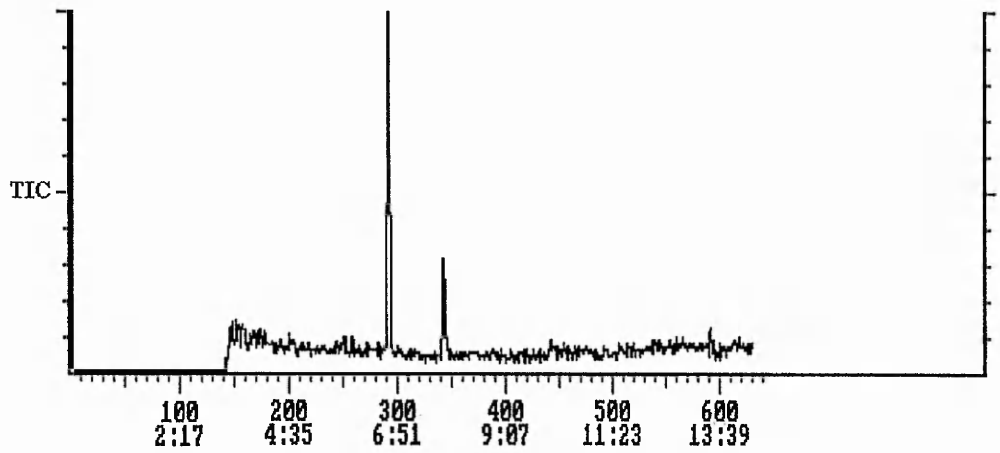

Figure 4.4. TIC for the $[C_6F_3H_2CO]^+$ CI GC/MS of methylacetoacetate.

allowing the diketo and enol tautomers to be distinguished. The enol product spectrum (Figure 4.5(a) was dominated by an ion at m/z 243, but the $[M\text{-}OH]^+$ ion at m/z 99 ion was absent. A similar effect was observed for the reaction of the $[C_6H_5CO]^+$ ion with the enol tautomer, in which no $[M\text{-}OH]^+$ ion was observed, probably because of the effect of the strong hydrogen bonding between the keto oxygen and the hydroxy group. The most likely point of attachment of the $[C_6F_3H_2CO]^+$ in the adduct ion is at the carbon - carbon double bond of the enol tautomer (as for the $[C_6H_5CO]^+$ ion), as illustrated in Scheme 4.4.

The spectrum of the products of the $[C_6F_3H_2CO]^+$ reaction of the diketo tautomer contained an adduct ion at m/z 275, which was not present in the enol product spectrum, as well as an $[M\text{-}OH]^+$ ion at m/z 99, indicating electrophilic attack by the $[C_6F_3H_2CO]^+$ ion occurs at one of the carbonyl oxygen atoms on the

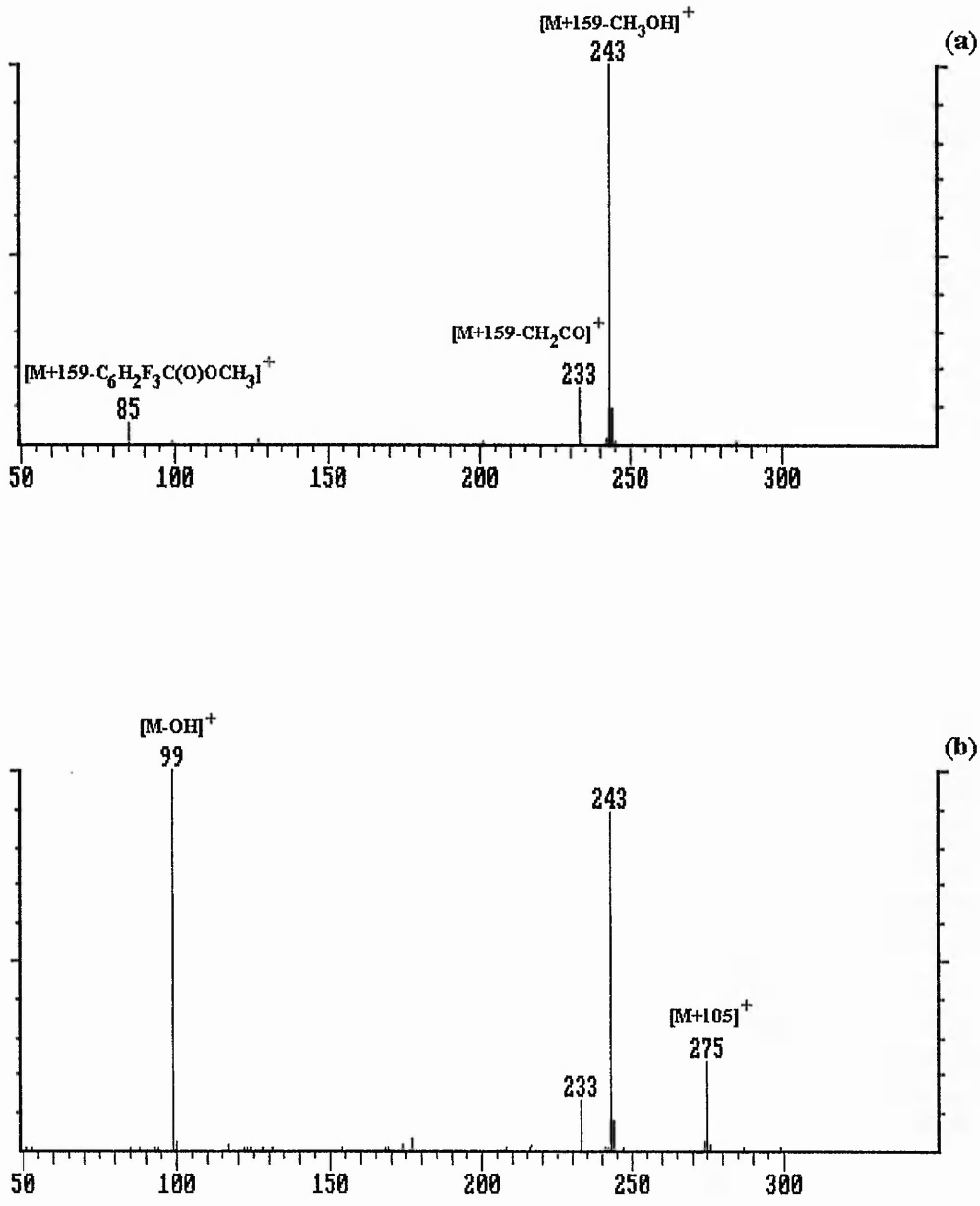

Figure 4.5. Spectra resulting from the reaction of $[C_6F_3H_2CO]^+$ with (a) enol and (b) keto tautomers of methylacetoacetate.

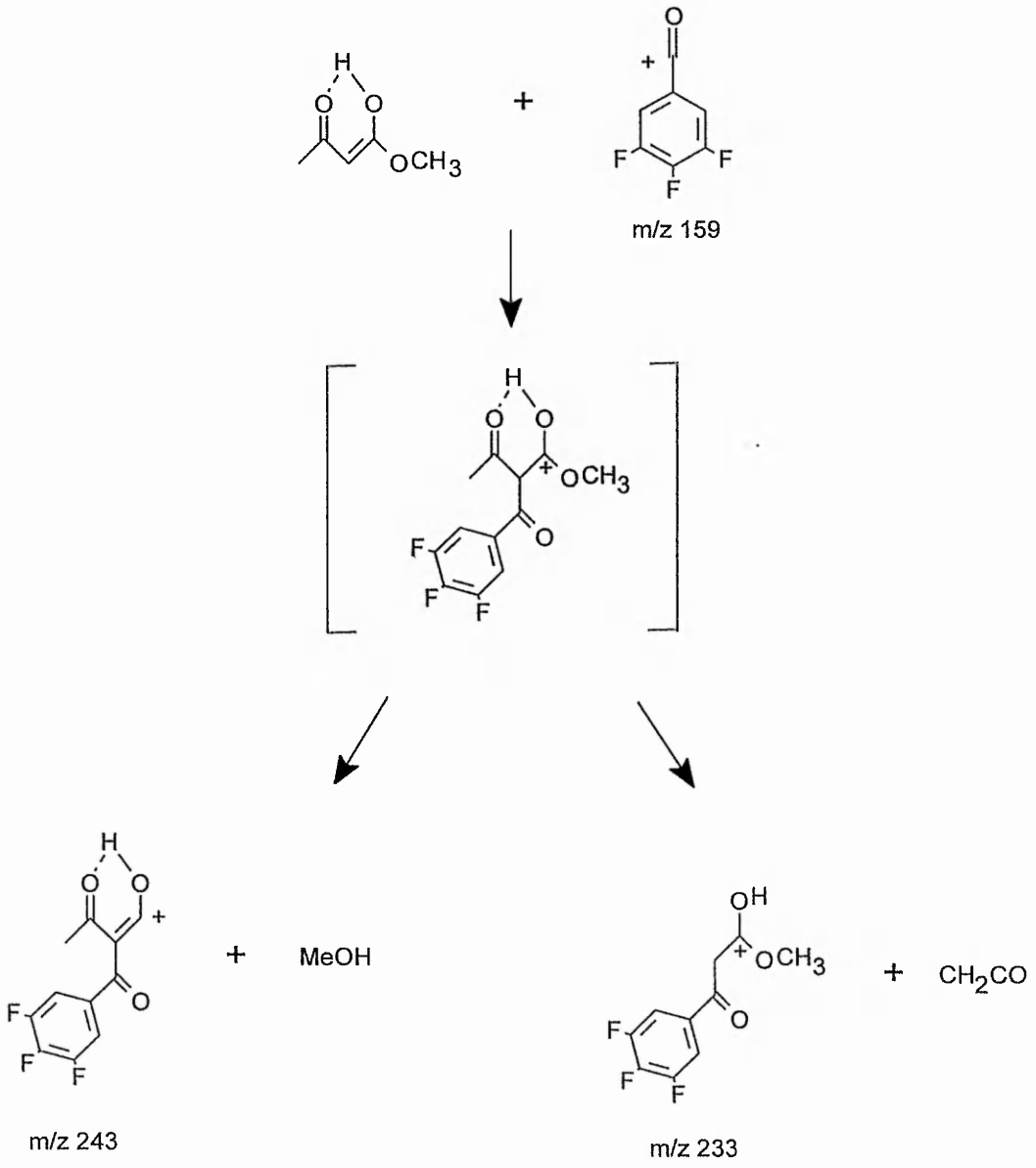

Scheme 4.4. Reaction pathway for the $[C_6F_3H_2CO]^+$ CI of the enol tautomer of methylacetoacetate.

methylacetoacetate molecule. The reaction pathway for these ions is illustrated in Scheme 4.5.

The structures of the adduct and fragment ions were further investigated by tandem mass spectrometry with CAD. Figure 4.6 shows the CAD product spectrum for the m/z 275 ion. Two ions at m/z 233, $[M\text{-}CH_2CO]^+$ and m/z 159, $[C_6F_3H_2CO]^+$, were formed but there was no ion at m/z 243, $[M\text{-}CH_3OH]^+$, or m/z 99, $[M\text{-}OH]^+$, the base peak in the original spectrum. This suggests that the m/z 243 and m/z 99 ions do not originate from the adduct ion. This can be rationalised if the formation of the adduct ion forms two structures, one long lived structure which is the ion seen at m/z 275 and dissociates to form m/z 233 and m/z 159 and one short lived structure which immediately dissociates to form the m/z 243 and m/z 99 ions. In order to form the ion at m/z 233, CH_2CO must be lost from the adduct. Without rearrangement, this can only occur if the diketo adduct has structure **a** and not **b**.

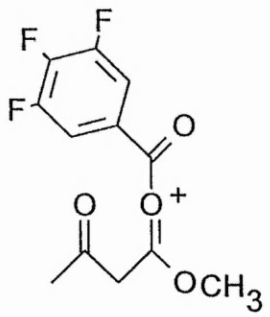

a

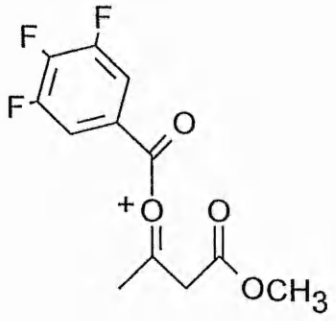

b

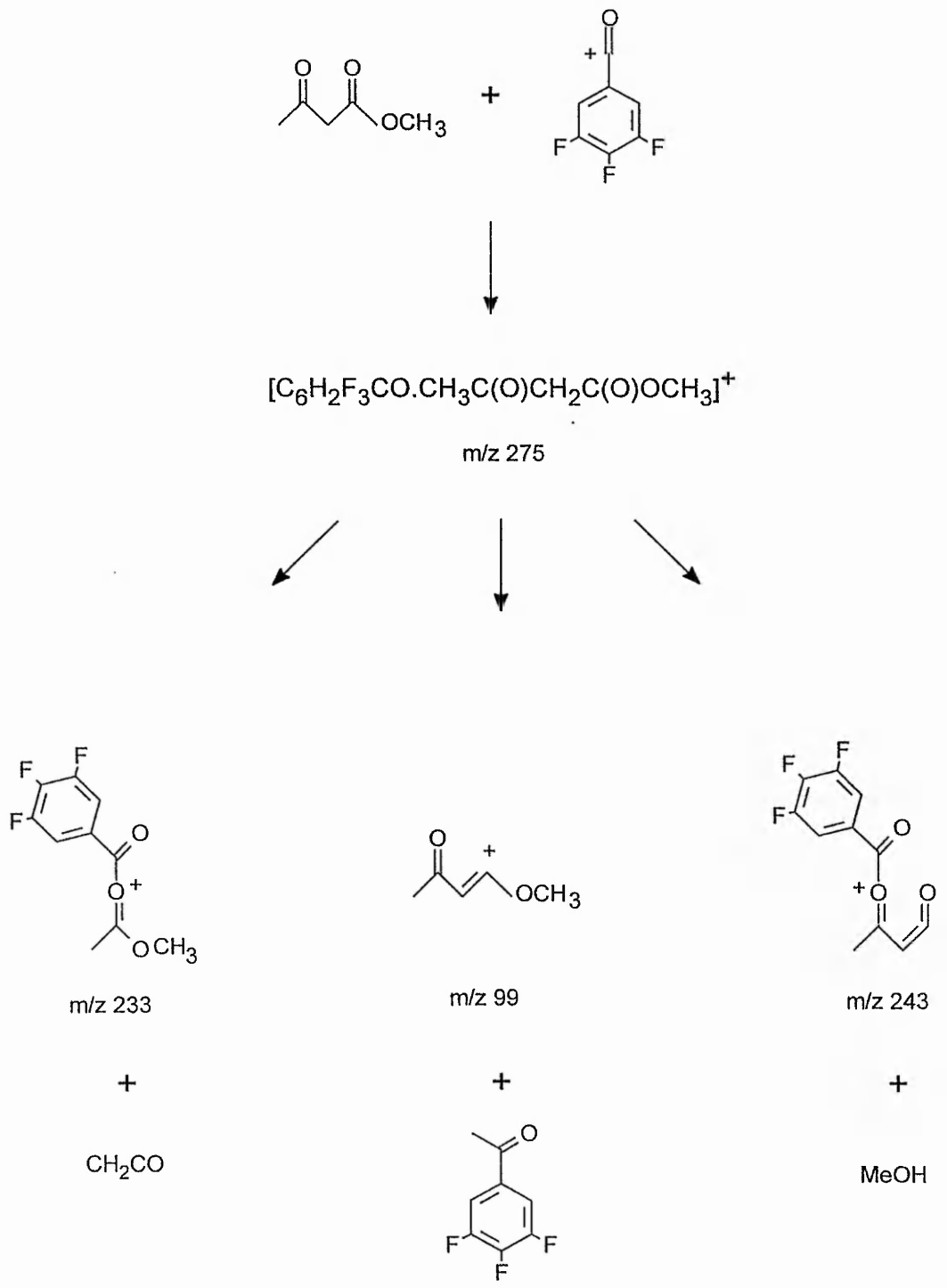

Scheme 4.5. Reaction pathway for the $[C_6F_3H_2CO]^+$ CI of the keto tautomer of methylacetoacetate.

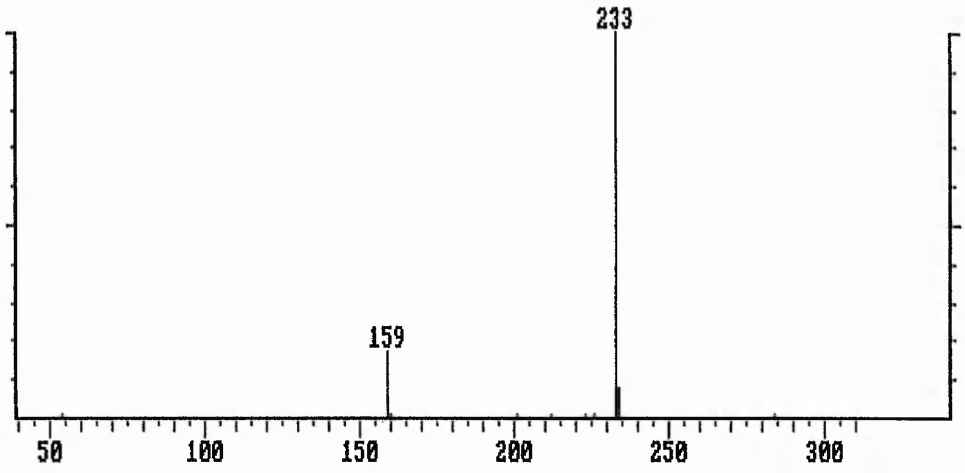

Figure 4.6. CAD products of the $[M+C_6F_3H_2CO]^+$ adduct ion at m/z 275

This indicates the possible structures of the adduct ion, which depend on the point of attachment of the $[C_6F_3H_2CO]^+$ ion. The electrophilic addition product possessing structure **a** is the long lived species observed at m/z 275 which dissociates to form m/z 233 and m/z 159 ions, and the addition product possessing structure **b** is the short lived species which immediately dissociates to form the ion at m/z 243 and m/z 99. A reaction procedure for this is proposed in Scheme 4.6. The structure of the ion at m/z 243 was investigated by tandem mass spectrometry using CAD. Figure 4.7 shows the product ion spectra for the m/z 243 ion derived from the diketo and enol tautomers. Both ions dissociate to give the $[C_6F_3H_2CO]^+$ ion at m/z 159, which is consistent with the structures proposed.

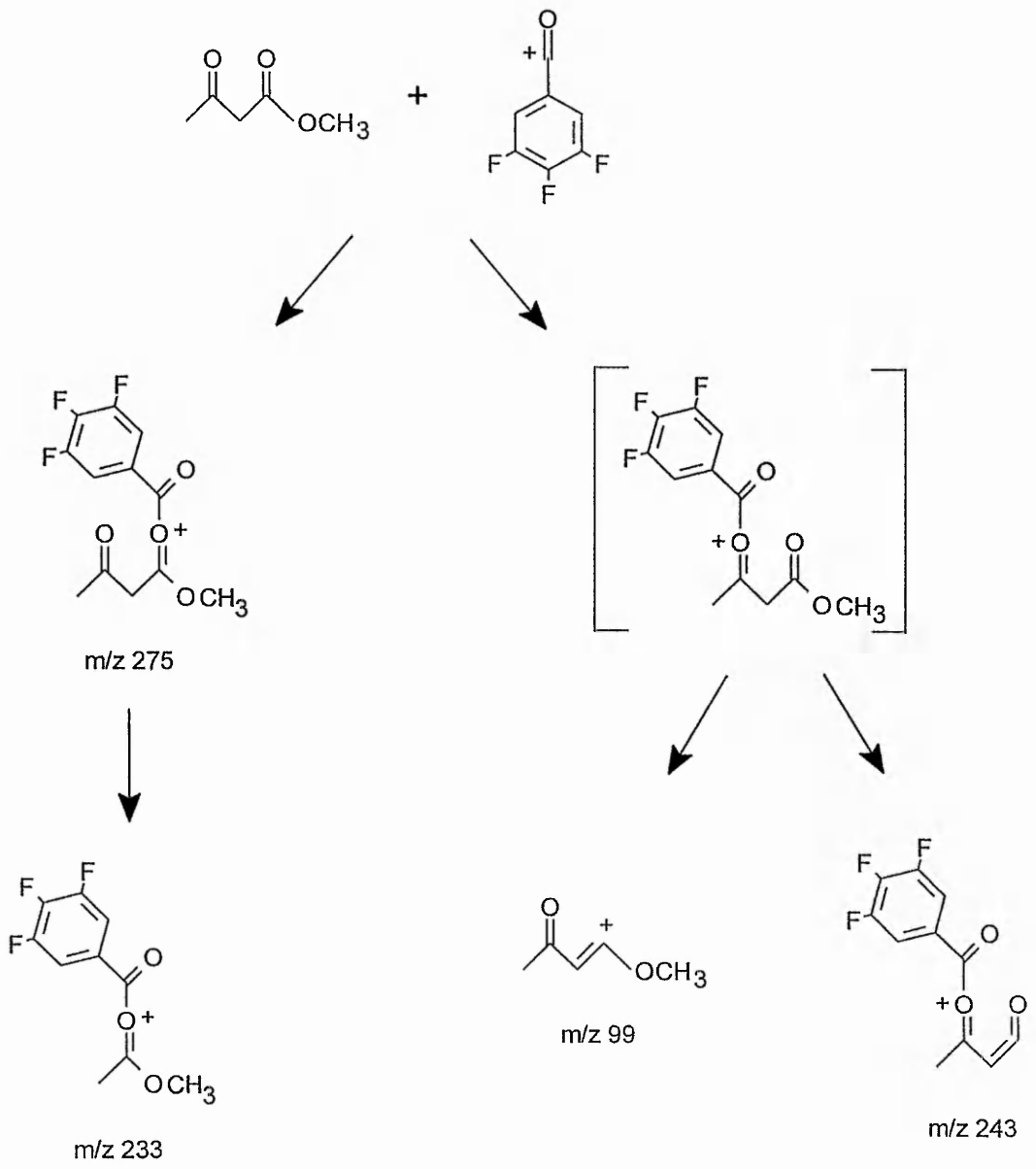

Scheme 4.6. The fragmentation pathway for the electrophilic addition products formed between $[C_6H_2F_3CO]^+$ and the diketo tautomer of methylacetoacetate

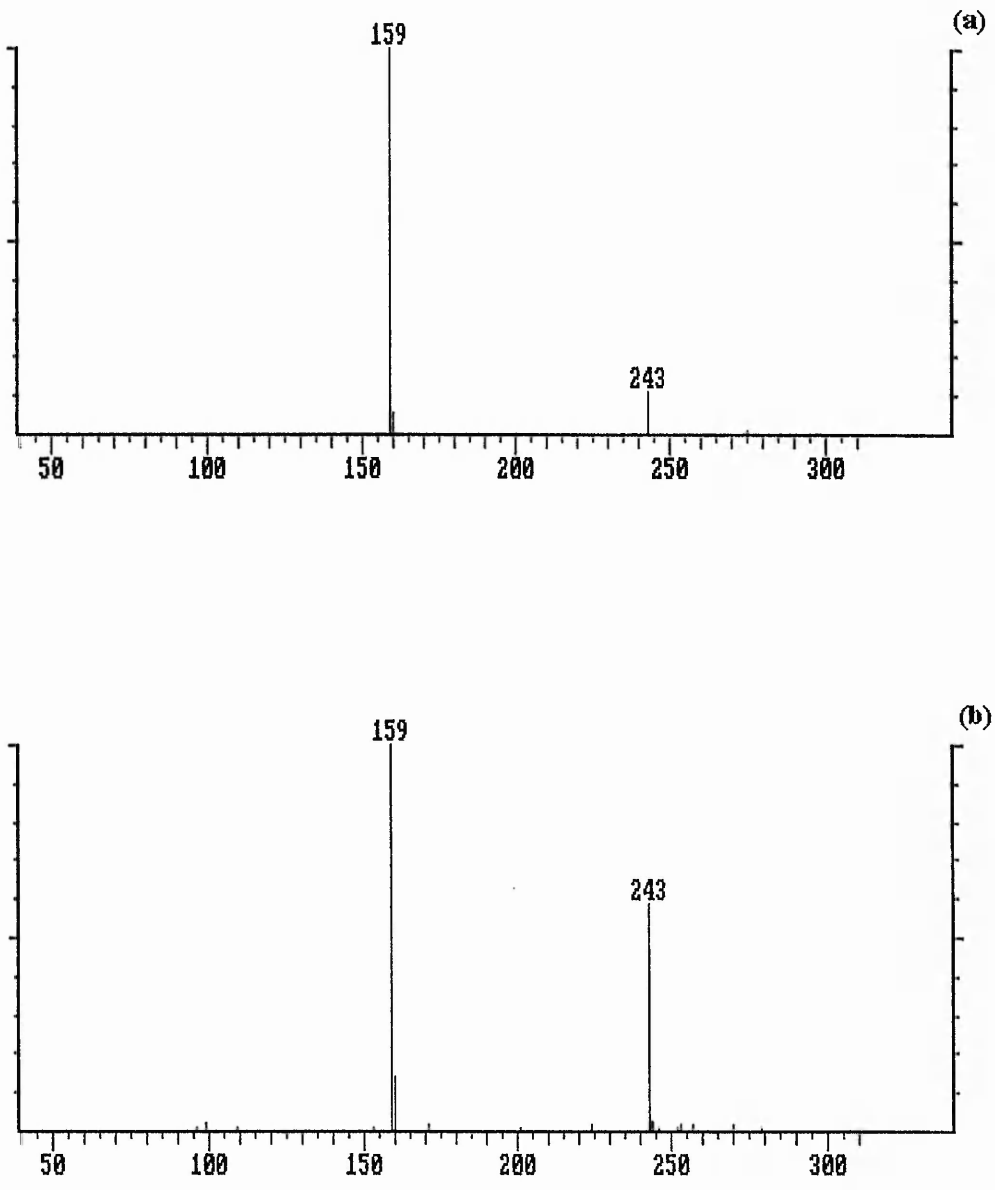

Figure 4.7. The CAD of the $[M+C_6F_3H_2CO\text{-}MeOH]^+$ ion at m/z 243 for (a) the enol and (b) the keto tautomers of methylacetoacetate.

The increased electrophilicity of the $[C_6F_3H_2CO]^+$ ion caused reactions to occur with both the diketo and enol tautomers of methylacetoacetate giving spectra that allowed easy differentiation of the two tautomers, which was not possible by conventional EI GC/MS techniques. Fragmentation products and tandem mass spectrometry suggest electrophilic addition by the $[C_6F_3H_2CO]^+$ ion with the enol tautomer occurs at the carbon - carbon double bond and the reaction with the diketo tautomer occurs at the oxygen atoms of both carbonyl groups.

4.3.2 The product related intermediates of 2-(8-phenyloctyl)benzaldehyde (POB)

2-(8-phenyloctyl)benzaldehyde, (POB), is the precursor of SK&F104353 (SmithKline Beecham), a peptidoleukotriene antagonist. The synthesis of POB results in the formation of many product related intermediates, which are often difficult to separate by GC. Therefore, the selectivity of the benzoyl cation as a CI reagent was applied to this complicated pharmaceutical mixture.

Table 4.1 illustrates the product related intermediates of POB. Figure 4.8a shows the total ion current observed for the EI GC/MS analysis of this mixture. The elution order is 1=benzyl chloride, 2=benzyl alcohol, 3=σ-tolualdehyde, 4=phenylheptene, 5=SB205268, 6=bibenzyl, 7=phenylheptyl chloride, 8=phenylheptyl alcohol, 9=dichlorodecane, 10=diphenyloctyl. The products of the ion-molecule reactions of the benzoyl ions with these intermediates (100 ms reaction time) in the ion trap are shown in Figure 4.8b-d. In each case residual

precursor was removed from the trap by resonance ejection prior to the spectral acquisition scan.

The $[C_6H_5CO]^+$ cation reacts with only four components of the mixture; benzyl alcohol, phenylheptene, bibenzyl and phenylheptyl alcohol (Figure 4.8b). Both hydroxy containing compounds, benzyl alcohol and phenylheptyl alcohol (Table 4.1) react to produce an $[M\text{-}OH]^+$ hydroxy abstraction ion as expected for these aromatic alcohols (Chapter2, Table 2.1). Ions at m/z 197, m/z 181 and m/z 169 in the benzyl alcohol spectrum were also present in spectrum resulting from the reaction between $[C_6H_5CO]^+$ and benzyl alcohol introduced on the probe.

Phenylheptene formed an $[M+105]^+$ adduct ion at m/z 279 (Scheme 4.7). Bibenzyl was ionised through a side reaction, which lead to the formation of $M^{+\cdot}$ by charge exchange. No reaction was observed with the nitrogen containing compound SB205268, this is probably due to the steric crowding around the nitrogen atom. The spectra resulting from the reaction of $[C_6H_5CO]^+$ with benzyl alcohol and phenylheptene are shown in Figure 4.9. The selective ionisation reactions of the $[C_6H_5CO]^+$ ion thus both greatly simplify the chromatogram and allow some assignment of functionality.

Table 4.1. Product related intermediates of 2-(8-phenyloctyl)benzaldehyde (POB)

COMPOUND	STRUCTURE
Benzyl chloride	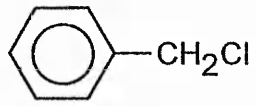
Benzyl alcohol	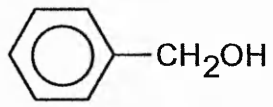
σ-tolualdehyde	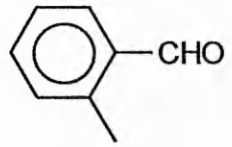
Phenyl heptene	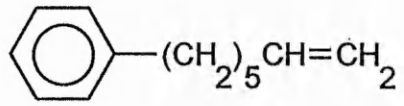
SB205268	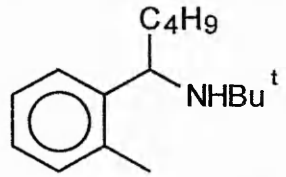
Bibenzyl	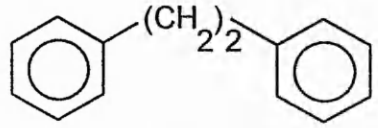
Phenylheptyl chloride	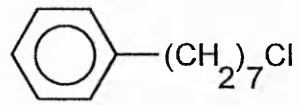
Phenylheptyl alcohol	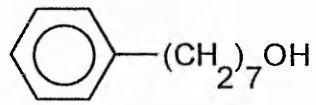
Dichlorodecane	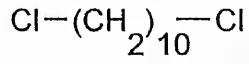
Diphenyloctyl	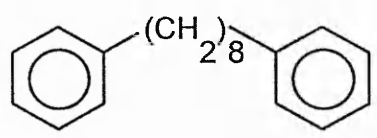

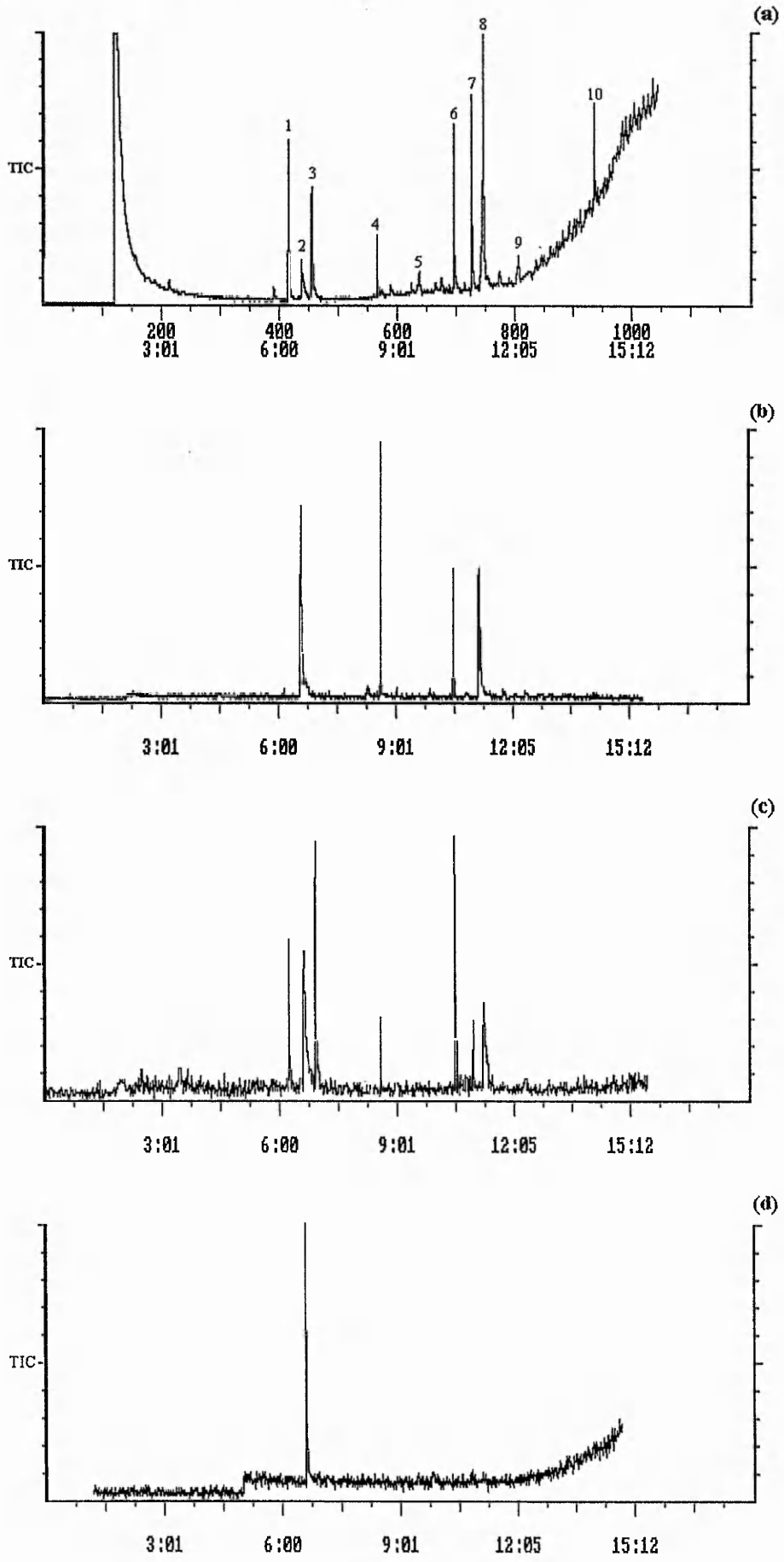

Figure 4.8. TIC for (a) EI, (b) $[C_6H_5CO]^+$ CI, (c) $[C_6F_5CO]^+$ CI and (d) $[4\text{-}MeC_6H_4CO]^+$ CI GC/MS of the product related intermediates of POB

The reactions of the pentaflurobenzoyl ion, a much stronger electrophile than $[C_6H_5CO]^+$ are illustrated in Figure 4.8c. The greater reactivity of this ion is apparent from the larger number of components which undergo ionising reactions. Benzyl alcohol yields product ions as before, and phenylheptyl alcohol produces $[M\text{-}OH]^+$, $[M+195\text{-}H_2O]^+$ and fragment ions from the hydroxy abstraction ion. However, the greater electrophilicity of the $[C_6F_5CO]^+$ ion also results in formation of an $[M\text{-}Cl]^+$ chloride abstraction ion from the reaction with benzyl chloride. Similarly, phenylheptyl chloride produces an $[M+195]^+$ adduct and an $[M\text{-}H]^+$ ion. The reaction with σ-tolualdehyde produces an adduct ion at m/z 315, an $[M\text{-}OH]^+$ hydroxy abstraction ion and an $[M\text{-}H]^+$ hydride abstraction ion. An ion at m/z 119 is produced from the reaction with phenylheptene, which is assigned to $[M+195\text{-}C_6F_5COC_4H_7]^+$. Bibenzyl also reacted to form $[M+195]^+$ and $[M+195\text{-}H_2O]^+$ ions in addition to the $M^{+\cdot}$ charge exchange products observed for the reaction with $[C_6H_5CO]^+$. The spectra resulting from the reaction of $[C_6F_5CO]^+$ with benzyl alcohol and phenylheptyl chloride are shown in Figure 4.10.

The reaction pathway of $[C_6F_5CO]^+$ with phenylheptyl chloride is illustrated in Scheme 4.8. Figure 4.8d illustrates the reactions of the 4-methylbenzoyl ion, $[CH_3C_6H_4CO]^+$, a weaker electrophile than $[C_6H_5CO]^+$, with the product related intermediates of POB. Only one reaction is observed, with benzyl alcohol to produce the characteristic $[M\text{-}OH]^+$ ion. The spectrum from this reaction is illustrated in Figure 4.11. The reactions of the benzoyl ions of the type

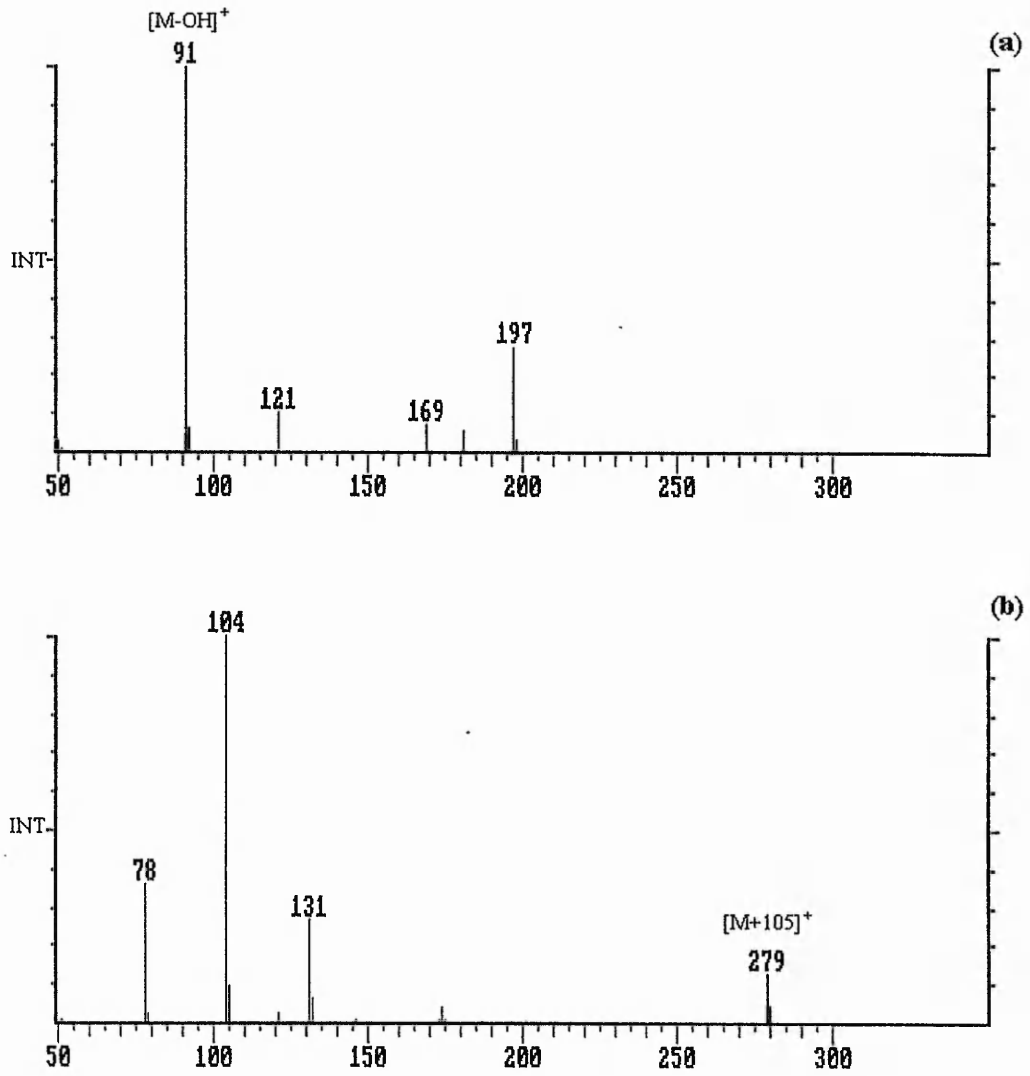

Figure 4.9. Spectra resulting from the reaction of $[C_6H_5CO]^+$ with (a) benzyl alcohol and (b) phenylheptene

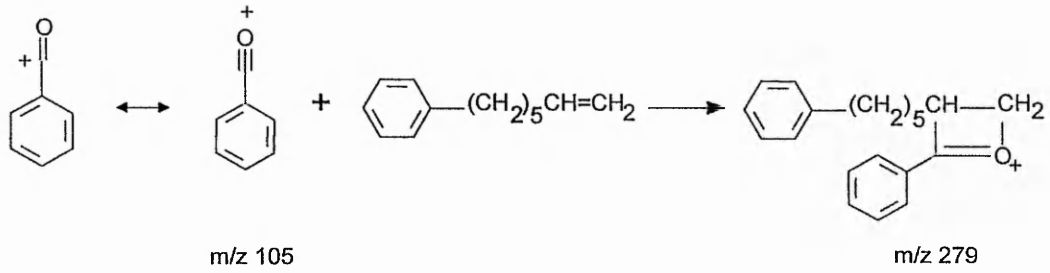

Scheme 4.7. The reaction pathway of $[C_6H_5CO]^+$ with phenylheptene

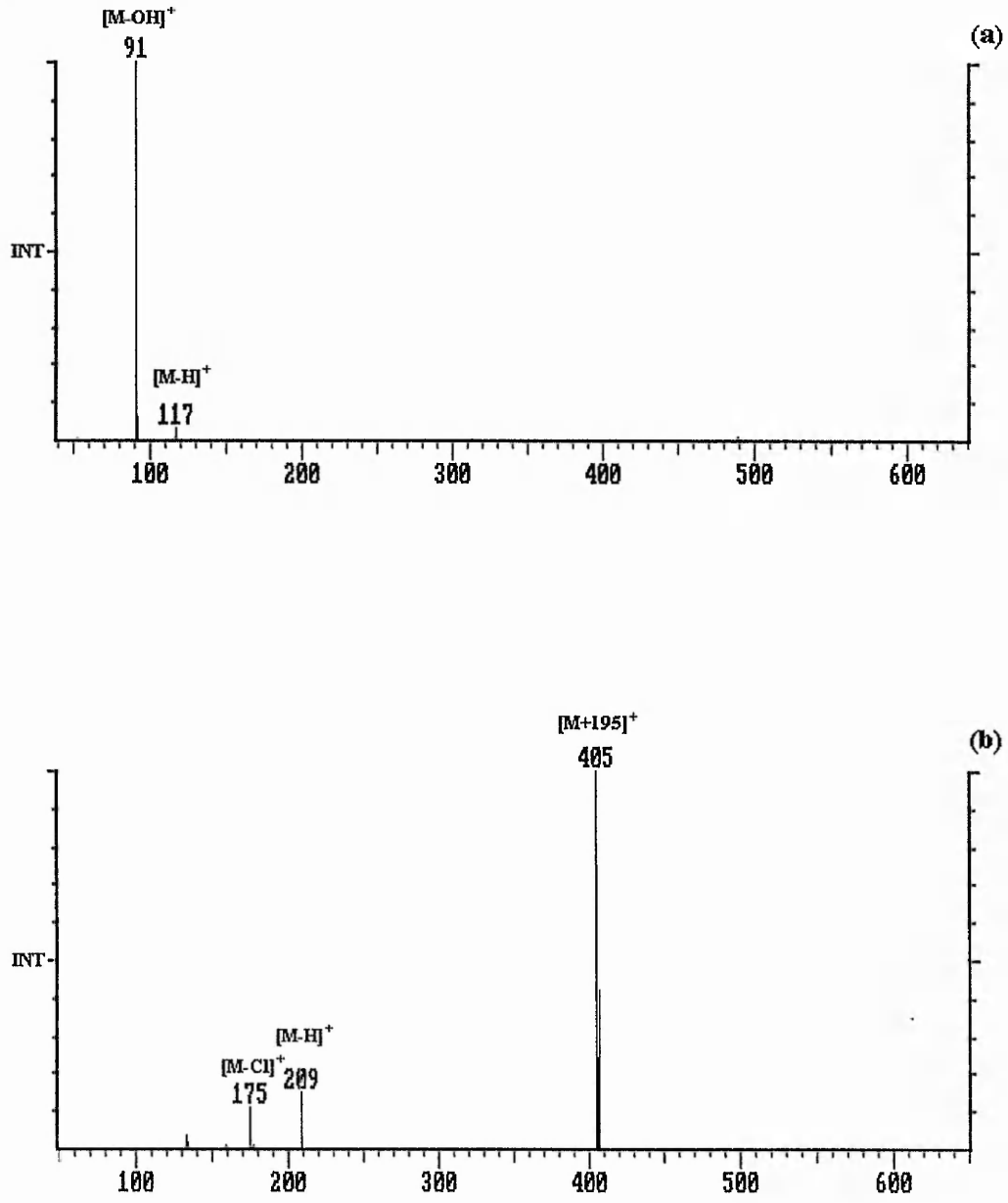

Figure 4.10. The spectra resulting from the reaction of $[C_6F_5CO]^+$ with (a) benzyl alcohol and (b) phenylheptyl chloride.

$[C_6X_nH_{5-n}CO]^+$, (X= H, F, 4-CH_3) with the product related intermediates of POB are summarised Table 4.2.

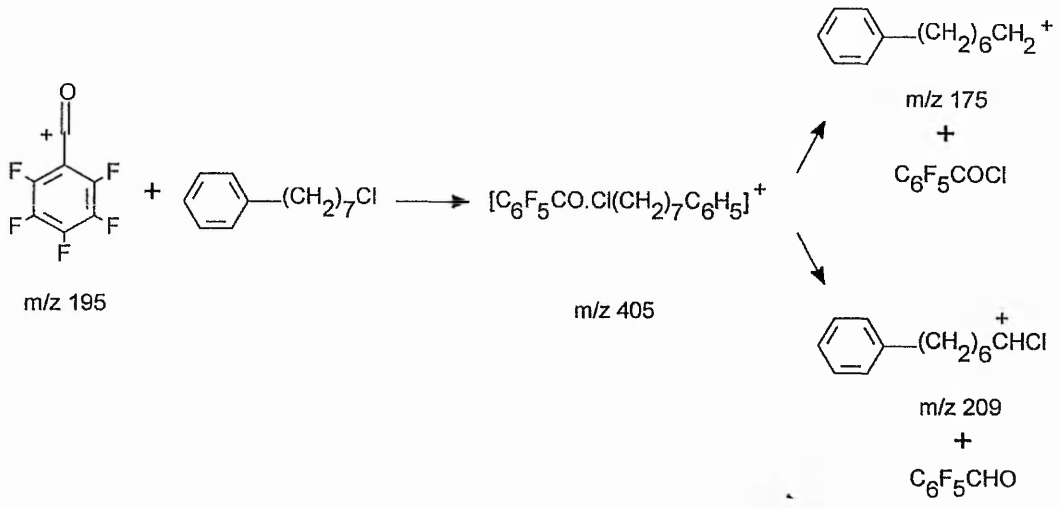

Scheme 4.8. The reaction pathway of $[C_6F_5CO]^+$ with phenylheptyl chloride

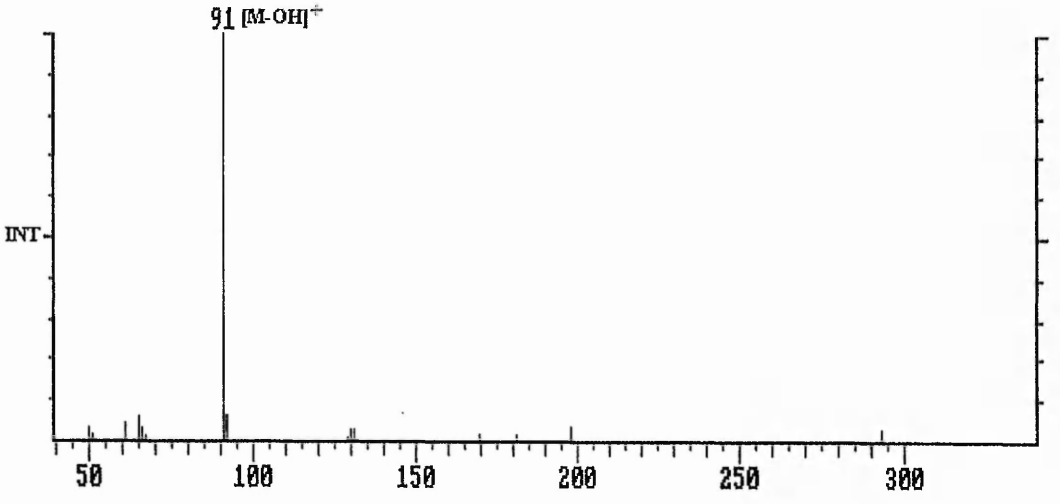

Figure 4.11. Mass spectrum resulting from the $[4\text{-}MeC_6H_4CO]^+$ ion reaction with benzyl alcohol.

Table 4.2. Product ions observed for the reactions of the substituted benzoyl ions with the POB mixture.

Compound	$[C_6H_5CO]^+$	$[C_6F_5CO]^+$	$[4\text{-}CH_3C_6H_4CO]^+$
Benzyl chloride	no reaction	$[M\text{-}Cl]^+$ (m/z 91)	no reaction
Benzyl alcohol	$[M\text{-}OH]^+$ (m/z 91) m/z 197, m/z 181, m/z 169	$[M\text{-}OH]^+$ (m/z 91) $[M\text{-}H]^+$ (m/z 117) m/z 181, m/z 169	$[M\text{-}OH]^+$ (m/z 91)
σ-Tolualdehyde	no reaction	$[M+195]^+$ (m/z 315) $[M\text{-}H]^+$ (m/z 119)	no reaction
Phenylheptene	$[M+105]^+$ (m/z 279) m/z 131, m/z 104, m/z 78	$[M+195\text{-}C_6F_5COC_4H_7]^+$	no reaction
SB205268	no reaction	no reaction	no reaction
Bibenzyl	$M^{+\cdot}$ (m/z 182)	$[M+195]^+$ (m/z 377) $[M+195\text{-}H_2O]^+$ (m/z 359)	no reaction
Phenylheptyl chloride	no reaction	[M+195] (m/z 405) [M-H] (m/z 209) $[M\text{-}Cl]^+$ (m/z 175)	no reaction
Phenylheptyl alcohol	$[M\text{-}OH]^+$	$[M+195\text{-}H_2O]+$ (m/z 369) $[M\text{-}OH]^+$ (m/z 175)	no reaction
Dichlorodecane	no reaction	no reaction	no reaction
Diphenyloctyl	no reaction	no reaction	no reaction

4.4 CONCLUSION

The potential of the benzoyl ions of the type $[C_6X_nH_{5-n}CO]^+$ (X= H, F, 4-Me) to act as selective chemical ionisation reagents is illustrated by their reactions with the keto-enol tautomers of methylacetoacetate and the product related intermediates of 2-(8-phenyloctyl)benzaldehyde (POB). $[C_6H_5CO]^+$ reacted with only the enol tautomer of methylacetoacetate, allowing assignment of the tautomers separated by GC. Fragmentation and CAD products of these electrophilic addition reactions also provided additional structural information. $[C_6F_3H_2CO]^+$ reacted with both tautomers producing spectra with structurally diagnostic ions, which are not present in the conventional EI spectra. The $[C_6H_5CO]^+$ ion reacted with only four components of the product related intermediates of POB, simplifying the chromatogram and allowing functional group assignment in some cases. The use of $[C_6F_5CO]^+$ and $[4\text{-}MeC_6H_4CO]^+$ caused ionisation of more or less components of the mixture respectively. These observations confirm that the electrophilic nature of the benzoyl ion is strongly influenced by variation of the ring substituents, allowing its selectivity to be controlled. The ion-molecule chemistry of the benzoyl cation therefore has potential as a selective chemical ionisation technique in structural and trace analysis with the product ion distributions, $[M+105]^+$, $[M\text{-}OH]^+$ and $[M\text{-}H]^+$ allowing functional group assignment.

4.5 REFERENCES

1. Creaser, C.S., Williamson, B.L., *J. Chem. Soc., Chem. Comm*, 1677 (1994)

2. Creaser, C.S., Williamson, B.L., *J. Chem. Soc., Perkin 2*, in press

3. Soni, M., Amy, J., Frankevich, V., Cooks, R.G., Taylor, D., McKewan, A. and Schwartz, J.C., *Rapid Comm. Mass Spectrom.*, 911, **9** (1995)

4. Bruins, A.P. and Nibbering, N.M.M., *Tetrahedron Lett.*, 4491, **50** (1975)

5. White, E.L.,Tabet, J.C. and Bursey, M., *Org. Mass. Spectrom.*, 132, **22** (1987)

6. Eberlin, M.N. and Cooks, R.G., *J. Am. Chem. Soc.*, 9226, **115** (1993)

7. Eberlin, M.N. and Cooks, R.G., *Org. Mass Spectrom.*, 679, **28** (1993)

8. Occhiucci, G., Patacchiola, A., Sparapani, C. and Speranza, M., *J. Chem. Soc., Chem. Commun.*, 1269 (1982)

9. Occhiucci, G., Speranza, M. and Cacace, F., *J. Chem. Soc., Chem. Commun.*, 723 (1984)

10. Occhiucci, G., Cacace, F. and Speranza, M., *J. Am. Chem. Soc.*, 872, **108** (1986)

11. Stockton, B.M. (SmithKline Beecham), *private communication* (1994)

12. Forth, M.A., Mitchell, M.B., Smith, S.A.C., Gombatz, K. and Snyder, L., *J. Org. Chem.* 2616, **59** (1994)

13. Gleason, J.G., Hall, R.F., Perchonock, C.D., Erhard, K.F., Frazee, J.S., Ku, T. W., Kondrad, K., McCarthy, M.E., Mong, S., Crooke, S.T., Chi-Rosso, G., Wasserman, M.A., Torphy, T.J., Muccitelli, R.M., Hay, D.W., Tucker, S.S. and Vickery-Clark, L., *J. Med. Chem.*, 959, **30** (1987)

14. Kaiser, R.E., Cooks, R.G., Syka, J.E.P. and Stafford, G.C., *Rapid Commun. Mass Spectrom.* 30, **4** (1990)

15. Busch, K.L., Glish, G.L., McLuckey, S.A., *Mass Spectrometry/Mass Spectrometry: techniques and applications in tandem mass spectrometry*, VCH, New York (1988)

16. McLafferty, F.W. (ed.), *Tandem Mass Spectrometry*, Wiley, New York (1983)

17. Yost, R.A. and Enke, C.G., *Anal. Chem.*, 1251A, **51** (1979)

18. McLuckey, S.A., *J. Am. Chem. Mass Spectrom.*, 599, **3** (1992)

19. Todd, J.F.J., *presented at the 2nd European Tandem Mass Spectrometry Conference*, Warwick, UK (1992)

20. Masur, M., Grutzmacher, H.F., Munster, H. and Budzikiewicz, H. *Org. Mass Spectrom.*, 493, **22** (1987)

CHAPTER 5

CHEMICAL IONISATION REACTIONS OF THE BENZOYL ANION

5.1 INTRODUCTION

There have been several reports [1] on the applications of negative ionisation with a quadrupole ion trap. These have mostly been concerned with the use of air sampling glow discharge ion (ASGDI) source/QITMS combinations, [2] to generate the negative ions in an external source which were injected into the trap, stored, reacted and ejected in the normal mass-selective axial instability scan of the ion trap mass spectrometer. [3] Samples of 2,4,6-trinitrotoluene (TNT) and 1,3,5-trinitroazacyclohexane (RDX) were analysed successfully by reagent anions such as $O_2^{\cdot-}$, NO_2^- and OH^- [4-7] with this (ASGDI) source/QITMS combination. The negative ion fragmentation pathways of TNT have also been reported using this technique. [8] However the use of an ASGDI source involves major modifications to the ITMS setup.

There are few reports on negative chemical ionisation involving reagent and sample ion generation inside a quadrupole ion trap. [9-11] This is due partly to the very low efficiency of negative ion formation in the quadrupole ion trap and to the problem of positive ion-negative ion recombination. [11] Polyatomic anions derived from several dinitrotoluene isomers, 2,4,6-trinitrotoluene and 1,3,5-trinitro-1,3,5-triacyclohexane have been formed by reaction with the negative reagent ions $[OH]^-$ and $[O]^-$, generated inside the ion trap by electron ionisation of water. [9] MS/MS product ions were obtained for most of these ions, however in some cases the precursor to product conversion efficiency was observed to be relatively low. This was interpreted as due to collisional electron detachment competing with CAD.

Two recent reports on the generation of negative ions inside the ion trap used dissociative electron capture to yield negative ion spectra for FC-43 and hexachlorobiphenyl compounds, [10] as well as the formation of $[OH]^-$ reagent ions from H_2O. [11] After an electron ionisation period, all positive ions were ejected from the ion trap before a negative ion spectrum was acquired. This is possible because the stability diagram nearest the origin in a_z q_z space for negative ions is the mirror image (reflected in the q_z axis) of the stability diagram for positive ions as shown in Figure 5.1, a_z and q_z being the Mathieu trapping parameters:

$$a_z = -\frac{8eU}{mr_o^2\Omega^2} \qquad q_z = -\frac{4eV}{mr_o^2\Omega^2} \qquad (5.1)$$

As the stability diagrams overlap, there is a region of a_z q_z space where both positive and negative ions have stable trajectories, so that ions of both polarity are stored together. However, applying a suitably large negative DC voltage to the ring electrode will move the working point to a region where the trajectories of all positive ions are radially unstable resulting in their ejection from the trap.

Using this technique of applying a negative DC voltage to the ring electrode to eject all positive ions, $[OH]^-$ CI has been performed inside the ion trap yielding $[M-H]^-$ ions for glycine, aniline, σ-cresol, phenyl acetonitrile, nitrobenzene, benzamide, n-butylbenzene and benzoic acid. [11] The hydroxy ion is a strong base which reacts principally by proton abstraction a wide range of compounds

containing an acidic hydrogen, yielding spectra which contain strong $[M-H]^-$ ions and few fragments. [12] $[OH]^-$ chemical ionisation has therefore been applied to the analysis of many compounds including amines and amino acids, [13] hydroxy compounds, [14] carbonyl compounds, [15, 16] aromatic hydrocarbons [17, 18] and in the molecular weight determination of tertiary alcohols which are difficult to analyse by most other mass spectrometric methods. [19, 20]

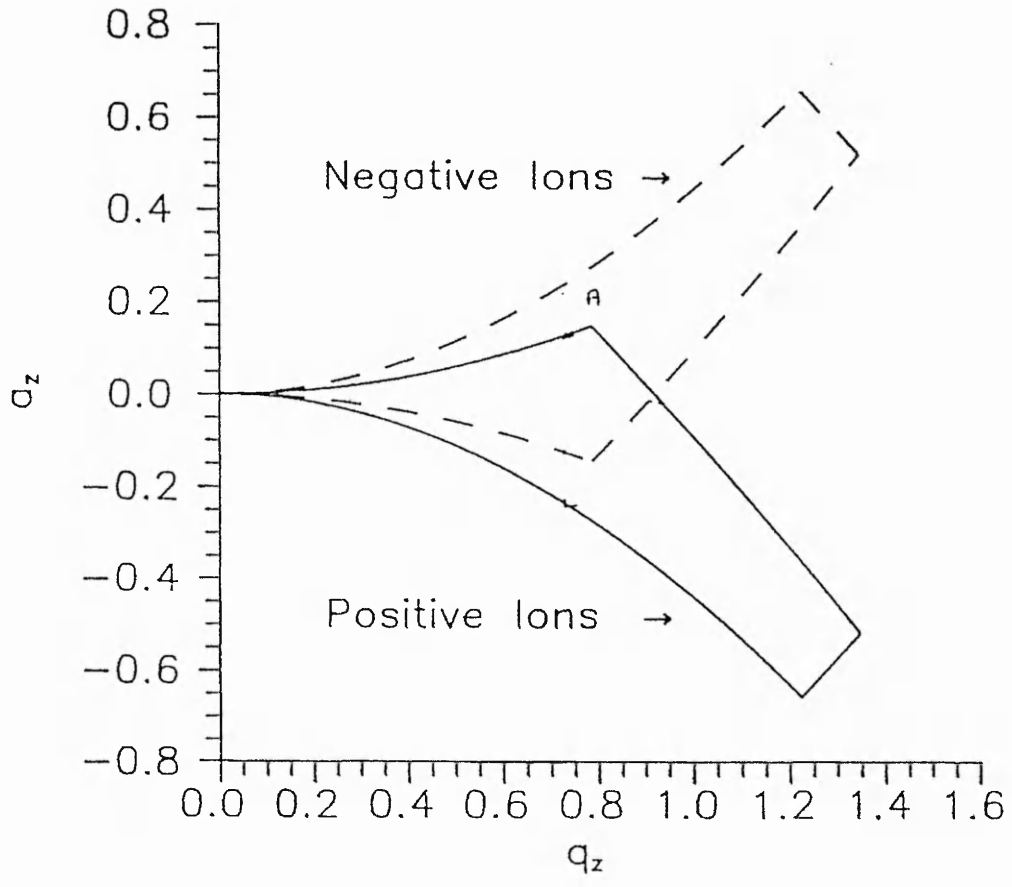

Figure 5.1. Stability diagrams in a_z, q_z space for positive ions (—) and negative ions (---) stored in a quadrupole ion trap.

In recent years the gas phase ion-molecule reactions of the benzoyl cation, $[C_6H_5CO]^+$, have received considerable attention. [21-26] This reagent ion has been shown to undergo selective, gas phase ion-molecule reactions with the hydroxy functional group (Chapter 2), amine containing compounds (Chapter 3) and has been shown to have potential as a selective chemical ionisation reagent in a quadrupole ion trap mass spectrometer (Chapter 4). In view of this interest in the benzoyl cation, it is some what surprising that very little work has been reported on the gas phase reactions of the benzoyl anion, $[C_6H_5CO]^-$. [27] Therefore a study was undertaken on the generation of $[OH]^-$ and $[C_6H_5CO]^-$ ions inside the ion trap and their reactions with model compounds containing carbonyl and hydroxy functional groups.

5.2 EXPERIMENTAL

Experiments were carried out using a quadrupole ion trap mass spectrometer (Finnigan MAT ITMS, San Jose, CA), operated at 120 °C in negative ion mode with the conversion dynode charged at + 4 kV. The electron multiplier voltage was typically -2 kV. All chemicals were obtained from Aldrich Chemical Co. (Dorset, UK) and used without further purification. Water and benzaldehyde were introduced *via* leak valves (Megg itt Avionics, Portsmouth, UK) at pressures of 2 x 10^{-5} and 5 x 10^{-6} torr respectively. Other samples were introduced on the solids probe. The helium buffer gas was introduced into the ion trap *via* a third leak valve (Megg itt Avionics, Portsmouth, UK) at a pressure of 1 x 10^{-4} torr. All pressures

are uncorrected, as measured using the ionisation gauge (Granville-Phillips) mounted on the vacuum chamber.

The $[OH]^-$ ion was generated by dissociative electron capture of water. [11] Electrons were gated into the trap for 100 ms with a low mass cut off of 10 amu and during this period a filtered noise waveform [28] was applied to the end cap electrodes to eject from the ion trap all positive and negative ions except those of m/z 17. A generalised scan routine for this experiment is shown in Figure 5.2. Following the ionising electron pulse the working point of the $[OH]^-$ ions was moved to $a_z = 0.20$, $q_z = 0.774$ (point A, Figure 5.1), where positive ions were unstable and ejected

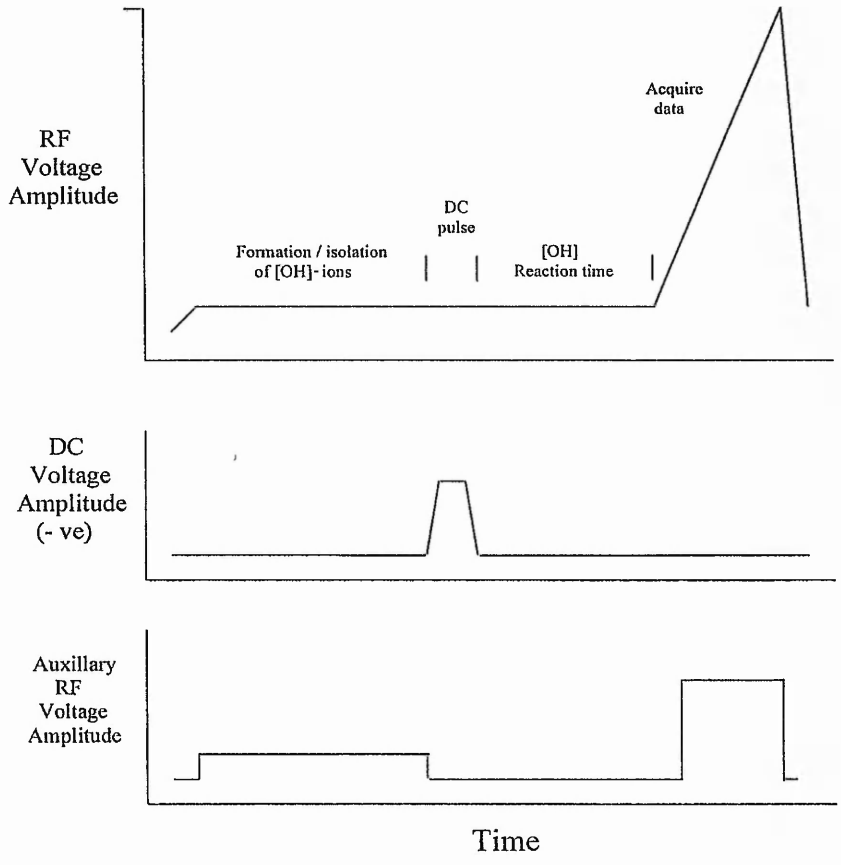

Figure 5.2. Scan routine for the reactions of $[OH]^-$

from the trap by application of a DC pulse to the ring electrode (-21 V for 2 ms). Isolation of $[OH]^-$ ions followed by a 50 ms reaction time during which $[OH]^-$ ions were allowed to react with neutral sample vapour.

5.3 RESULTS AND DISCUSSION

A long ionisation time (100 ms) was required to generate a sufficiently large $[OH]^-$ ion population from the water admitted into the mass spectrometer. The $[OH]^-$ CI spectra of benzophenone, benzhydrol, phenoxyacetic acid and benzaldehyde are shown in Figure 5.3 and Figure 5.4. All produce strong $[M-H]^-$ ions. The benzophenone and benzhydrol spectra showed no fragment ions with significant intensity. Fragment ions were present in the spectrum obtained for phenoxyacetic acid (Figure 5.4(a)) at m/z 107 and m/z 89 and m/z 45, which can be assigned to $[M-HCO_2]^-$, $[M-H_3CO_3]^-$ and $[M-C_7H_6O]^-$ respectively. In the case of benzaldehyde (Fig 5.4b), the formation of $[M-H]^-$, the $[C_6H_5CO]^-$ ion, was detected at m/z 105 and the ion at m/z 123 is assigned to the $[M+17]^-$ adduct ion. Two additional peaks were observed at m/z 211 and m/z 183 and these prompted further investigation.

In order to investigate the origin of the two high mass ions at m/z 211 and m/z 183 in the $[OH]^-$ CI spectrum of benzaldehyde, the $[C_6H_5CO]^-$ ion was isolated using the resonance hole technique [29] (with a low mass cut off of 20 amu and

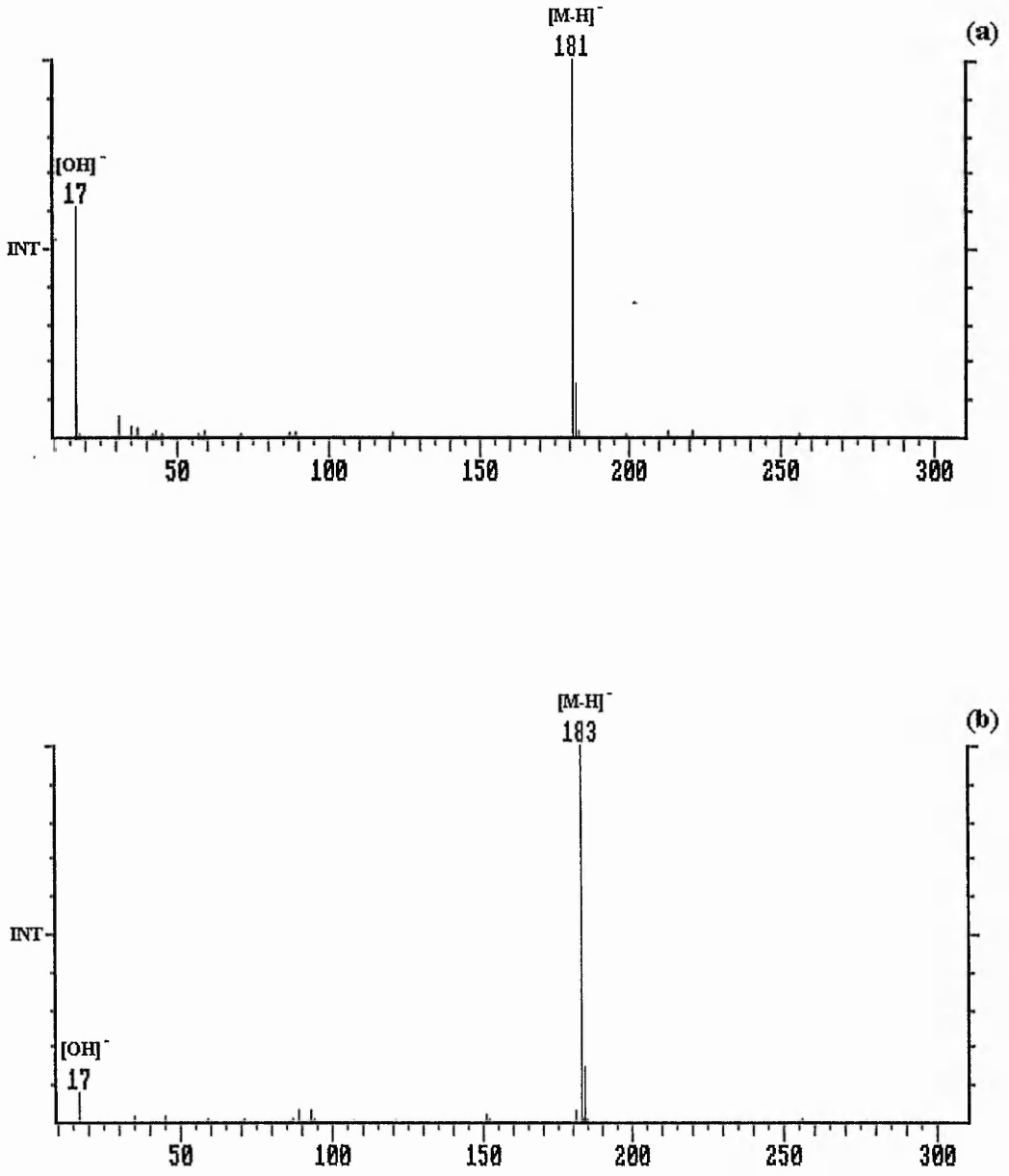

Figure 5.3. The reaction of $[OH]^-$ with (a) benzophenone and (b) benzhydrol

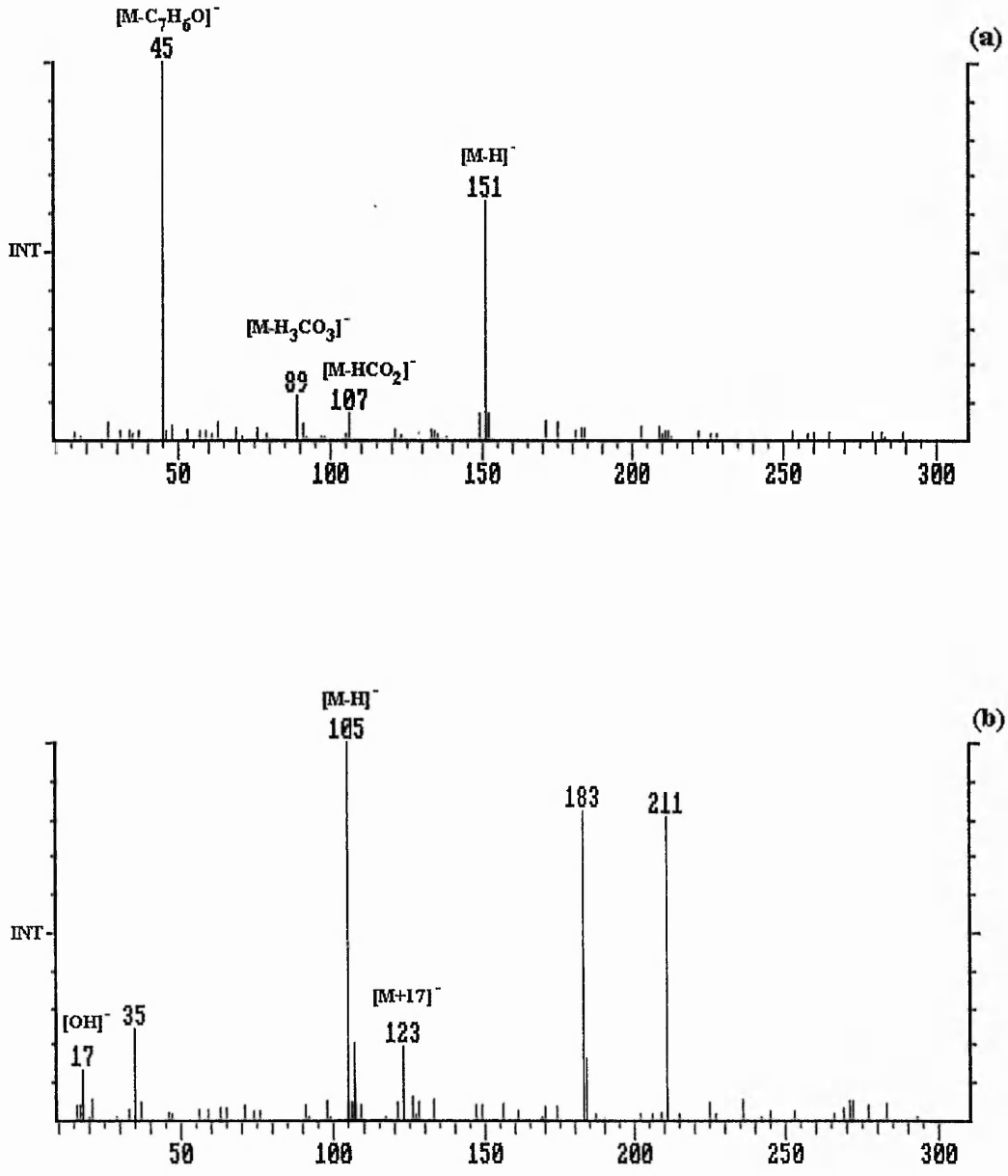

Figure 5.4. The reaction of [OH]- with (a) phenoxyacetic acid and (b) benzaldehyde

q_z $[C_6H_5CO]^-$ = 0.173) and allowed to react with benzaldehyde sample vapour for 100 ms. The scan routine for this experiment is shown in Figure 5.5 and the resulting spectrum is given in Figure 5.6. The m/z 211 and 183 ions were observed in the spectrum and are assigned to an ion arising from nucleophilic addition of $[C_6H_5CO]^-$ to benzaldehyde and a related $[M+105-CO]^-$ fragment ion respectively, establishing the origin of these ions in the $[OH]^-$ CI spectrum of benzaldehyde. The reaction of the benzoyl anion with benzaldehyde is summarised in Scheme 5.1. The additional ion at m/z 121

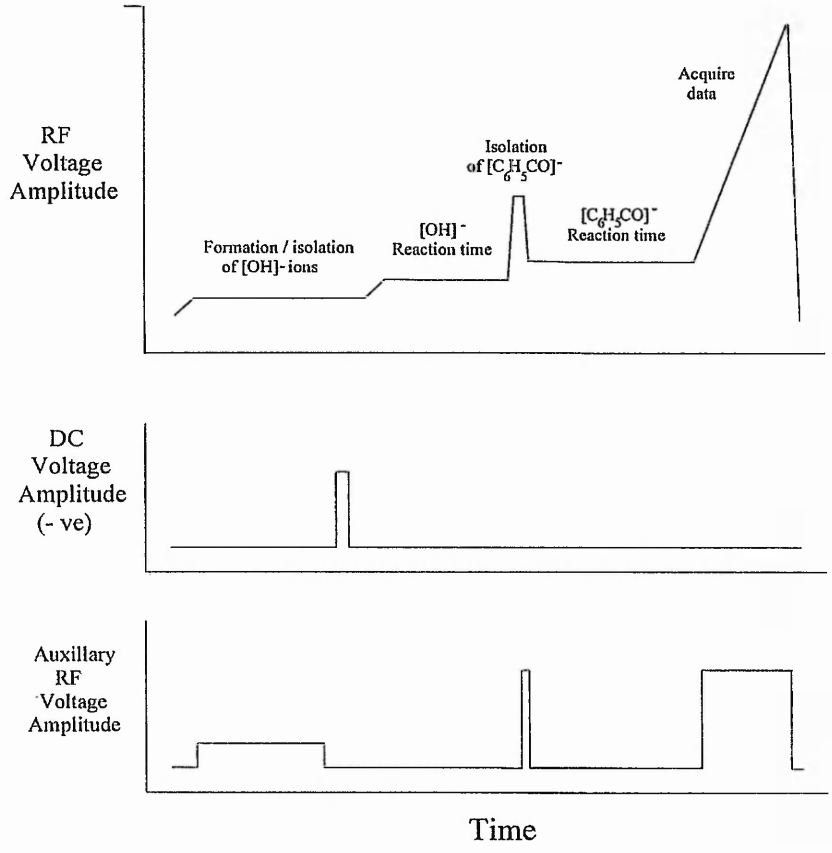

Figure 5.5. Scan routine for the reaction of $[C_6H_5CO]^-$ with benzaldehyde

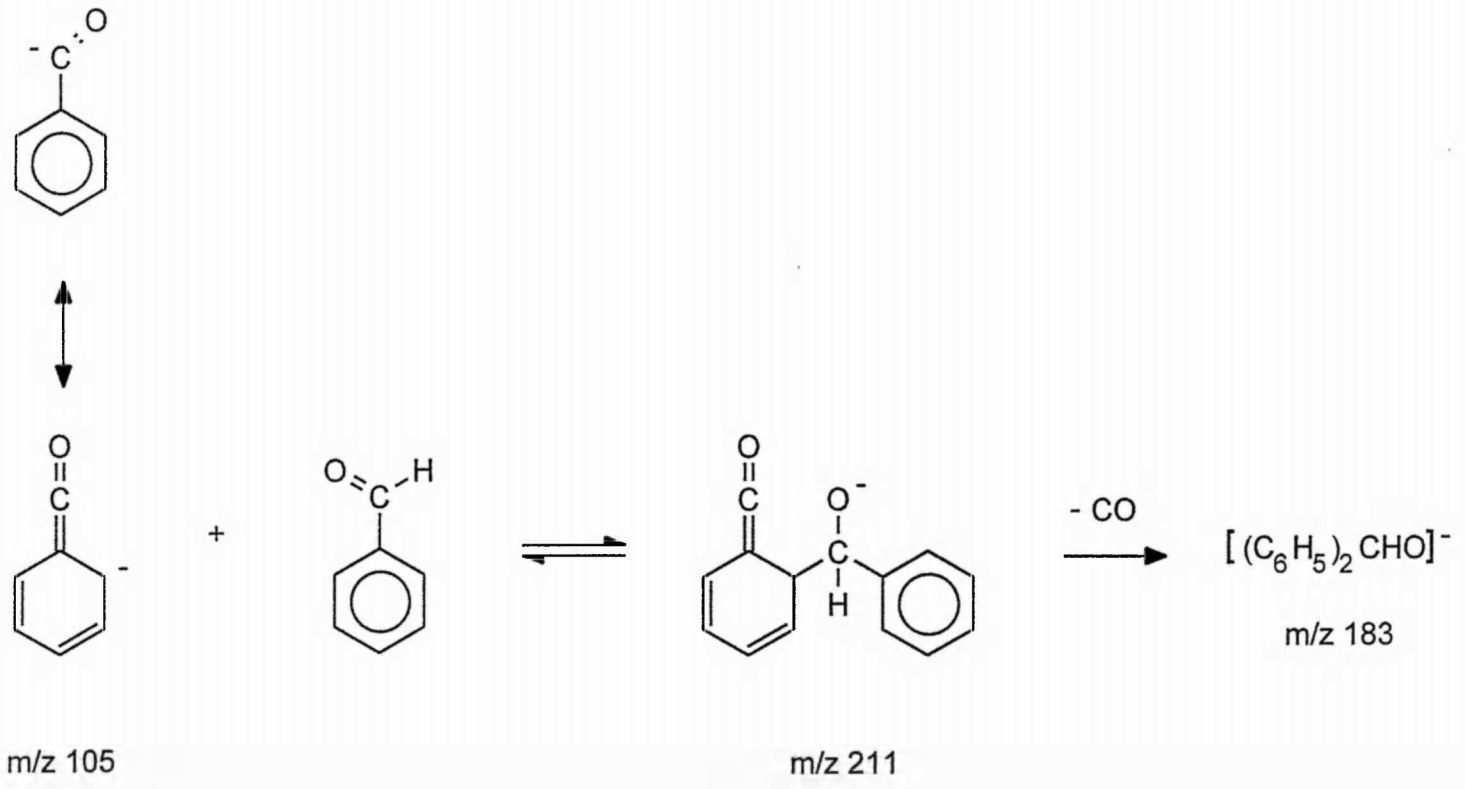

Scheme 5.1. The reaction of $[C_6H_5CO]^-$ with benzaldehyde

(Figure 5.6) is assigned to the benzoate anion formed by the addition of oxygen to the benzoyl anion.

The product and product ion intensity ratios observed in these ion trap experiments differ significantly from those in an FT-ICR investigation of the reactions of the benzoyl anion [4] where m/z 133 ($[C_6H_5(CO)_2H]^-$) and m/z 183 were the principal products, with m/z 209 ($[C_6H_5COCOC_6H_5]^-$) and m/z 211 present to only a minor extent. These differences may be explained by the pressures and time scales of the QITMS and FT-ICR experiments. Collisional stabilisation of the adduct (m/z 211) being expected to the more efficient in the mtorr region of the ion trap, [25, 26] than the lower pressures (10^{-8} torr) of the FT-ICR instrument.

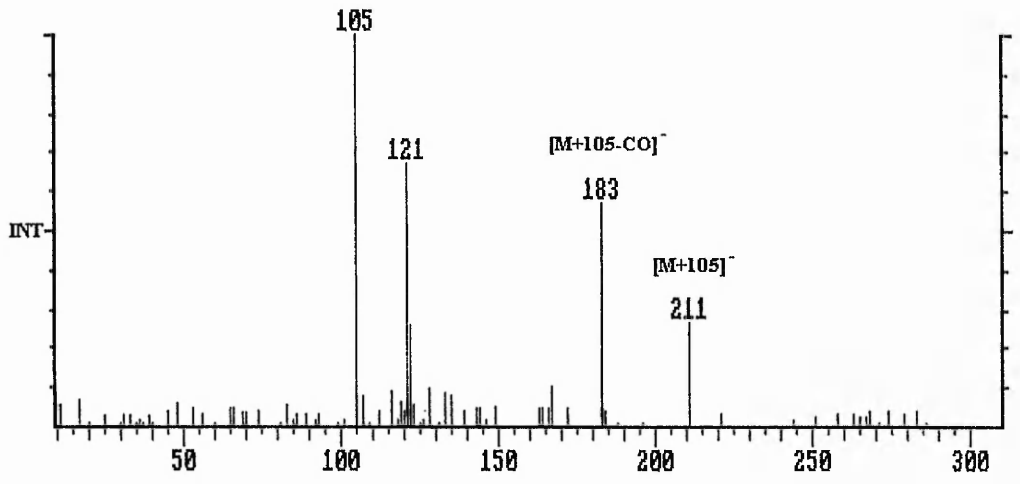

Figure 5.6. The reaction of $[C_6H_5CO]^-$ with benzaldehyde

Investigation of the reactions of the $[C_6H_5CO]^-$ ion was extended to reactions with benzophenone, phenoxyacetic acid and benzhydrol. Figure 5.7 illustrates the spectrum obtained following a 100 ms reaction time with benzophenone. The ions at m/z 211 and m/z 183 are observed as benzaldehyde is present in the trap as the precursor to the $[C_6H_5CO]^-$ ion. However, additional ions are present at m/z 287 and m/z 259, which can be assigned to an $[M+105]^-$ adduct ion with benzophenone and the $[M+105-CO]^-$ fragment ion. These processes are summarised in Scheme 5.2. No reaction was detected when $[C_6H_5CO]^-$ was reacted with phenoxyacetic acid or benzhydrol. These observations suggest that the benzoyl anion reacts preferentially where the carbonyl group is adjacent to the aromatic ring, as it is for benzaldehyde and benzophenone.

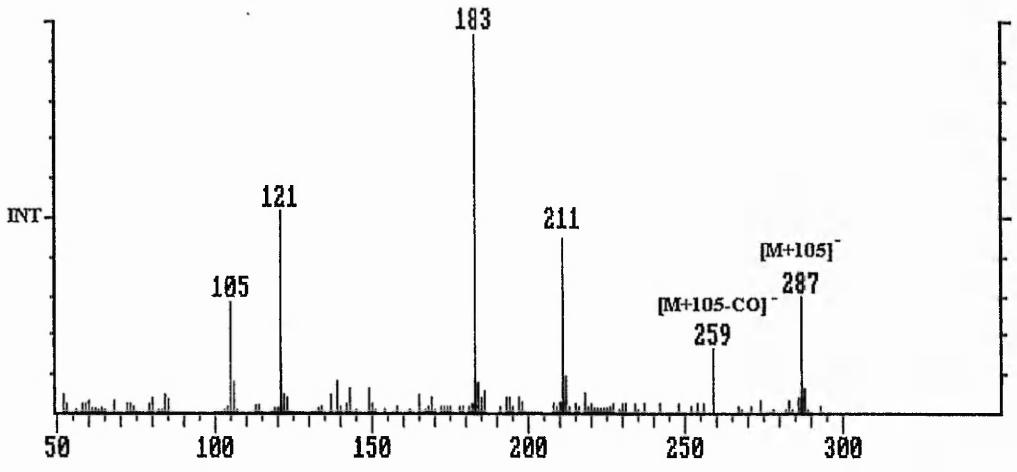

Figure 5.7. The reaction of $[C_6H_5CO]^-$ with benzophenone

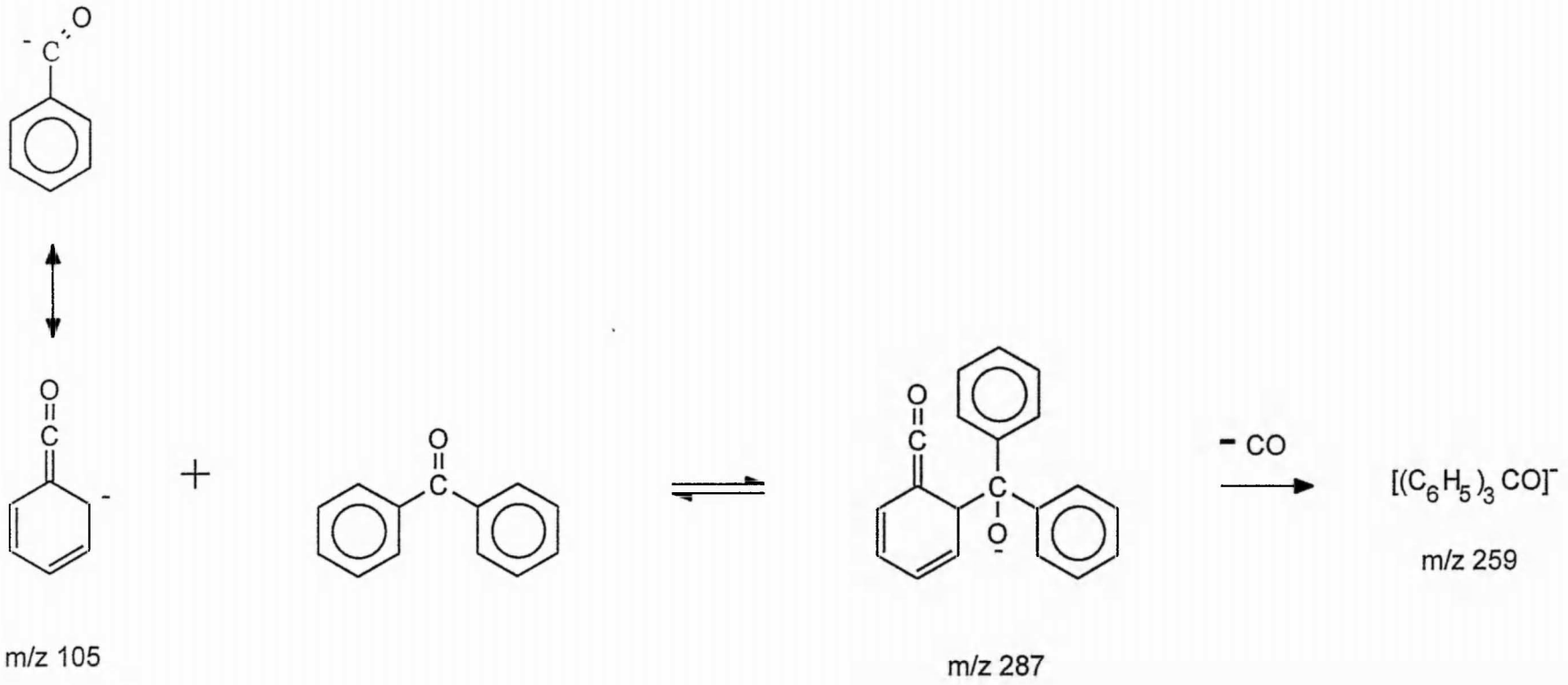

Scheme 5.2. The reaction of $[C_6H_5CO]$- with benzophenone

5.4 CONCLUSION

The data reported in this investigation confirm earlier observations that $[OH]^-$ negative CI works well in the quadrupole ion trap and is demonstrated in this chapter to form $[M-H]^-$ ions with the oxygenated compounds benzaldehyde, benzophenone, benzhydrol and phenoxyacetic acid. The benzoyl anion, $[C_6H_5CO]^-$, formed as the $[M-H]^-$ ion from the $[OH]^-$ CI reaction with benzaldehyde, undergoes ion-molecule reactions with benzaldehyde and benzophenone, but not with phenoxyacetic acid or benzhydrol. This suggests that the $[C_6H_5CO]^-$ ion acts selectively as a nucleophile towards the carbonyl functional group in the aldehyde and ketone compounds investigated and the benzoyl anion may therefore have potential as a selective chemical ionisation reagent for these classes of compounds, although further investigations is required to establish the range of analytes amenable to this ionisation process.

5.5 REFERENCES

1. March, R.E. and Hughes, R.J., *Quadrupole Storage Mass Spectrometry*, Vol. 102, Chemical Analysis Series, John Wiley, New York (1989)

2. McLuckey, S.A., Glish, G.L. and Asano, K.G., *Anal. Chim. Acta*, 25, **225** (1989)

3. Stafford, G.C., Kelley, P.E., Syka, J.E.P., Reynolds, W.E. and Todd, J.F.J., *Int. J. Mass Spectrom. Ion Processes*, 85, **60** (1984)

4. Eckenrode, B.A., Glish, G.L. and McLuckey, S.A., *Int. J. Mass Spectrom. Ion Processes*, 151, **99** (1990)

5. McLuckey, S.A., Asano, K.G. and Glish, G.L., *proceedings of the 36th ASMS Conference on Mass Spectrometry and Allied Topics*, San Francisco (1988)

6. McLuckey, S.A., Glish, G.L. and Grant, B.C., *proceedings of the 3rd Symposium on the Analytical Determination of Explosives*, Germany (1989)

7. McLuckey, S.A., Goeringer, D.E. and Glish, G.L., *J. Am. Soc. Mass Spectrom.*, 11, **2** (1991)

8. Langford, M.L. and Todd, J.F.J., *Org. Mass Spectrom.*, 773, **28** (1993)

9. McLuckey, S.A. and Glish, G.L., *Anal. Chem.*, 1670, **59** (1987)

10. Catinella, S., Traldi, P., Jiang, X., Londry, F.A., Morrison, J.S., March, R.E., Gregoire, S., Mathurin, J.C. and Tabet, J.C., *Rapid Commun. Mass Spectrom.*, 1302, **9** (1995)

11. Berberich, D.W. and Yost, R.A., *J. Am. Soc. Mass Spectrom.*, 757, **5** (1994)

12. Chapman, J.R, *Practical Organic Mass Spectrometry*, Wiley, New York (1985)

13. Smit, A.L.C. and Field, F.H., *J. Am. Chem. Soc.*, 6471, **99** (1977)

14. Houriet, R., Stahl, D. and Winkler, F.J., *Environ. Health Perspect.*, 63, **36** (1980)

15. Hunt, D.F., Sethi, S.K. and Shabanowitz, J., *Environ. Health Perspect.*, 33, **36** (1980)

16. Hunt, D.F., Shabanowitz, J. and Giordani, A.B., *Anal. Chem.*, 386, **52** (1980)

17. Sieck, L.W., Jennings, K.R. and Burke, P.D., *Anal. Chem.*, 2232, **51** (1979)

18. Sieck, L.W., *Chem. Brit.*, 38, **16** (1980)

19. Dougherty, R.C., Whitaker, M.J., Smith, L.M., Stalling, D.L. and Kuel, D.W. *Environ. Health Perspect.*, 103, **36** (1980)

20. Hunt, D.F., Harvey, T.M. and Russel, J.W., *J. Chem. Soc. Chem. Commun.*, 151 (1975)

21. Eberlin, M.N. and Cooks, R.G., *J. Am. Chem. Soc.* 9226, **115** (1993)

22. Eberlin, M.N. and Cooks, R.G., *Org. Mass Spec.*, 679, **28** (1993)

23. Occhiucci, G., Cacace, F. and Speranza, M., *J. Am. Chem. Soc.*, 872, **108** (1986)

24. Soni, M., Amy, J., Frankevich, V., Cooks, R.G., Taylor, D., Mckewan, A. and Schwartz, J. C., *Rapid Comm. Mass. Spectrom.*, 911, **9** (1995)

25. Creaser, C.S. and Williamson, B.L., *J. Chem. Soc., Chem. Comm.*, 1677 (1994)

26. Creaser, C.S. and Williamson, B.L., *J. Chem. Soc., Perkin 2,* in press

27. Kleingeld, J.C. and Nibbering, N.M.M., *Tetrahedron*, 2789, **40** (1984)

28. Asano, K.G., Goeringer, D.E., McLuckey, S.A., Hoekman, D., Stiller, S.W., *Proceedings of the 41st ASMS*, San Francisco, 1993, p 700a

29. P.E. Kelly, J.E.P. Syka, P.C. Ceja, G.C. Stafford, J.N. Louris, H.F. Grutzmacher, D. Kuck and J.F.J. Todd, *proceedings of the 34th ASMS*, Cinncinatti, 1986.

CHAPTER 6

NON-COVALENT INCLUSION COMPLEXES OF PROTONATED AMINES WITH CROWN ETHERS

6.1 INTRODUCTION

The study of host-guest chemistry in the gas phase has received considerable interest only in the last five years, despite extensive investigations in the solution phase since the discovery of crown ethers in 1967. [1, 2] Crown ethers are particularly useful in modelling biologically relevant ion transport processes, antibody-antigen association and enzyme catalysis. Intermolecular and intramolecular hydrogen bonds and other electrostatic interactions are also important interactions in solution chemistry molecular recognition. The study of the gas-phase chemistry of inclusion complexes in the mass spectrometer is particularly important since these non-covalent interactions may be observed in the absence of solvent effects, which opens up new avenues for understanding some of the fundamental details of molecular recognition.

The area of host-guest chemistry in the mass spectrometer has been recently reviewed. [3] The first reports of gas-phase crown ether complexes were published in the mid-1980s and describe the formation of transition metal ion complexes of 12-crown-4 in a FT-ICR mass spectrometer. [4, 5] In the same year the formation of host-guest complexes between RNH_3^+ (R=CH_3, c-C_6H_{11}), $[(CH_3)_3NH]^+$ and [pyridine+H]$^+$ and the crown ethers (12-crown-4, 15-crown-5 and 18-crown-8) were described. [6] These crown ethers were observed to be much more efficient ligands than their acyclic analogues. There have been several other reports in recent years on the interaction of crown ethers with alkali metal ions, [7, 8, 9] other metal ions [10] and anions. [11, 12]

The ammonium ion has been shown to demonstrate unusually high gas-phase affinities for the crown ethers 18-crown-6 and 21-crown-7 relative to the acyclic ethers. [13, 14] This is attributed to the large cavity sizes (1.34-1.43 A and 1.68 - 2.12 A respectively) being more able to accommodate the configuration necessary for optimum hydrogen bond interactions to the bulky tetrahedral ammonium ion (radius = 1.43 A). The kinetic method [15] and the ligand exchange technique [16] were used to determine this high affinity of the ammonium ion for 18-crown-6 and 21-crown-7. [17]

There have been few accounts of the gas phase mass spectrometric complexation reactions between crown ethers and protonated amine ions since Meot-Ner's preliminary investigations. [6] A study on the non-covalent inclusion complexes formed between a variety of protonated amines and the crown ethers 12-crown-4, 15-crown-5 and 18-crown-6 has been reported [18] in which the nature of the hydrogen bond interactions of the ion complexes was evaluated by comparison of their CAD spectra. The amines investigated were propylamine, 2,5-dimethylpyrrole, 2-chloro-6-methylpyridine, 2-methylaziridine, pyridine, 2-aminoethanol, 3-aminopropanol, diethylamine, 3,5-lutidine, ethylene diamine, 4- and 5-aminobutanol. Weakly bonded complexes were found to dissociate following collisional activation, to form intact protonated polyether molecules and/or ammonium ions by simple hydrogen bond cleavage. These weakly bonded complexes included all the 12-crown-4 inclusion complexes and all the 15-crown-5 complexes except those formed with propylamine, 2-methylaziridine, 2-

aminoethanol and ethylene diamine. Those complexes strongly bond by multiple hydrogen bonds, such as the complexes between 18-crown-6 and propylamine, 2-methylaziridine, 2-aminoethanol, 3-aminopropanol and ethylene diamine dissociate not only to form the protonated polyether and/or ammonium ions, but also by extensive covalent bond cleavage of the protonated ether skeleton. It is only with the larger crown ethers that the multiple hydrogen bonding needed for the formation of a strongly non-covalently bonded complex can occur. In cases were the crown ether host can only bind to the amine part of the molecule, such as ion complexes of crown ethers with methyl- and tosylhydrazine, covalent bond cleavage of the nitrogen-sulphur bond of the guest substrate occurs. [19] These results suggest that the association energy for the multiple hydrogen-bonding interactions of the crown ether/ammonium ion complex is of the same order as the covalent macrocyclic or nitrogen-sulphur bonds.

Recently, complexation reactions between modified crown ethers and substituted ammonium ions have been used to enable chiral recognition by mass spectrometry. Fast atom bombardment (FAB) and FT-ICR mass spectrometry have been used in enantioselective recognition of diastereomeric host-guest complexes between chiral crown ether hosts and chiral organic ammonium guests on the basis of the relative peak intensity (RPI). [20] This work has included chiral differentiation of the enantiomers of phenylalanine methyl esters [21, 22] and (1-(1-naphthyl)ethyl)amine. [23, 24]

In this chapter a study on the gas phase interactions of a variety of crown ethers with aromatic and aliphatic protonated amines is described. The effect of varying the structure of the protonated amine on the stability of a crown ether amine complexes has been determined by a novel quadrupole ion trap technique which compares the relative affinities of the protonated amines for the crown ether hosts. This method allowed the relative stabilities of these non-covalent inclusion complexes to be assigned.

6.2 EXPERIMENTAL

Experiments were performed using a quadrupole ion trap mass spectrometer (Finnigan MAT ITMS, San Jose, CA), operated at 120 ^{o}C. Helium bath gas pressure was maintained at $1x10^{-4}$ torr (uncorrected) measured by the ion trap vacuum chamber ion gauge. All chemicals were obtained from Aldrich Chemical Co. (Dorset, UK) except (s)-phenyl-18-crown-6 which was obtained from Dr Chris Anson (School of Chemical Sciences, University of East Anglia, Norwich) and used without further purification. Reaction times were varied using key sequences [25] to automatically increase the reaction time. Total reaction times were calculated from the end of the protonated amine isolation period, taking into account electron multiplier warm-up and the time taken to eject the $[M+H]^+$ ion. Key sequences were also employed in the tandem mass spectrometry studies of the inclusion complexes involving the variation

of the tickle voltages (0-3V) applied to the end cap electrodes. [26] Isolation of the inclusion complexes was achieved using the filtered noise technique, [27] with a low mass cut off of 50 amu.

In each experiment the amine was ionised by electron ionisation and held in the trap for 50 ms to form the $[M+H]^+$ ion by self-CI. [28] The $[M+H]^+$ ion was isolated using the filtered noise technique and allowed to react with the neutral crown ether, for typically 100 ms. A scan routine for this experiment is shown in Figure 6.1. In experiments comparing the relative stabilities of the protonated propylamine/benzo-18-crown-6 and protonated phenethylamine/benzo-18-crown-6 inclusion complexes, propylamine was introduced *via* a leak valve (Megg itt. Avionics, Portsmouth, UK) at a pressure of 4 x 10^{-6} torr (uncorrected). A 1 μL sample of a solution of 0.05 M phenethylamine and 0.1 M benzo-18-crown-6 dissolved in DCM was introduced on the solids probe and heated to 110 °C and then forty scans were averaged. This gave reasonable intensities of the protonated amine/benzo-18-crown-6 inclusion complexes. In experiments comparing the relative stabilities of the protonated propylamine/18-crown-6 and protonated phenethylamine/18-crown-6 inclusion complexes, the same procedure was used as above, apart from a 1μL solution of 0.05 M phenethylamine and 0.1 M 18-crown-6 dissolved in DCM was introduced on the solids probe and heated to 110 °C and then forty scans were averaged. For experiments involving the comparison of the stabilities of the phenethylamine/benzo-18-crown-6 and 4-nitrophenethylamine/benzo-18-crown-6 inclusion complexes, a 1 μL sample of a solution of 0.1 M 4-nitrophenethylamine,

0.05 M phenethylamine and 0.05 M benzo-18-crown-6 in DCM was introduced on the probe and heated to 110 °C. This then gave reasonably constant pressure of each compound. The intensity of protonated phenethylamine and 4-nitrophenethylamine was checked before introduction of the benzo-18-crown-6 to ensure similar intensities of the $[M+H]^+$ ions.

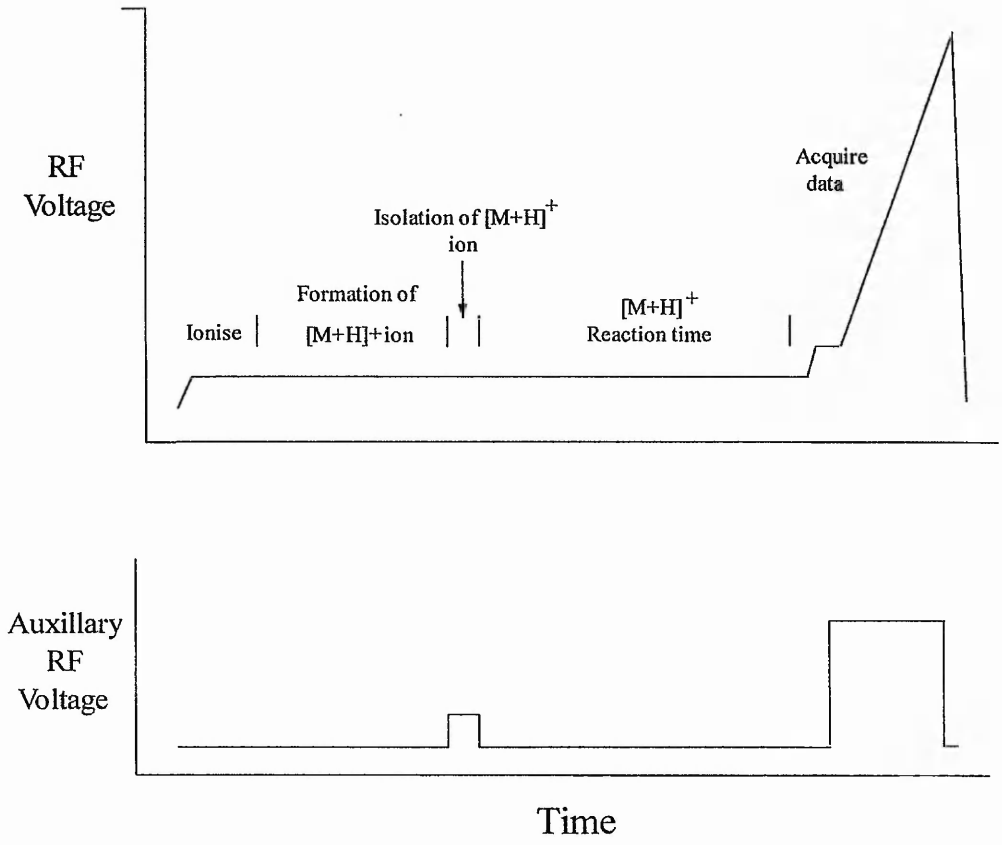

Figure 6.1. Scan routine for the formation of an inclusion complex between a protonated amine and a crown ether

The (r) and (s) enantiomers of phenylalanine were chosen to investigate chiral recognition using host guest chemistry as both enantiomers were commercially available. A constant pressure of phenylalanine was achieved inside the mass spectrometer by heating a solid sample of phenylalanine to 300 °C on the solids probe for approximately two minutes. This then gave a constant background of phenylalanine for several hours. The ionisation period (typically 1 ms) was adjusted to ensure similar intensities of the $[M+H]^+$ ion for both (r) and (s)-phenylalanine. At least 12 hours was allowed between experiments using different enantiomers of phenylalanine. In experiments comparing the relative stabilities of protonated phenylalanine/(s)-phenyl-18-crown-6 and protonated phenylalanine/18-crown-6 non-covalent inclusion complexes, a 1 μL sample of a 0.05 M solution containing equimolar amounts of 18-crown-6 and (s)-phenyl-18-crown-6 dissolved in DCM was introduced on the solids probe which was heated to 150 °C. 40 scans were then averaged.

In experiments comparing the relative affinity of protonated phenylalanine for (s)-phenyl-18-crown-6 and 18-crown-6, a 1 μL sample of the 0.05 M solution containing equimolar amounts of 18-crown-6 and (s)-phenyl-18-crown-6 was introduced on the solids probe and heated to 150 °C. The inclusion complex between either protonated phenylalanine and (s)-phenyl-18-crown-6 or protonated phenylalanine and 18-crown-6 was then isolated using the filtered noise technique and retained in the trap for 100 ms.

The ions were then ejected from the trap and a spectrum acquired. The scan routine for this experiment is illustrated in Figure 6.2.

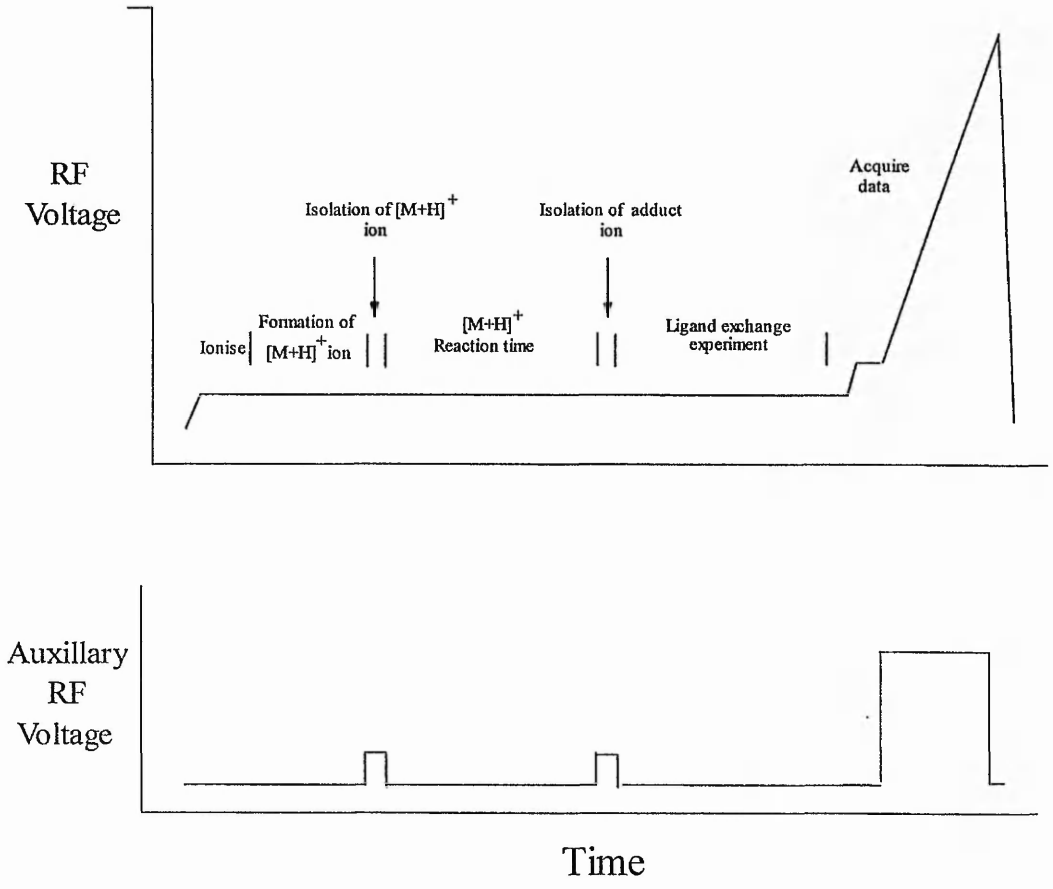

Figure 6.2. The scan routine for the comparison of the relative affinity of protonated phenylalanine for (s)-phenyl-18-crown-6 and 18-crown-6.

6.3 RESULTS AND DISCUSSION

6.3.1 Reactions of $[R\text{-}CH_2CH_2NH_3]^+$ (where R = CH_3, C_6H_5 or $O_2NC_6H_5$) with benzo-18-crown-6 and 18-crown-6.

In order to investigate the relative affinities of 18-crown-6 and benzo-18-crown-6 for protonated amines, the reactions of $[R\text{-}CH_2CH_2NH_3]^+$, where R = CH_3, C_6H_5 or $O_2NC_6H_4$ with these crown ethers were studied. The spectrum resulting from the reaction of protonated propylamine (m/z 60), generated by self CI, with benzo-18-crown-6 is shown in Figure 6.3(a) and demonstrates the formation of a non-covalent inclusion complex between protonated propylamine and benzo-18-crown-6 (m/z 372). The variation of ion intensity for m/z 60 and m/z 372 over a 110 ms reaction time is illustrated in Figure 6.3(b) and shows the fall of protonated propylamine (m/z 60) and the rise in the non-covalent complex intensity (m/z 372) as the reaction approaches equilibrium. A 100 ms reaction time was used in subsequent reactions.

The relative affinities of benzo-18-crown-6 for protonated propylamine and phenethylamine were determined. The spectrum obtained following isolation of the $[M+H]^+$ ions for propylamine and phenethylamine with no crown ether present is shown in Figure 6.4(a). The ions were retained in the trap for 100 ms and show the m/z 60 ($[C_3H_7NH_3]^+$) and m/z 122 ($[C_6H_5(CH_2)_2NH_3]^+$) have similar intensity. The

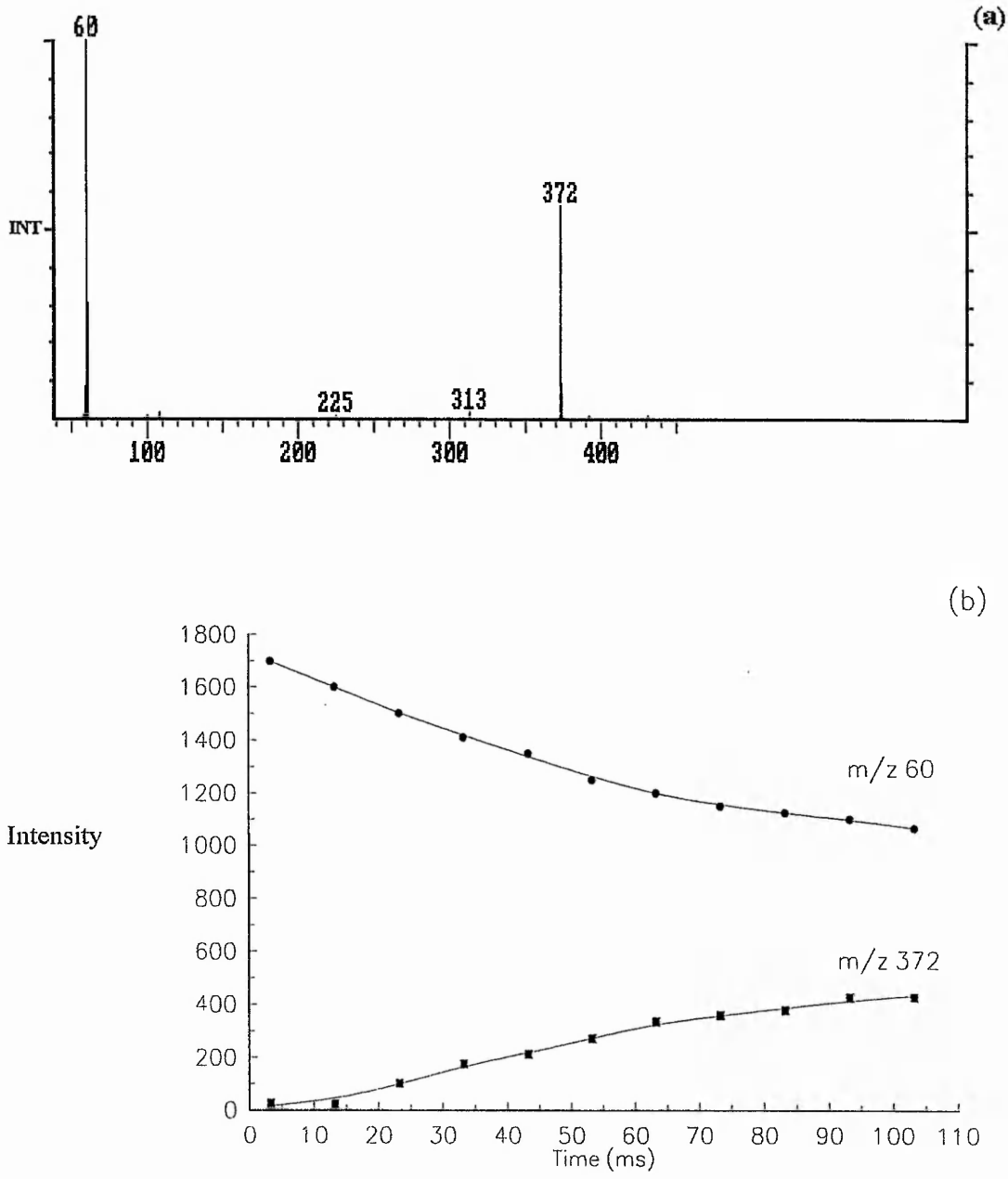

Figure 6.3. The reaction of protonated propylamine with benzo-18-crown-6 (a) spectrum resulting from 100 ms reaction time and (b) the variation of ion intensity with time.

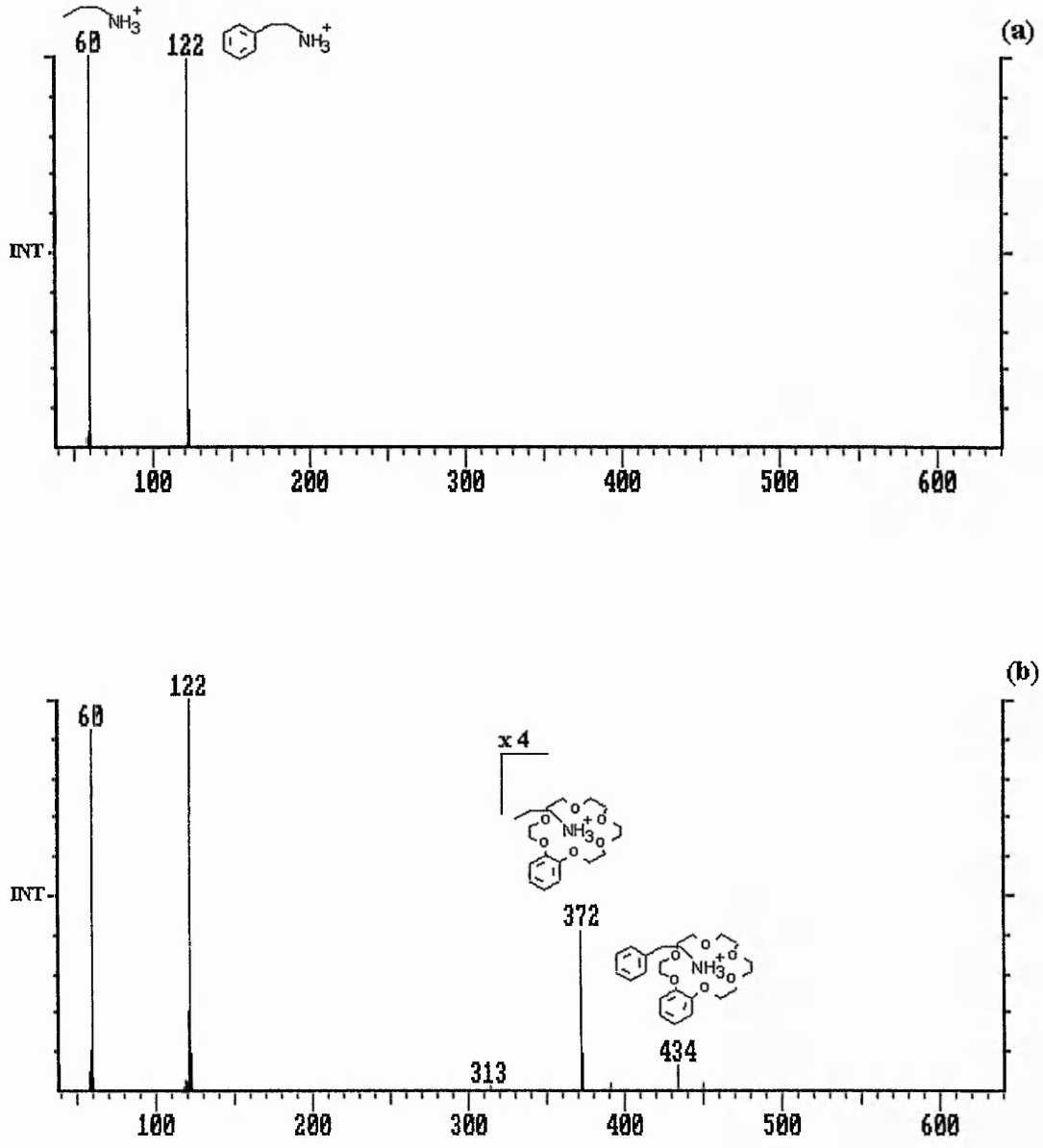

Figure 6.4. The reaction of the isolated $[M+H]^+$ ions from propylamine and phenethylamine with (a) no crown ether present and (b) benzo-18-crown-6 present.

spectrum obtained following the reaction with benzo-18-crown-6 is illustrated in Figure 6.4(b) and shows adduct ions with both propylamine and phenethylamine at m/z 372 and m/z 434 respectively. There is a small amount of protonated benzo-18-crown-6 at m/z 313 due to the loss of neutral amine from both complexes. The higher intensity of the benzo-18-crown-6 complex at m/z 372 indicates that this crown ether has a greater affinity for protonated propylamine then protonated phenethylamine. This is surprising as the aromatic ring of the phenethylamine complex may have a weak secondary π-π interaction with the aromatic ring of the crown which might be expected to increase the stability of the adduct compared to the protonated propylamine benzo-18-crown-6 complex, which does not have this capability for π-π stacking. These π-π stacking interactions have been observed in solution studies of benzo crown ethers containing a tricarbonyl chromium group.[29]

The relative stabilities of the non-covalent inclusion complexes of protonated propylamine and protonated phenethylamine with benzo-18-crown-6 were studied further by comparing their affinities for 18-crown-6 using the same experimental procedure (Figure 6.5). The resulting spectrum also shows an increased intensity for the protonated propylamine/18-crown-6 inclusion complex (m/z 324) compared to the protonated phenethylamine/18-crown-6 complex (m/z 386). This indicates a much greater stability of the propylamine inclusion complex relative to the phenethylamine

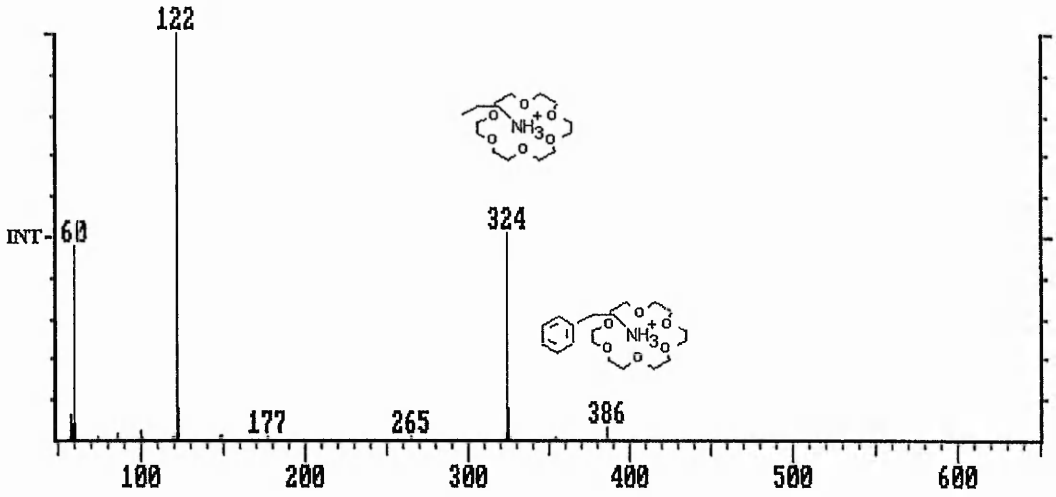

Figure 6.5. The reaction of the $[M+H]^+$ ions of propylamine and phenethylamine with 18-crown-6.

complex and it would therefore appear that the aromatic ring on phenethylamine destabilises the crown ether adduct. The stronger interaction between protonated propylamine and 18-crown-6 was further supported by tandem mass spectrometry of the two inclusion complexes using collisionally activated dissociation, which show significantly different product ion spectra (Figure 6.6). The MS/MS spectrum of the protonated propylamine/18-crown-6 inclusion complex (Figure 6.6(a)) showed fragment ions at m/z 265 (loss of neutral propylamine), m/z 221 and m/z 177 which correspond to the loss of 1 and 2 ethylene oxide units respectively together with neutral propylamine from the crown ether ring. This fragmentation of the crown ether

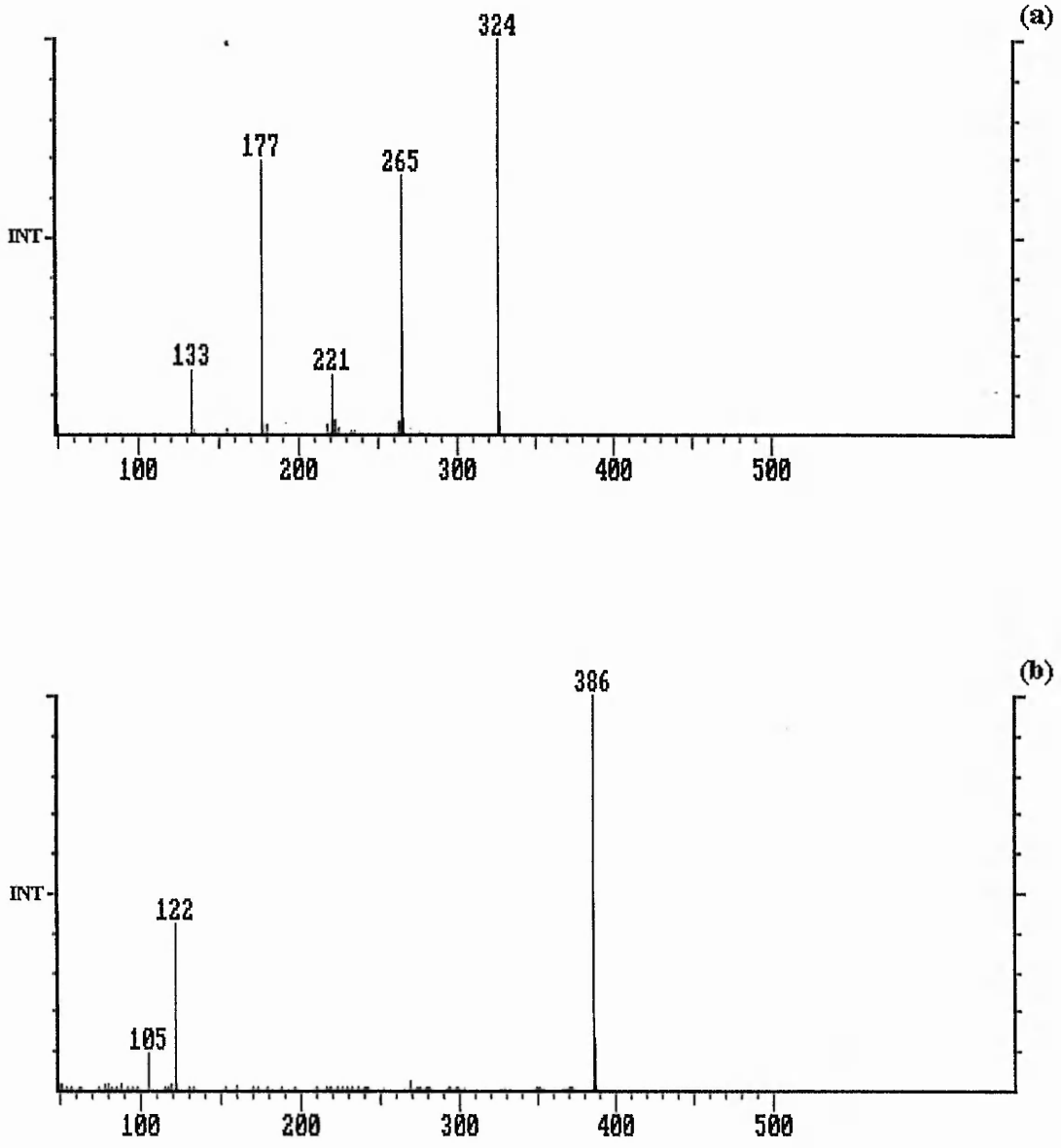

Figure 6.6. Tandem mass spectrometry of the inclusion complex between 18-crown-6 and (a) $[M+H]^+$ of propylamine and (b) $[M+H]^+$ of phenethylamine

is associated with a strongly bonded crown ether adduct. [18] In comparison, the product ion spectrum of the protonated phenethylamine/18-crown-6 inclusion complex (m/z 386) produces two fragment ions, one at m/z 122 the loss of the neutral 18-crown-6 to form protonated phenethylamine and m/z 105, the loss of ammonia and 18-crown-6 (Figure 6.6(b)). These product ions suggest a weakly bonded crown ether complex, [18] arising from the poor interaction of the crown ether with the aromatic ring.

The presence of an electron deficient aromatic group in 4-nitrophenethylamine might be expected to enhance the π-π introduction with the aromatic group on the benzo-18-crown-6. The reactions of phenethylamine and 4-nitrophenethylamine with benzo-18-crown-6 were therefore also investigated. The spectrum resulting from the isolation of protonated phenethylamine and 4-nitrophenethylamine followed by a 100 ms period when these ions were retained in the trap with no benzo-18-crown-6 present is shown in Figure 6.7(a) and shows the equal intensity of both ions. The spectrum obtained following the reaction with benzo-18-crown-6 for 100 ms is shown in Figure 6.7(b) and indicates a slightly greater intensity of the complex between 4-nitrophenethylamine and benzo-18-crown-6 at m/z 479 compared to the unnitrated inclusion complex at m/z 434. The spectrum also shows fragment ions at m/z 390, the loss of ethylene oxide from the protonated phenethylamine/benzo-18-crown-6 complex, m/z 313 the loss of the neutral amine from one or both inclusion complexes, m/z 225 the loss of two ethylene oxide units and neutral amine from the adducts and m/z 105 the loss of ammonia and neutral crown ether from the protonated

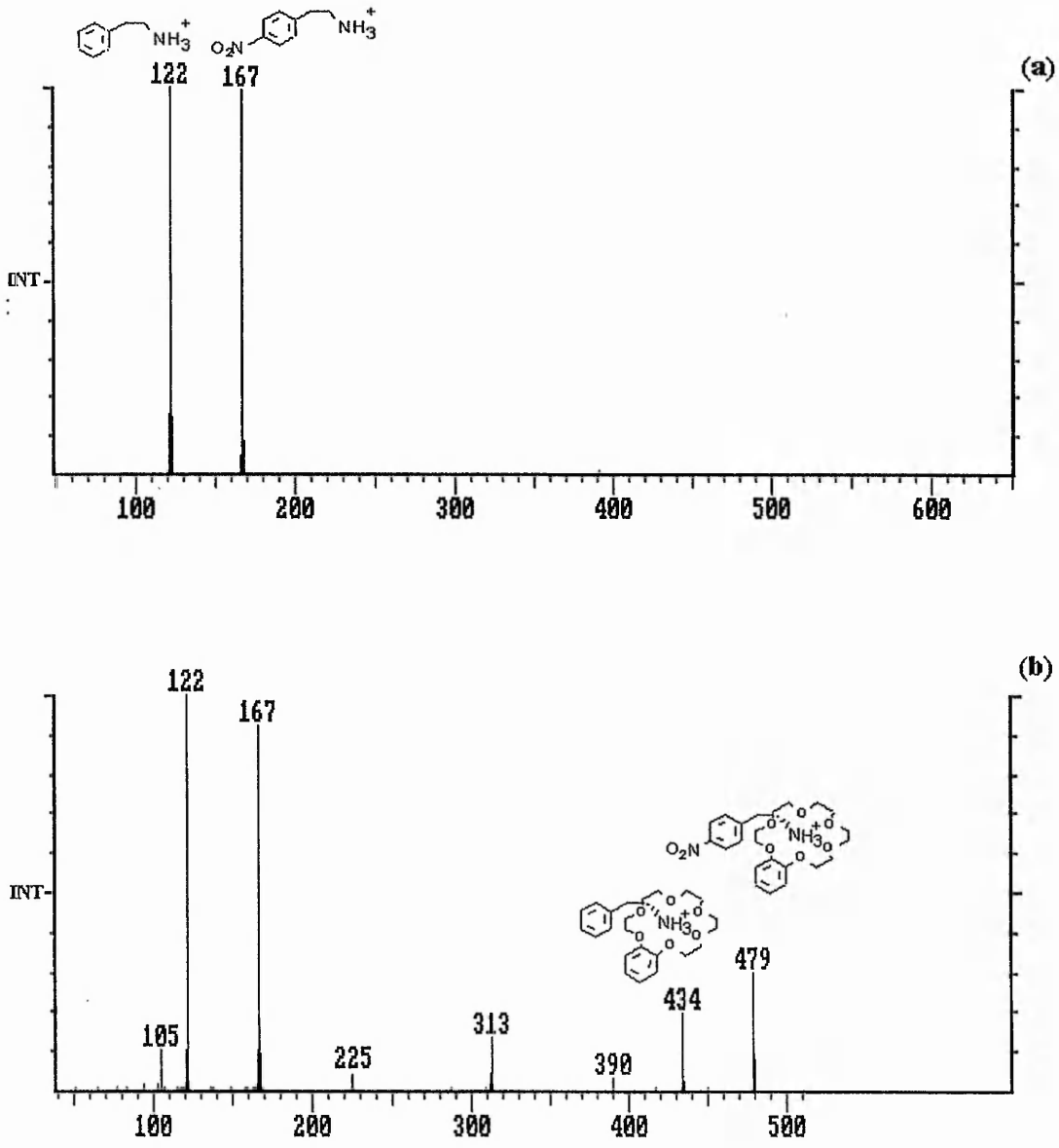

Figure 6.7. The reaction of the isolated [M+H]+ ions from phenethylamine and 4-nitrophenethylamine with (a) no benzo-18-crown-6 present and (b) benzo-18-crown-6 present.

phenethylamine/benzo-18-crown-6 complex. The greater intensity of the protonated 4-nitrophenethylamine/benzo-18-crown-6 inclusion complex indicates weak π-π bonding is occurring in this complex, increasing its stability. These observations suggest the following order of affinity for the crown ether amine non-covalent inclusion complexes.

$[p+H+18\text{-crown-}6]^+ > [phen+H+18\text{-crown-}6]^+$; and $[p+H+benzo\text{-}18\text{-crown-}6]^+ > [nitro+H+benzo\text{-}18\text{-crown-}6]^+ > [phen+H+benzo\text{-}18\text{-crown-}6]^+$

where p = propylalanine, nitro = 4-nitrophenethylamine and phen = phenethylamine

The increased stability of the protonated propylamine/18-crown-6 inclusion complex compared to phenethylamine/18-crown-6 inclusion complex (Figure 6.5) and the increased stability of the protonated propylamine/benzo-18-crown-6 inclusion complex compared to phenethylamine/benzo-18-crown-6 inclusion complex (Figure 6.4) would suggest introduction of the aromatic ring into the amine destabilises the complex. This is further supported by the observation of fragment ions corresponding to a strongly bonded inclusion complex being observed in the product ion spectrum of the protonated propylamine/benzo-18-crown-6 ion and fragment ions corresponding to a weakly bonded inclusion complex being observed in the product ion spectrum of the protonated phenethylamine/benzo-18-crown-6 ion (Figure 6.6). The increased stability of the 4-nitrophenethylamine/benzo-18-crown-6 inclusion complex compared to the

phenethylamine/benzo-18-crown-6 complex (Figure 6.7) would suggest that the stability of the protonated 4-nitrophenethylamine/benzo-18-crown-6 inclusion complex lies in between that of the inclusion complexes formed between propylamine/benzo-18-crown-6 and phenethylamine/benzo-18-crown-6.

6.3.2 Reaction of phenylalanine with (s)-phenyl-18-crown-6 and 18-crown-6

Protonation of the amine group on phenylalanine to produce an $R_1R_2R_3C\text{-}NH_3^+$ ion (where $R_1=C_6H_5CH_2$, $R_2=H$, $R_3=COOH$) should lead to a reaction with (s)-phenyl-18-crown-6 to produce a covalently bonded inclusion complex.

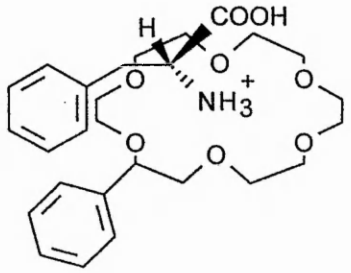

The spectrum resulting from the isolation of the $[M+H]^+$ of (s)-phenylalanine (m/z 166) followed by retention of this ion in the trap with no crown ether present is illustrated in Figure 6.8(a) and shows that only the m/z 166 ion is present. In comparison, Figure 6.8(b), the introduction of (s)-phenyl-18-crown-6 into the mass spectrometer resulted in the formation of an inclusion complex at m/z 506, together

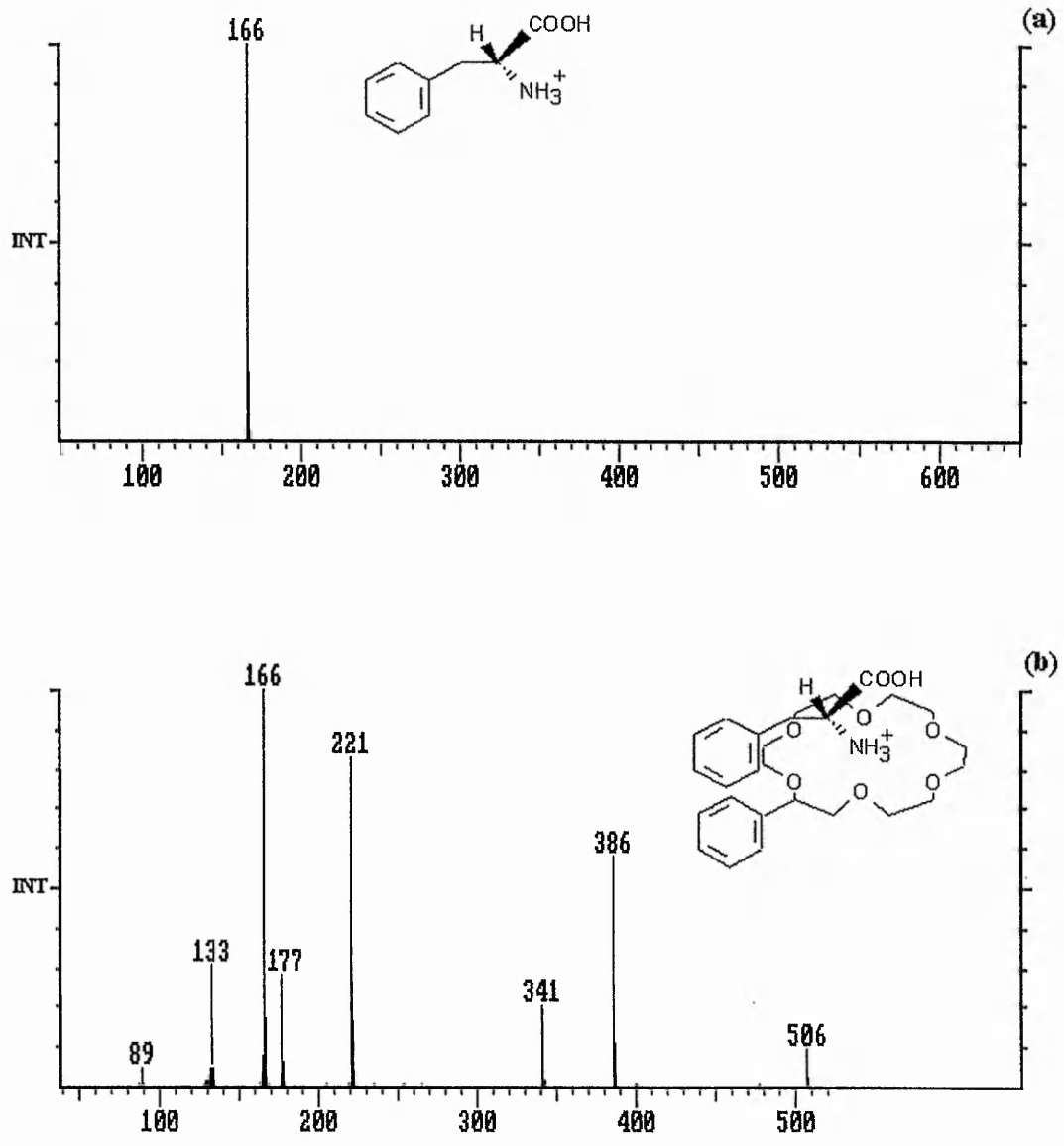

Figure 6.8. Spectra resulting from the isolation of $[M+H]^+$ of (s)-phenylalanine followed by 100 ms reaction time with (a) no crown ether present and (b) introduction of s-phenyl-18-crown-6

with fragment ions at m/z 386, which arises from the elimination of $C_6H_5C_2H_3O$ from the adduct, m/z 341, assigned to protonated (s)-phenyl-18-crown-6 resulting from the loss of (s)-phenylalanine and m/z 221, m/z 177, m/z 133 which correspond to the loss of 1,2 or 3 ethylene oxide units in conjunction with the elimination of phenylalanine and $C_6H_5C_2H_3O$. These fragment ions are analogous to those seen in the low energy collisionally activated dissociation mass spectra of the 18-crown-6 ammonium ion complexes[19] and this extensive fragmentation of the inclusion complex suggests adduct formation is strongly exothermic.

The possibility of chiral recognition of (r) and (s)-phenylalanine was investigated by the relative peak intensity (RPI) method [20] by (s)-phenyl-18-crown-6. In this approach the peak intensity of the target host (M)-guest (A^+) complex ion, I($[M+A]^+$), is compared to that of an internal standard host (R)-guest (A^+) ion I($[R+A]^+$: the RPI value = I($[M+A]^+$)/I($[R+A]^+$). The internal standard chosen was 18-crown-6. The spectrum resulting from the reaction of the $[M+H]^+$ ion of (s)-phenylalanine with (s)-phenyl-18-crown-6 and 18-crown-6 (100 ms) is shown in Figure 6.9(a). It shows the two inclusion complex ion at m/z 506 and m/z 430 respectively, together with ions at m/z 341 and 265 relating to the protonated crown ether arising from elimination of (s)-phenylalanine. The fragment ions observed in Figure 6.8(b) are also present. The $[M+H]^+$ from (s)-phenylalanine appears to have a greater affinity for 18-crown-6 compared to (s)-phenyl-18-crown-6 and this would suggest little π-π interaction between the aromatic rings. This is consistent with the earlier work (section 6.3.1) in

which the $[M+H]^+$ from propylamine was observed to have a greater affinity for benzo-18-crown-6 compared to the $[M+H]^+$ ion from phenethylamine. The RPI value (averaged over three experiments) was calculated to be 0.180 ± 0.020. The reaction of (r)-phenylalanine with (s)-phenyl-18-crown-6 and 18-crown-6 is illustrated in Figure 6.9(b). The spectrum can be seen to be very similar to Figure 6.9(a) and the RPI value (averaged over three experiments) was calculated to be 0.209 ± 0.013. The RPI values for the two enantiomers are therefore not significantly different and (s)-phenyl-18-crown-6 does not appear to be able to distinguish between the two enantiomers of phenylalanine.

Tandem mass spectrometry using collisionally activated dissociation with resonance excitation was employed to investigate the structure of the diastereomeric inclusion complex of phenylalanine. The spectrum obtained from the tandem mass spectrometry of the (S, S) inclusion complex is illustrated in Figure 6.10. The main product ion (m/z 341) resulted from the elimination of phenylalanine from the ring. The formation of the other low intensity product ions were due to fragmentation of the ring following elimination of $C_6H_5C_2H_3O$ and phenylalanine. There was also a small amount of protonated (s)-phenylalanine present in the spectrum. The main product ion being the decomplexation of phenylalanine from the crown ether would suggest a weakly bonded complex, however the formation of low intensity skeletal fragment ions would suggest the stability of this complex lies somewhere in between the stability of the propylamine benzo-18-crown-6 and phenethylamine-18-crown-6 complexes. [18]

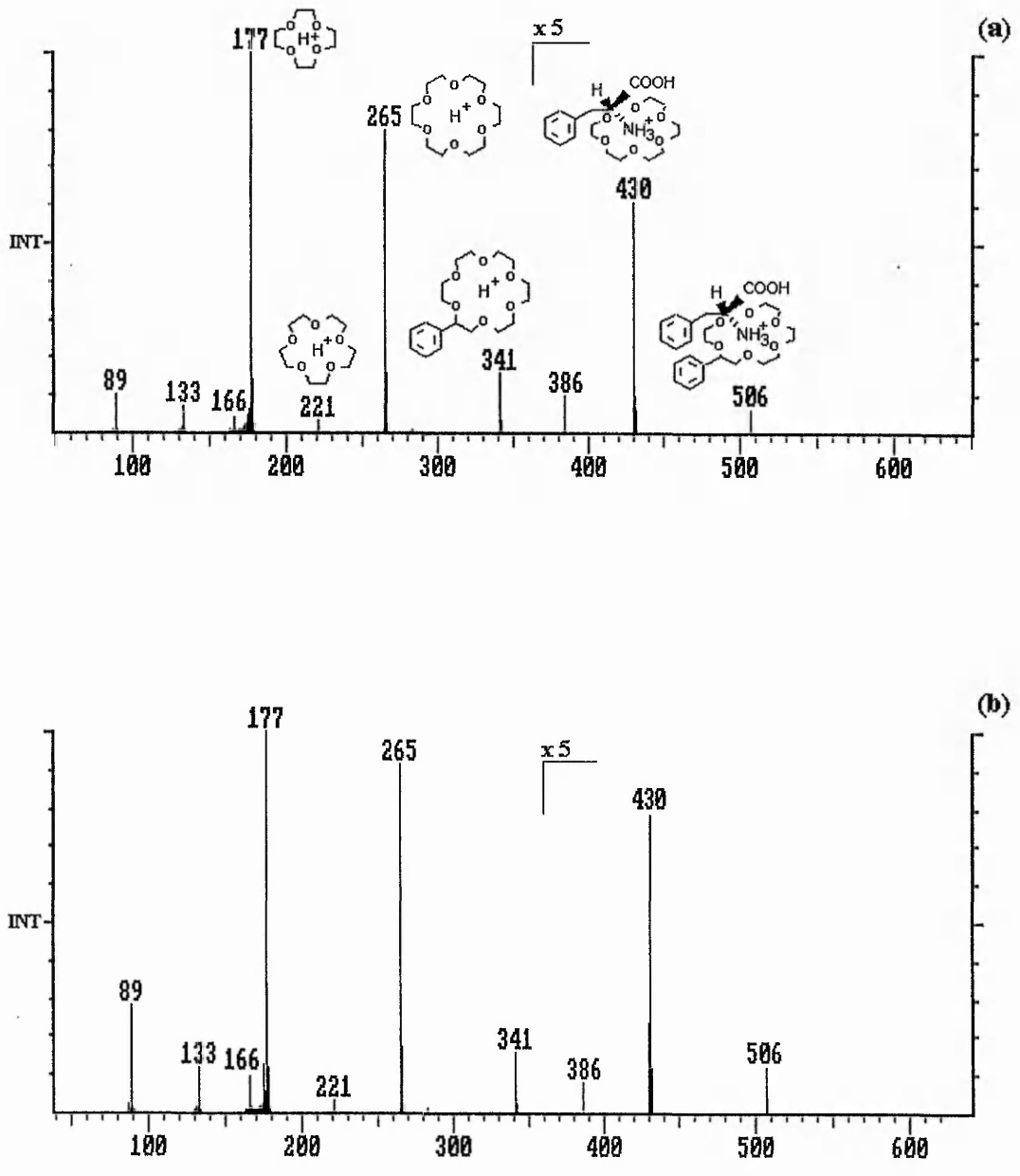

Figure 6.9. Spectrum resulting from the reaction of $[M+H]^+$ from (a) s-phenylalanine and (b) r-phenylalanine with s-phenyl-18-crown-6 and 18-crown-6.

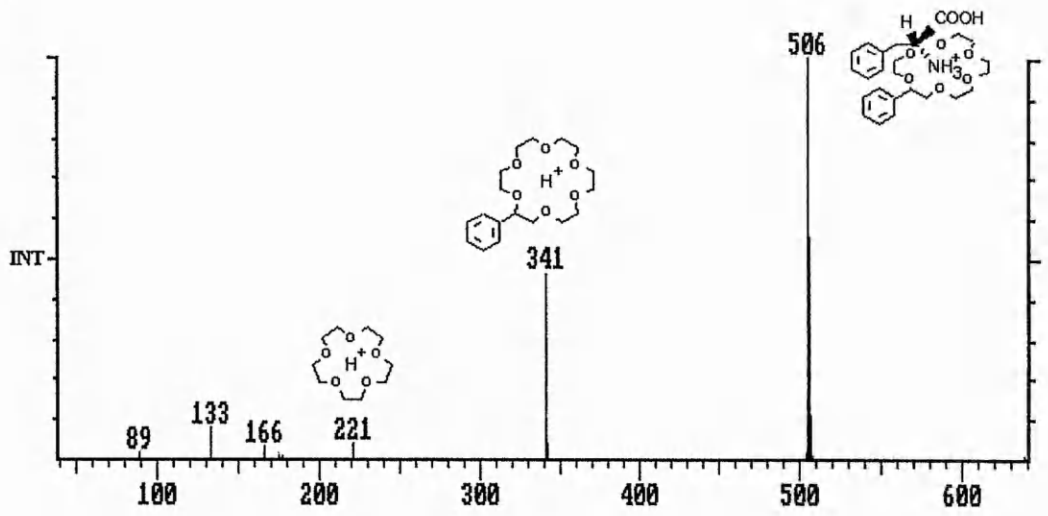

Figure 6.10. Product ion spectrum resulting from the tandem MS of the inclusion complex between s-phenyl-18-crown-6 and the $[M+H]^+$ ion from s-phenylalanine

The effect of the variation of auxiliary RF (tickle) voltage at a constant tickle time (1 ms) on the resulting CAD spectra of the [(s)-phenylalanine+H+(s)-phenyl-18-crown-6]$^+$ ion was evaluated to obtain additional information about the dissociation of the complex. As the amplitude of the activation voltage is increased, the average internal energy deposition should also increase. Comparison of the relative appearance thresholds for the decomplexation process and the ring fragment ions may reveal whether there is a significant difference in the energy needed to promote decomplexation versus skeletal fragmentation. The results of the tandem mass spectrometry are illustrated in Figure 6.11, which shows a small off-set between the threshold for decomplexation (formation of m/z 341) at approximately 250 mV and the

threshold for skeletal fragmentation (formation of m/z 221, 133 and 89) at 800 mV. This is consistent with the energy resolved mass spectra of the [15-crown-5+H+2-aminoethanol]$^+$ complex, where a threshold of about 20 mV activation voltage was reported. [18] The tandem mass spectrometry of the [(r)-phenylalanine+H+(s)-phenyl-18-crown-6]$^+$ inclusion complex showed virtually identical fragment ions with a similar energy resolved mass spectrum to the S,S inclusion complex.

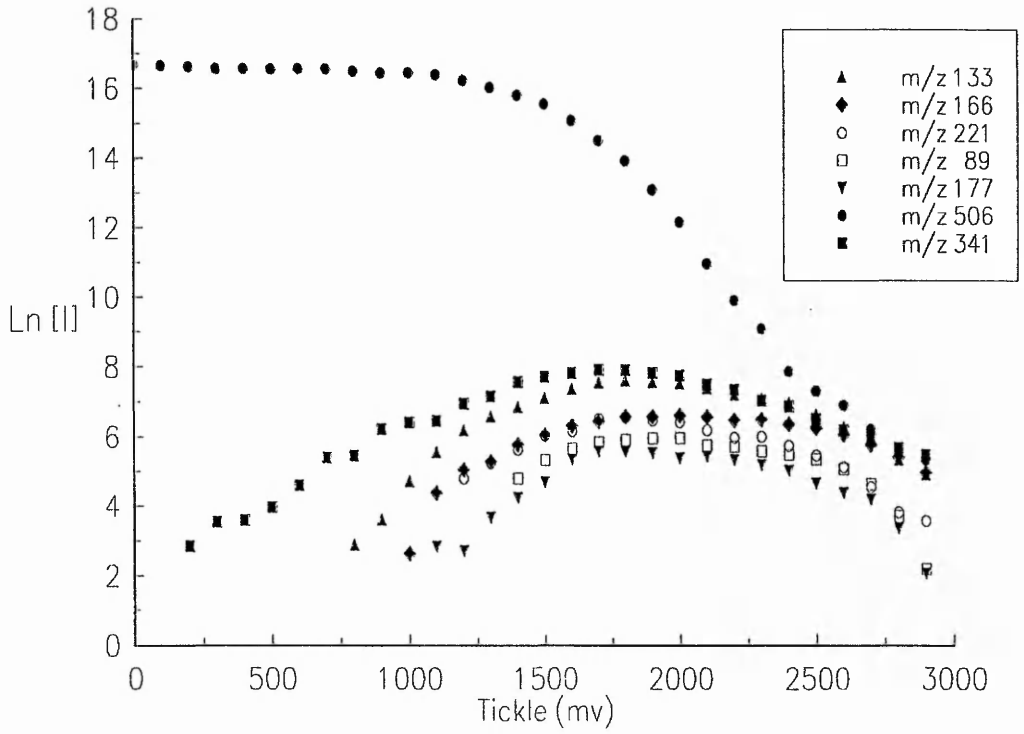

Figure 6.11. Variation of ion intensity with CAD tickle voltage for the [s-phenylalanine+H+s-phenyl-18-crown-6]$^+$ inclusion complex.

The ligand exchange technique [17] has been employed to give an indication of the ion binding affinities of two inclusion complexes. In this method a protonated amine crown ether inclusion complex is isolated and allowed to interact with a second uncomplexed crown ether molecule. Observation of the transfer of the protonated amine to the second crown ether indicates that this second crown ether has a higher gas phase affinity for the protonated amine. The reaction needs to be done in the reverse direction to confirm the order of affinities and pressures of the two crown ethers must roughly equal.

The spectrum resulting from the isolation of the $[(s)\text{-phenylalanine}+H]^+$/(s)-phenyl-18-crown-6 non-covalent inclusion complex followed by retention of this ion in the trap for 100 ms in the presence of neutral 18-crown-6 is illustrated in Figure 6.12(a) and indicates the presence of a $[(s)\text{-phenylalanine}+H+18\text{-crown-}6]^+$ ion at m/z 430, formed by abstraction of protonated phenylalanine from the (s)-phenyl-18-crown-6 complex. However, this is absent in the reverse reaction between the $[(s)\text{-phenylalanine}+H+18\text{-crown-}6]^+$ inclusion complex and neutral (s)-phenyl-18-crown-6, shown in Figure 6.12(b), which indicates the greater affinity of 18-crown-6 for $[(s)\text{-phenylalanine}+H]^+$.

The overall order of the strength of the non covalent complexes can be tentatively assigned as:

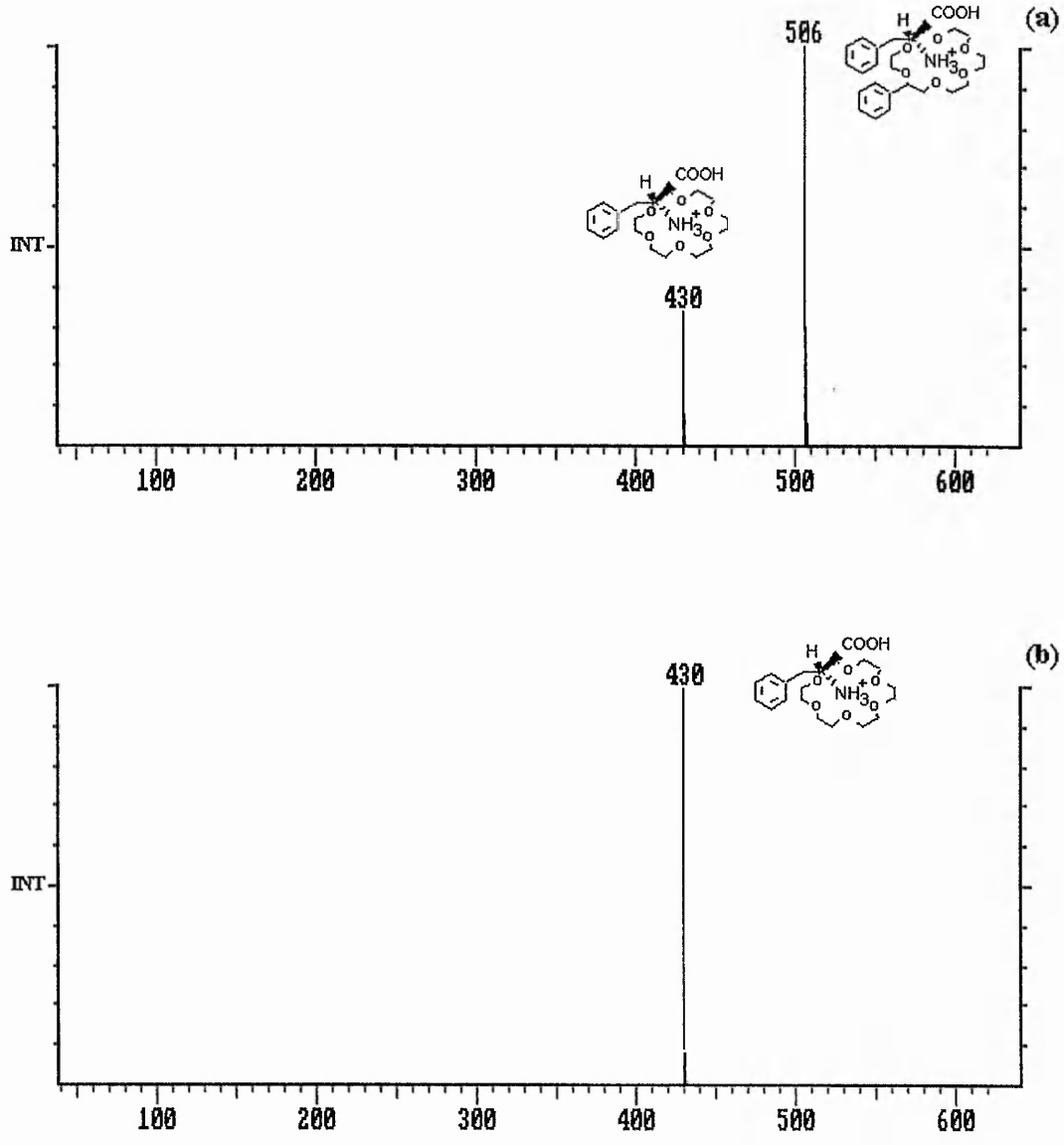

Figure 6.12. Ligand exchange experiment between the $[M+H]^+$ ion of s-phenylalanine and s-phenyl-18-crown-6 and 18-crown-6. (a) isolation of the inclusion complex of the $[M+H]^+$ ion of s-phenylalanine and s-phenyl-18-crown-6 followed by 100 ms reaction time; (b) isolation of the [M+H]+ ion from s-phenylalanine and 18-crown-6 followed by 100 ms reaction time.

$[p+H+18\text{-crown-6}]^+ > [p+H+benzo\text{-}18\text{-crown-6}]^+ > [(r)\text{-phenyl}+H+18\text{-crown-6}]^+ = [(s)\text{-phenyl}+H+18\text{-crown-6}]^+ > [(s)\text{-phenyl}+H+(s)\text{-phenyl-}18\text{-crown-6}]^+ > [nitro+H+18\text{-crown-6}]^+ > [phen+H+18\text{-crown-6}]^+ \sim [phen+H+benzo\text{-}18\text{-crown-6}]^+$

where p = propylamine, phen = phenethylamine, phenyl = phenylalanine and nitro = 4-nitrophenylalanine

The increased stability of the protonated phenylalanine/18-crown-6 non-covalent inclusion complex compared to the protonated phenylalanine/(s)-phenyl-18-crown-6 (Figures 6.9 and 6.12) indicates the aromatic ring on (s)-phenyl-18-crown-6 destabilises the inclusion complex. Therefore this would suggest that the protonated propylamine/18-crown-6 complex is a stronger non-covalent inclusion complex than the protonated propylamine/benzo-18-crown-6 complex. The observation of skeletal fragment ions in the product ion spectrum of the protonated phenylalanine/(s)-phenyl-18-crown-6 ion would suggest that the stability of this complex lies in between the stability of the propylamine/benzo-18-crown-6 and phenethylamine/18-crown-6 complexes.

6.4 CONCLUSION

Crown ethers form stable non-covalent inclusion complexes with protonated amines, which allow some structural recognition to be attained for protonated amino-containing analytes. The effect of varying the substituents on protonated amines of the type $[RNH_3]^+$ (R= $CH_3(CH_2)_2$, $C_6H_5(CH_2)_2$, $O_2NC_6H_4(CH_2)_2$ or $C_6H_5CH_2C(H)COOH$) can have a striking effect on the stability of the inclusion complex formed with crown ethers. Introduction of an aromatic ring on the protonated amine reduces the stability of the complex. Benzo-18-crown-6 forms less stable complexes with protonated propylamine than 18-crown-6. Phenylalanine forms much more stable complexes with 18-crown-6 than (s)-phenyl-18-crown-6, but tandem mass spectrometry would suggests that the stability of the (s)-phenyl-18-crown-6 protonated phenylalanine complex lies somewhere in between that of protonated propylamine benzo-18-crown-6 and protonated phenethylamine-18-crown-6 complexes.

The use of tandem mass spectrometry to obtain information on the strength of an inclusion complex would allow structural information to be gathered on an unknown compound by isolation of its $[M+H]^+$ ion in the presence of a crown ether host followed by tandem mass spectrometry.

6.5 REFERENCES

1. Pedersen, C.J., *J. Am. Chem. Soc.*, 2495, **89** (1967)

2. Pedersen, C.J., *J. Am. Chem. Soc.*, 7017, **89** (1967)

3. Vincenti, M., J. of Mass Spectrom., 925, **30** (1995)

4. Huang, S. K., Lee,Y.C., Allison, J. and Popov, A. I., *Spectrosc. Lett.*, 215, **16** (1983)

5. Huang, S.K. and Allison, J., *Organometallics*, 883, **2** (1983)

6. Meot-Ner, M., *J. Am. Chem. Soc.*, 4912, **105** (1983)

7. Chu, I.-H. and Dearden, D.V, *J. Am. Chem. Soc.* 8197, **117** (1995)

8. Liou, C.C. and Brodbelt, J.S., *J. Am. Soc. Mass Spectrom.,* 543, **3** (1992)

9. Maleknia, S., Brodbelt, J., *J. Am. Chem. Soc.*, 4295, **114** (1992)

10. Wu, H.F. and Brodbelt, J.S., *J. Inclus. Phenom. Mol. Recog. Chem.*, 37, **18** (1994)

11. Brodbelt, J., Maleknia, Liou, C.C. and Lagow, R., *J. Am. Chem. Soc.*, 5913, **113** (1991)

12. Liou, C.C., Brodbelt, J.S., *J. Am. Chem. Soc.*, 242, **4** (1993)

13. Liou, C.C. and Brodbelt, J.S., *J. Am. Chem. Soc.*, 6761, **114** (1992)

14. Brodbelt, J.S. and Liou, C.C., *Pure and Appl. Chem.*, 409, **65** (1993)

15. McLuckey, S.A., Cameron, D., Cooks, R.G., *J. Am. Chem. Soc.*, 1313, **103** (1981)

16. Munson, M.S.B., Field, F.H., *J. Am. Chem. Soc.*, 3294, **87** (1965)

17. Wu, H.F., Brodbelt, J.S., *J. Am. Soc. Mass Spectrom.*, 718, **4** (1993)

18. Liou, C.C., Wu, H.F. and Brodbelt, J.S., *J. Am. Soc. Mass Spectrom.*, 260, **5** (1994)

19. Maleknia, S. and Brodbelt, J., *J. Am. Chem. Soc.*, 2837, **115** (1993)

20. Sawada, M., Shizuma, M., Takai, Y., Yamada, H., Kaneda, T., Hanafusa, T., *J. Am. Chem. Soc.*, 4405, **114** (1992)

21. Sawada, M., Okumura, Y., Yamada, H., Takai, Y., Takahashi, S., Kaneda, T., Hirose, K. and Misumi, S., *Org. Mass Spectrom.*, 1525, **28** (1993)

22. Sawada, M., Takai, Y., Yamada, Hirayama, S., Kaneda, T., Tanaka, T., Kamada, K., Mizooku, T., Takeuchi, S., Ueno, K., Hirose, K., Tobe, Y. and Naemura, K., *J. Am. Chem. Soc.*, 7726, **117** (1995)

23. Sawada, M., Okumura, Y., Shizuma, M., Takai, Y., Hidaka, Y., Yamada, H., Tanaka, T., Kaneda, T., Hirose, K., Misumi, S. and Takahashi, S., *J. Am. Chem. Soc.*, 7381, **115** (1993)

24. Chu, I.H., Dearden, D.V., Bradshaw, J.S., Huszthy, P. and Izatt, R.M., *J. Am. Chem. Soc.*, 4318, **115** (1993)

25. Todd, J.F.J., Penman, A.D., Thorner, D.A. and Smith, R.D., *Rapid Commun. Mass Spectrom.*, 108, **4** (1990)

26. Louris, J.N., Cooks, R.G., Syka, J.E.P., Kelly, P.E., Stafford, G.C. and Todd, J.F.J., *Anal. Chem.*, 1677, **59** (1987)

27. K.G. Asano, D.E. Goeringer, S.A. McLuckey, D. Hoekman, S.W. Stiller, *Proceedings of the 41st ASMS*, San Francisco, 1993, p 700a

28. McLuckey, S.A., Glish, G.L., Asano, K.G. and Van Berkel, G.J., *Anal. Chem.*, 2312, **60** (1988)

29. Anson, C.I., Creaser, C.S. and Stephenson, G.R., *Spectrochim. Acta*, submitted for publication